

[276/160]

RUHR
UNIVERSITÄT
BOCHUM

RUB

Modern Techniques in
Hadron Spectroscopy

July, 2024

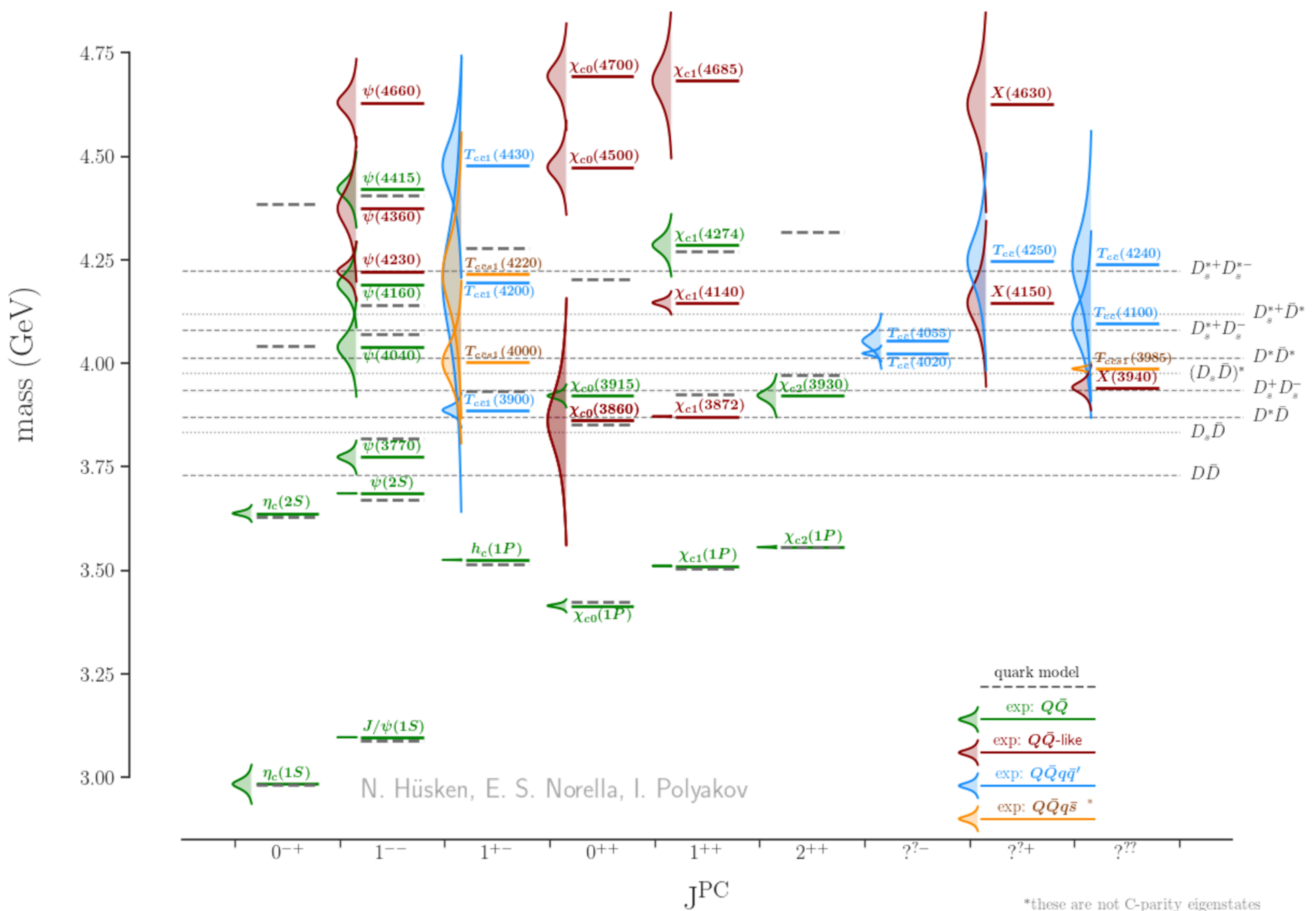
QCD PHENOMENOLOGY -- EXOTICS

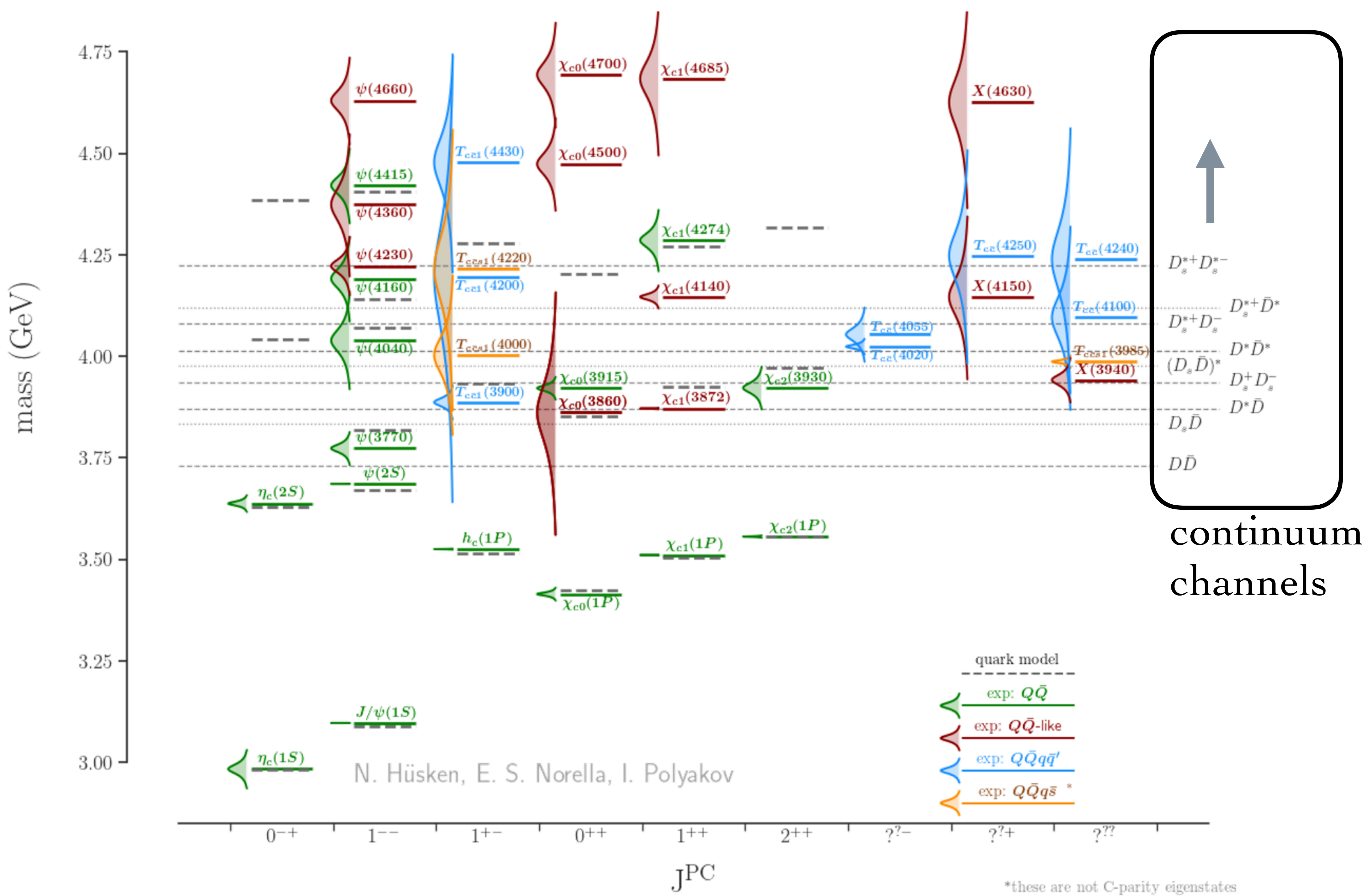
Eric Swanson

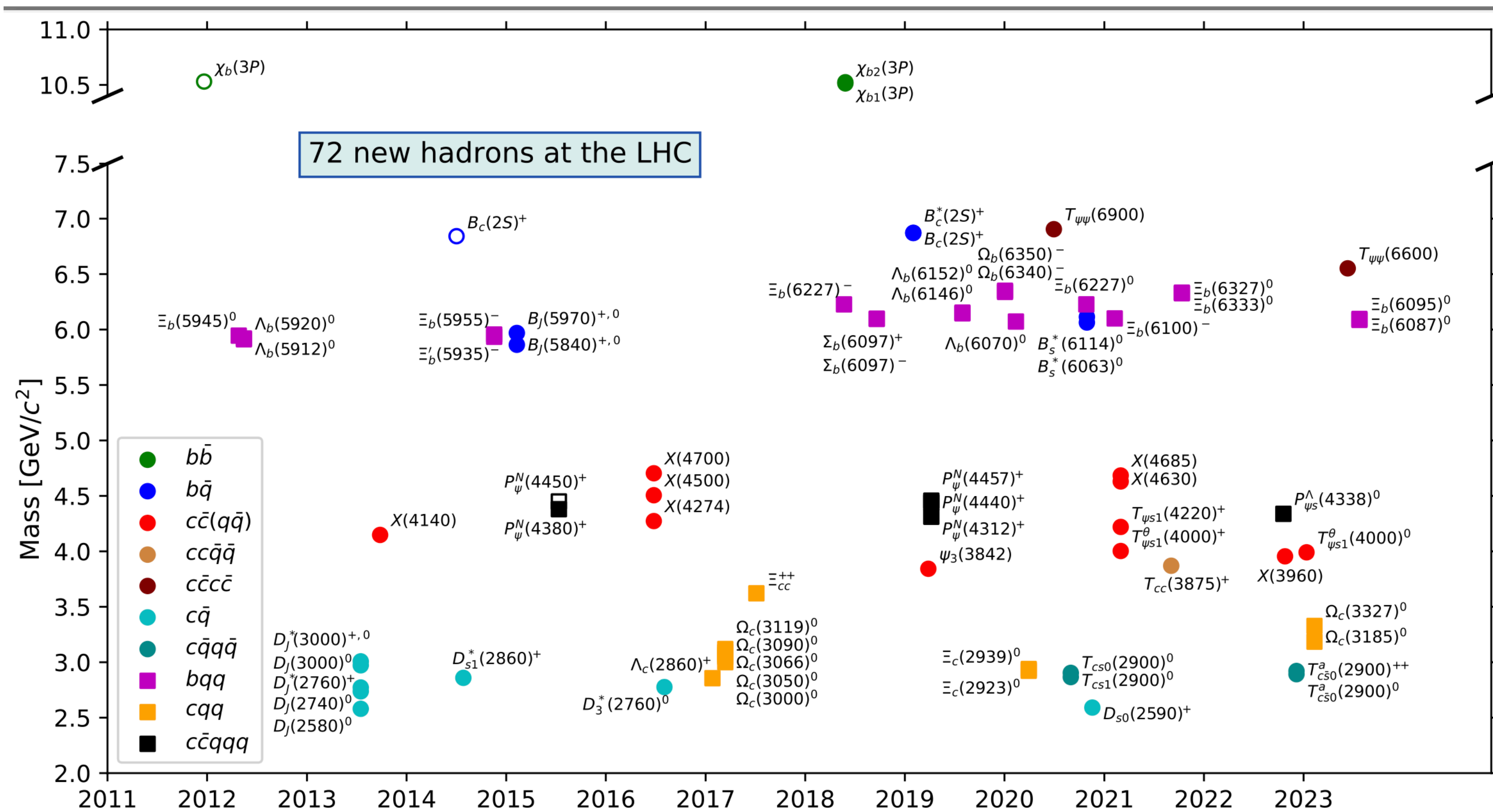


things need not be as simple as $q\bar{q}$ or qqq .

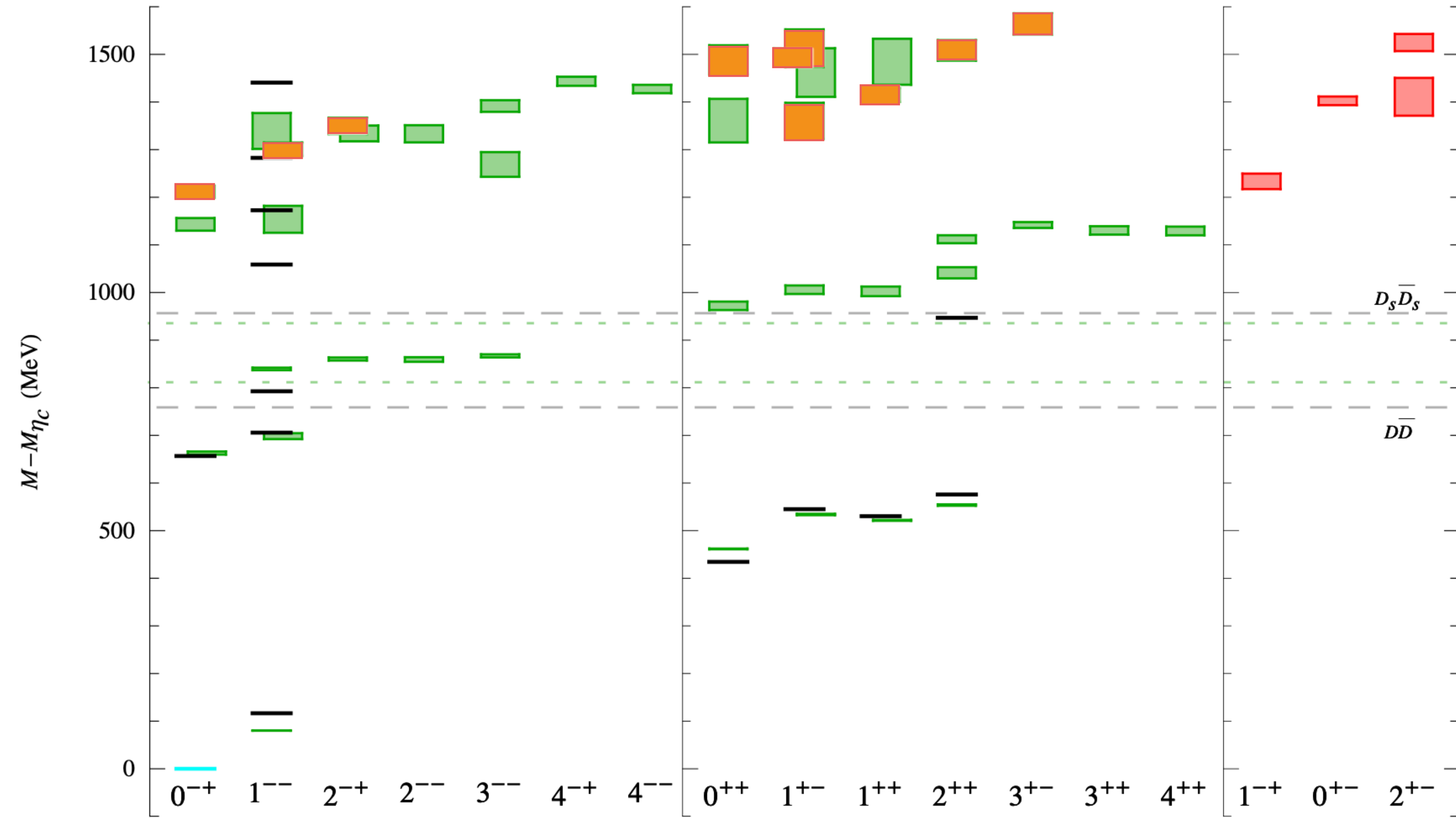
... and there is overwhelming evidence that they are not





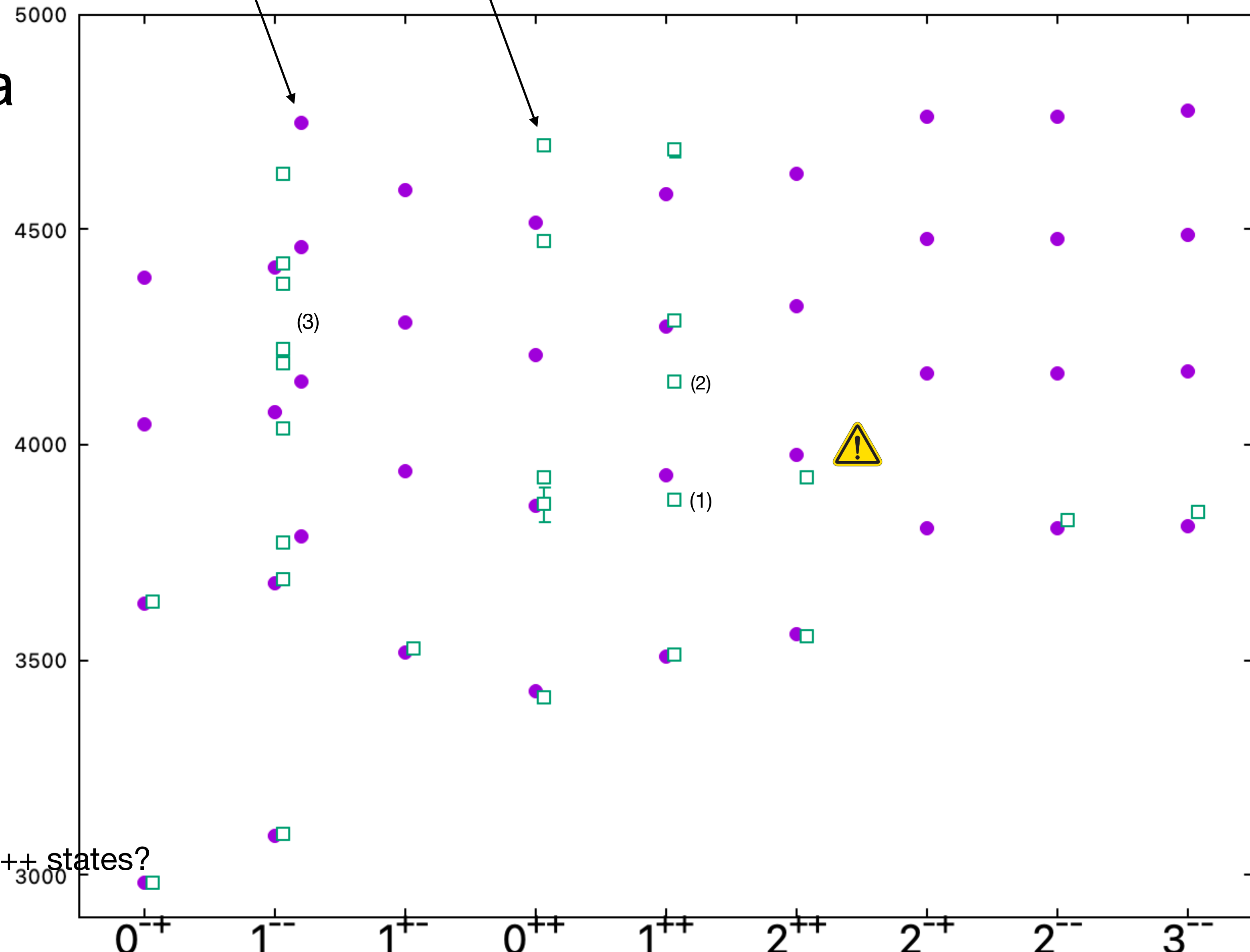


Lattice Charmonia



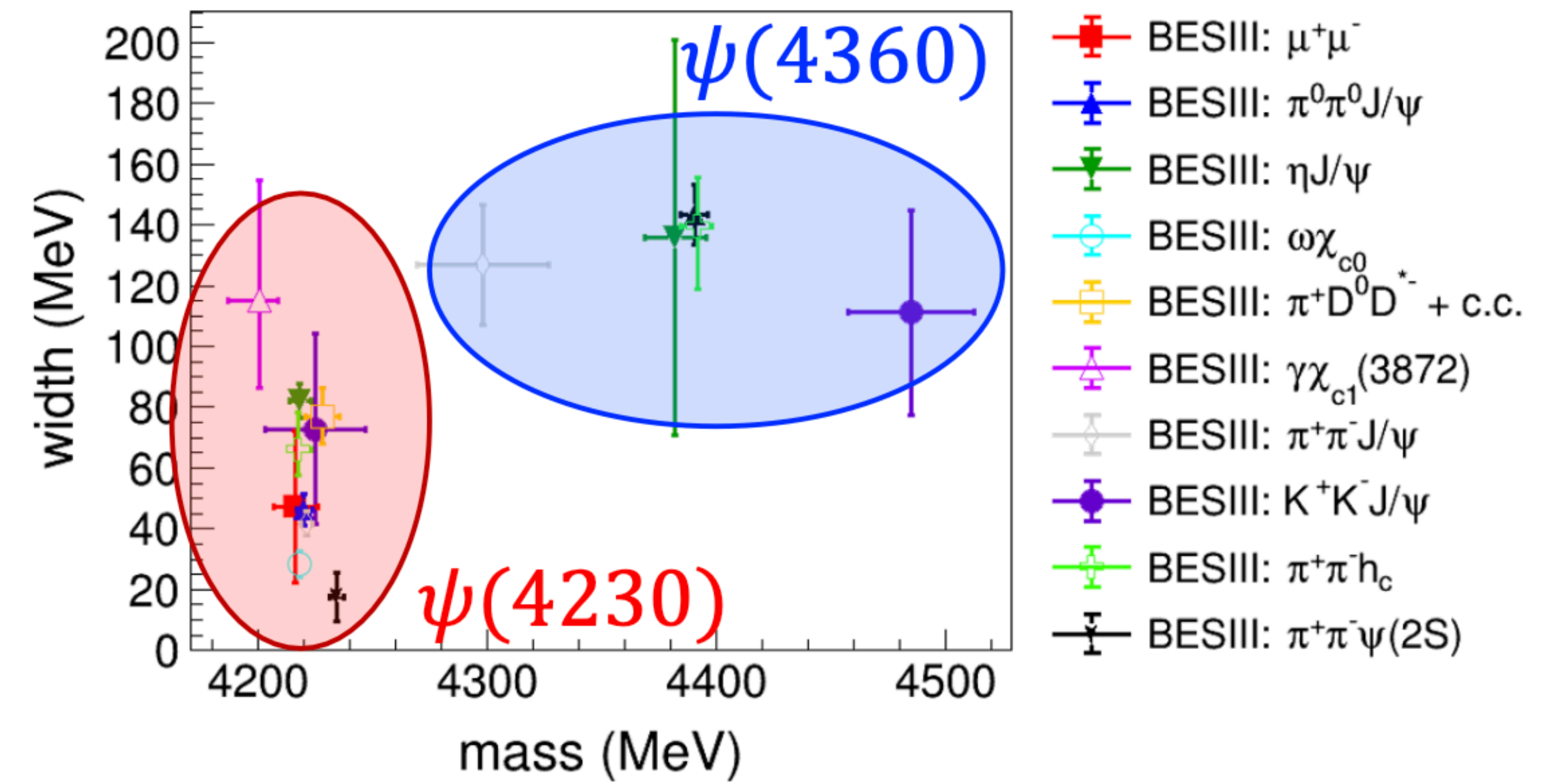
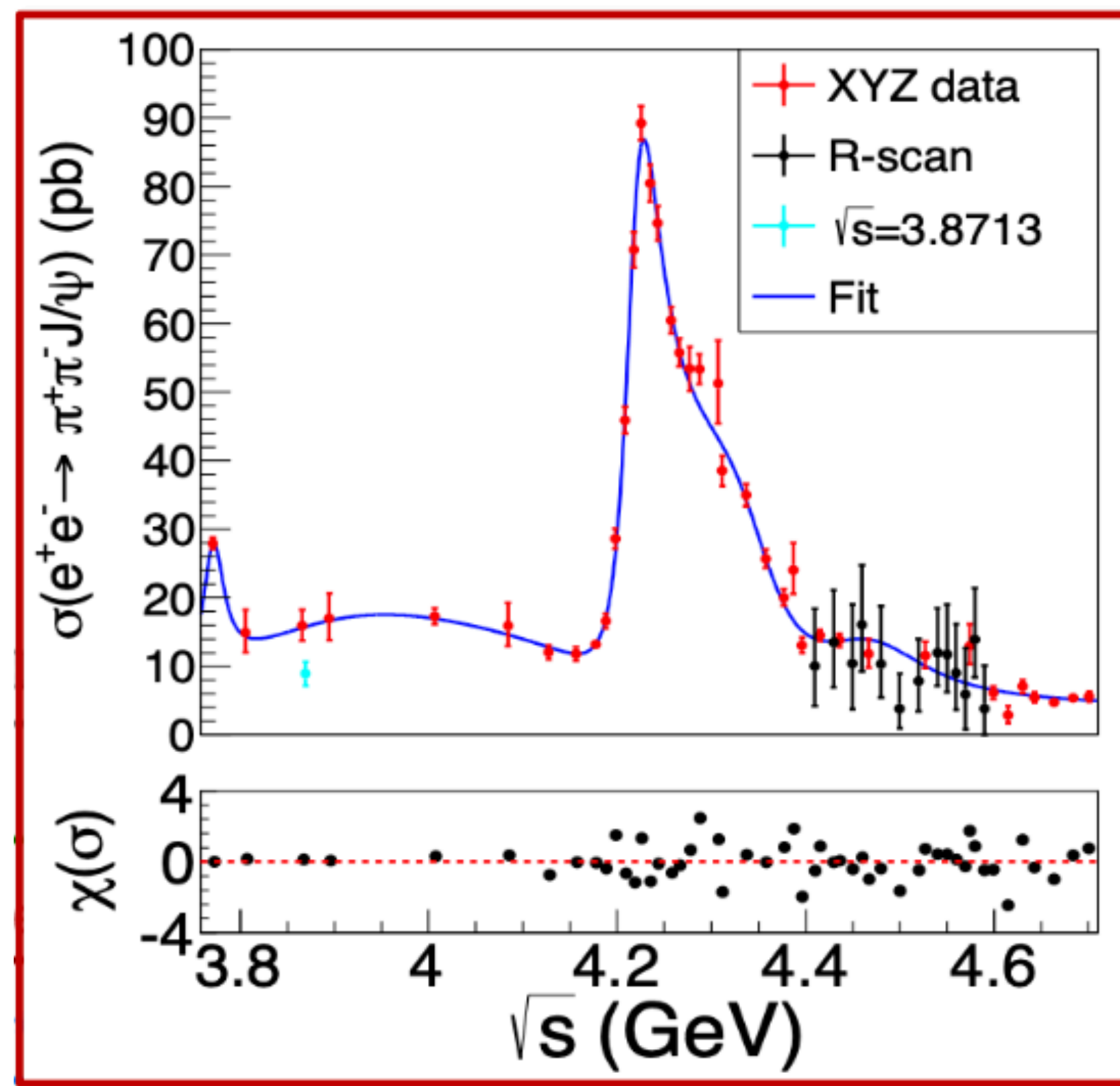
Model + PDG Charmonia

non rel model + pert VSD PDG

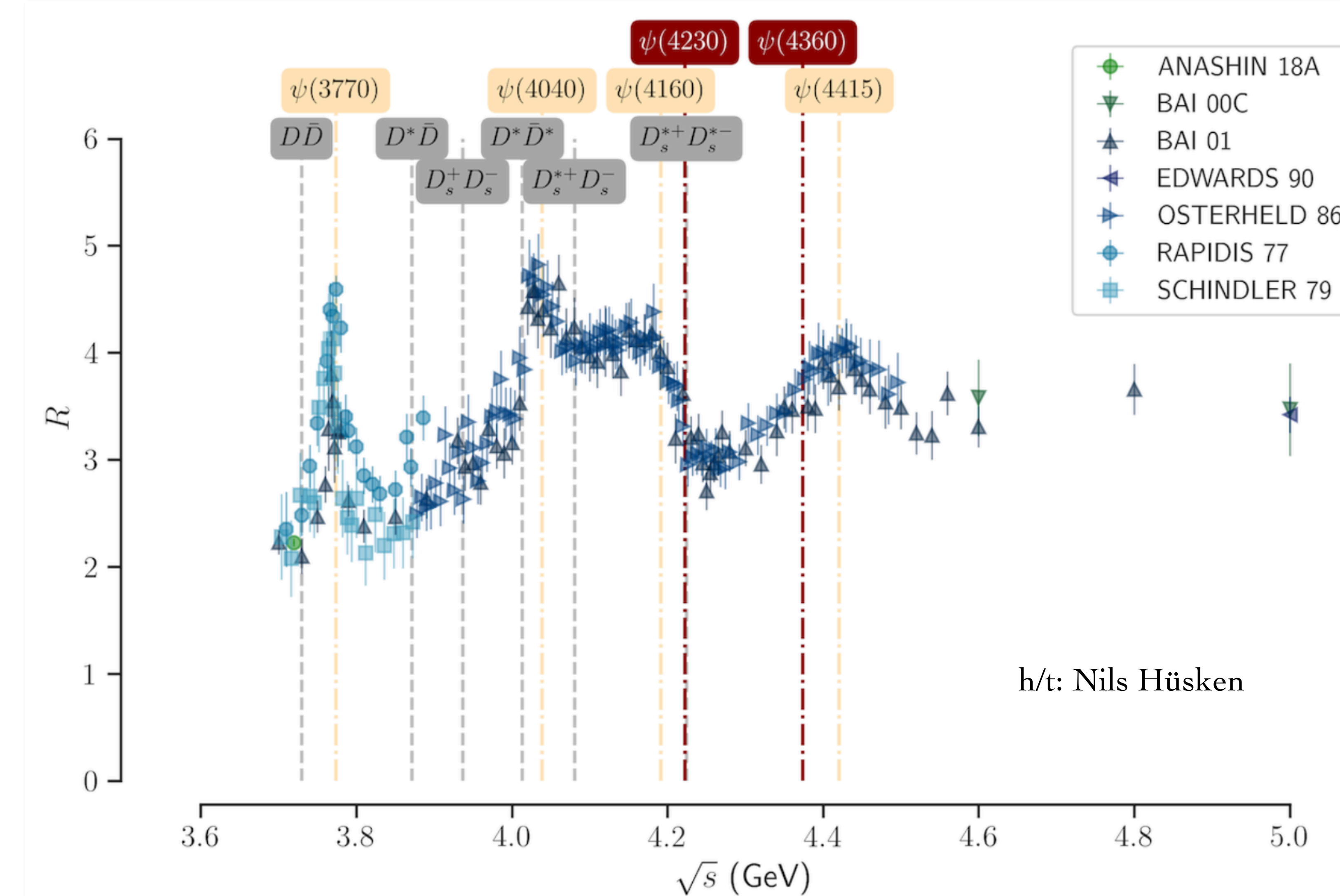


an example:

$\psi(4320)$ & $\psi(4360)$



another example:



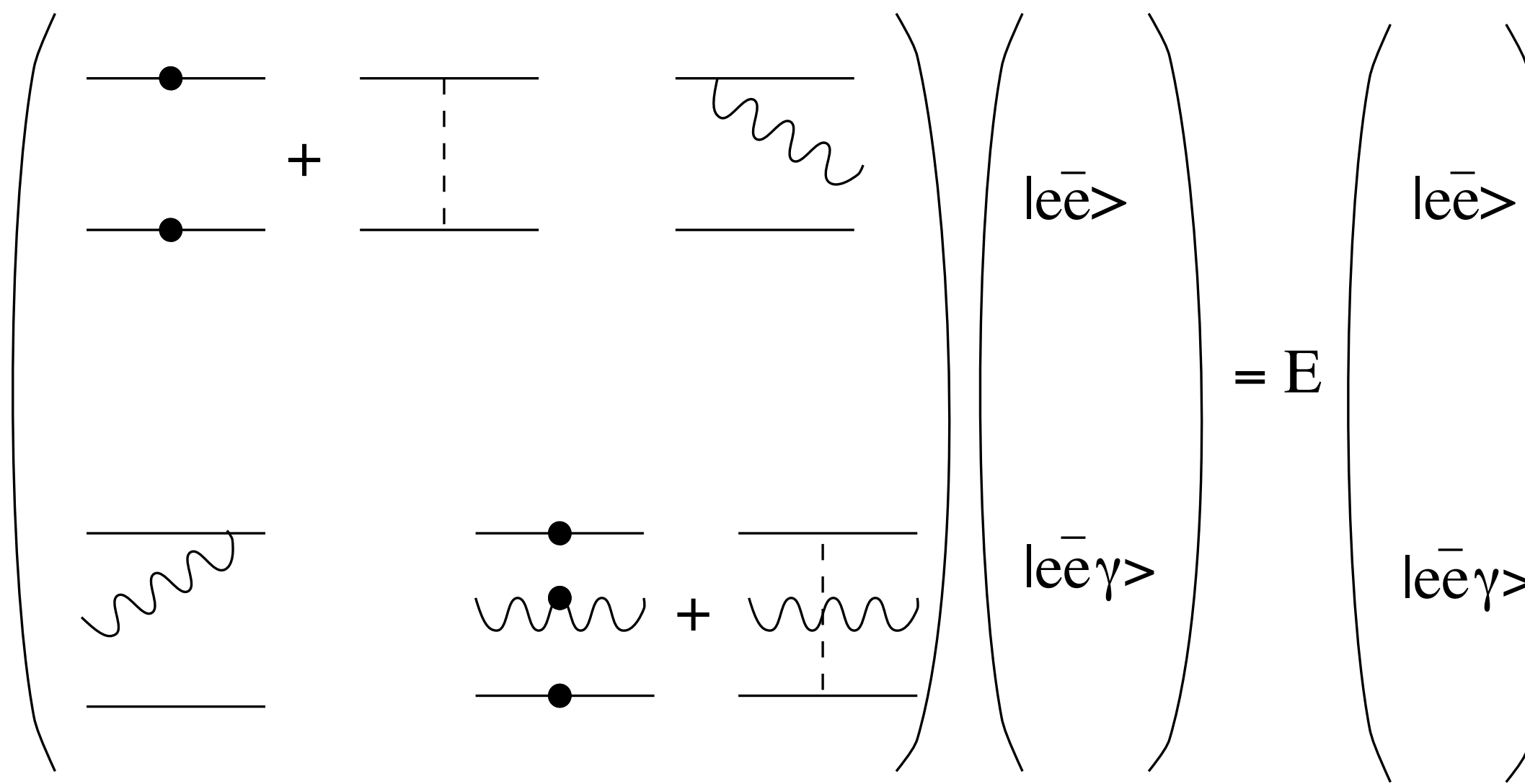
The situation is even worse: we rely on R for much information! This is not robust!

hybrids

$$|M\rangle = |q\bar{q}\rangle + \boxed{|q\bar{q}g\rangle} + |q\bar{q}q\bar{q}\rangle + \dots$$

what is a hybrid?

QED

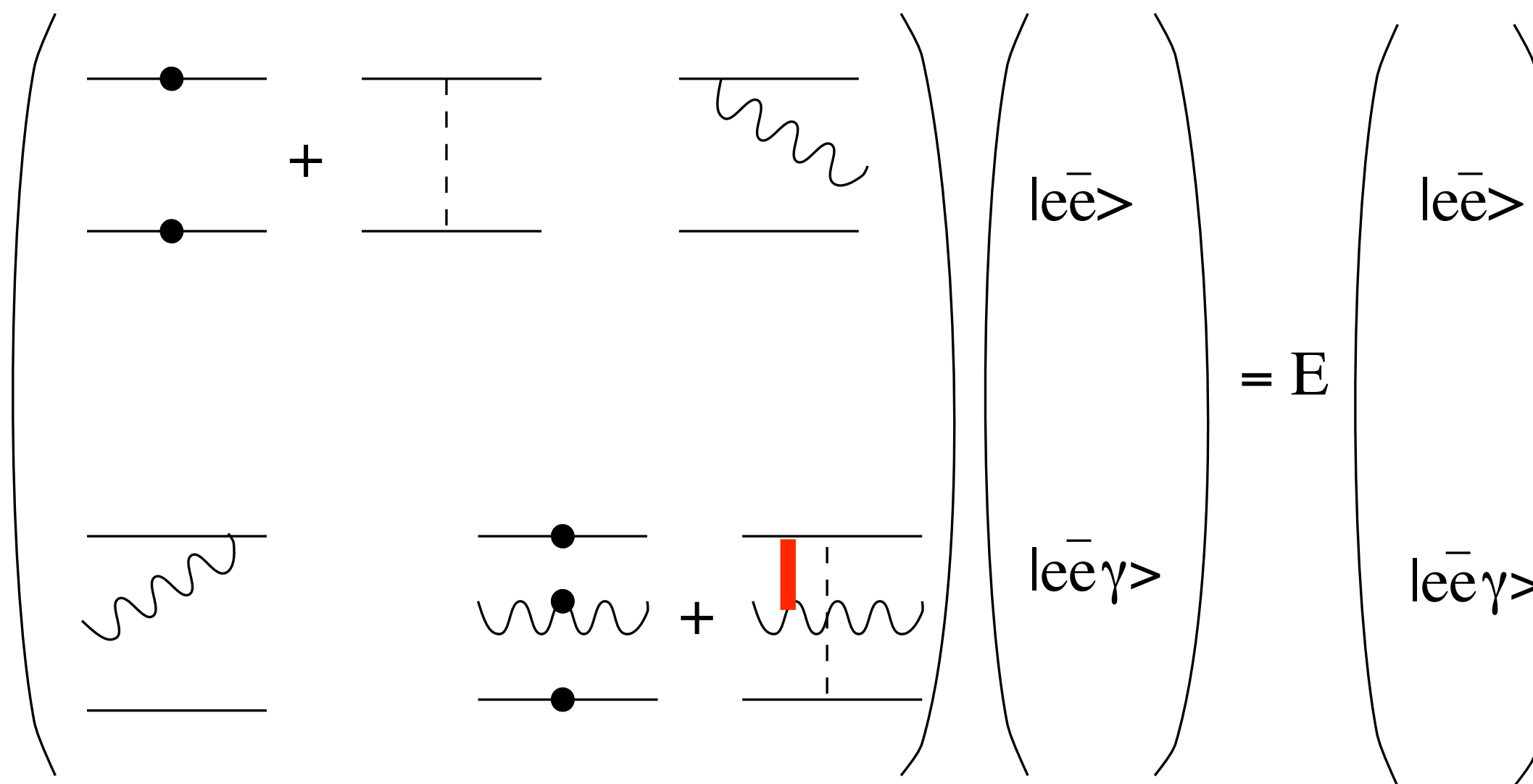


$$\begin{aligned} |0\rangle &= \sqrt{1-\epsilon^2}|e\bar{e}\rangle + \epsilon|e\bar{e}\gamma\rangle, \\ |1\rangle &= -\epsilon|e\bar{e}\rangle + \sqrt{1-\epsilon^2}|e\bar{e}\gamma\rangle. \end{aligned}$$

$$\begin{aligned} \langle r|0\rangle &\approx \phi(r) \\ \langle Rr|1\rangle &\approx \phi(r)\psi(R) \end{aligned}$$

what is a hybrid?

QCD



$$|0\rangle = \sqrt{1 - \epsilon^2} |e\bar{e}\rangle + \epsilon |e\bar{e}\gamma\rangle,$$

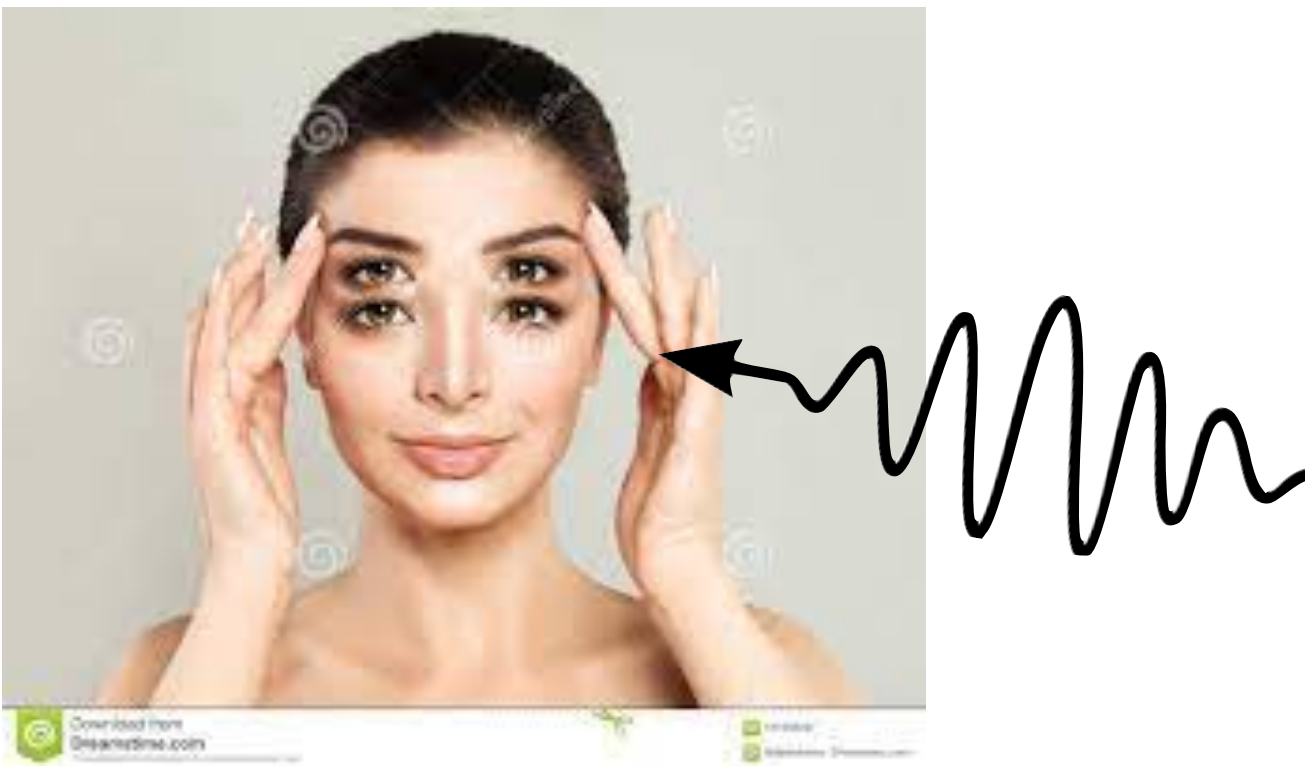
$$|1\rangle = -\epsilon |e\bar{e}\rangle + \sqrt{1 - \epsilon^2} |e\bar{e}\gamma\rangle.$$

$$\langle r|0\rangle \approx \phi(r)$$

$$\langle Rr|1\rangle \approx \phi(r)\psi(R)$$

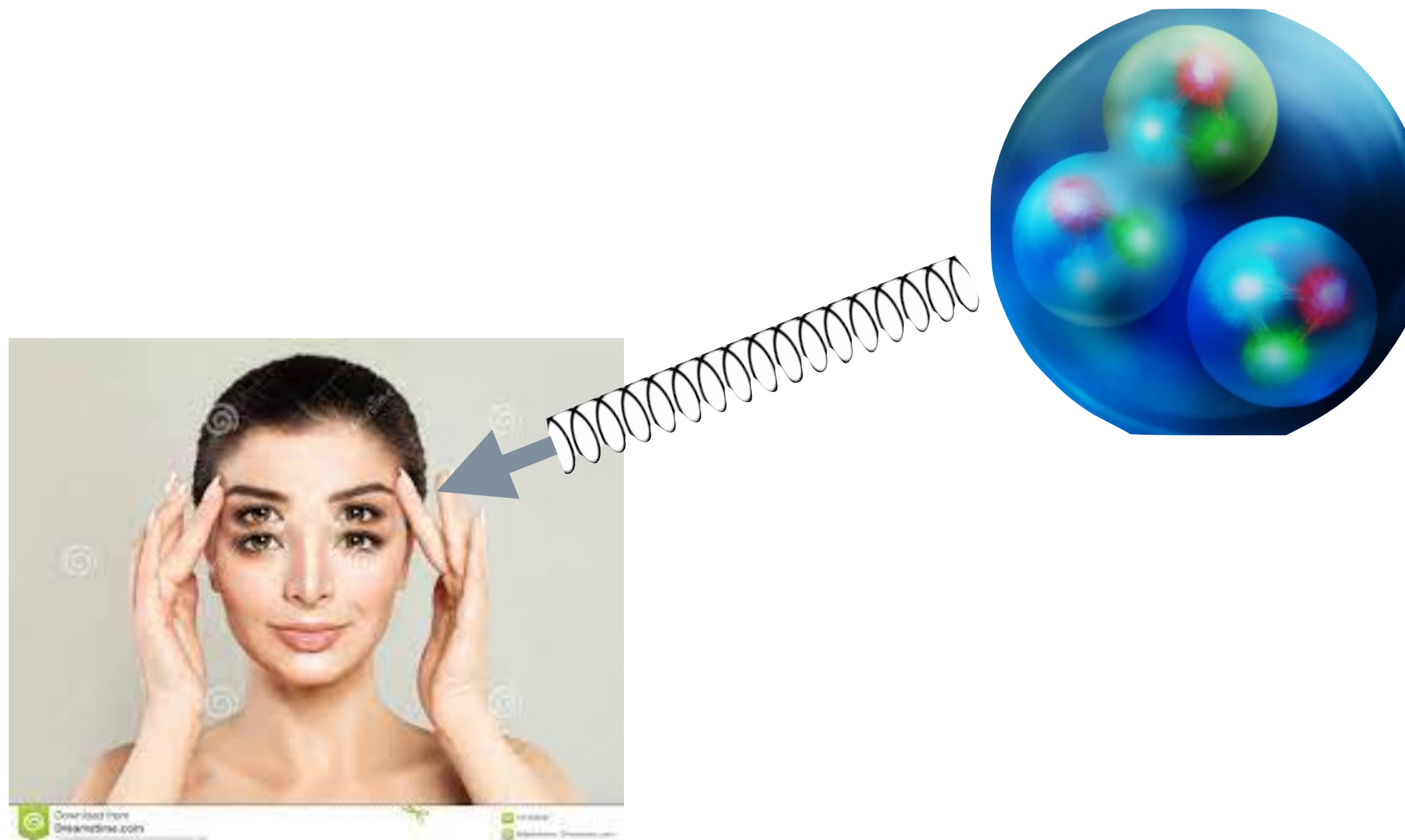
Modelling: gluons

gluonic degrees of freedom must manifest in the spectrum somewhere.



Modelling: gluons

gluonic degrees of freedom must manifest in the spectrum somewhere.



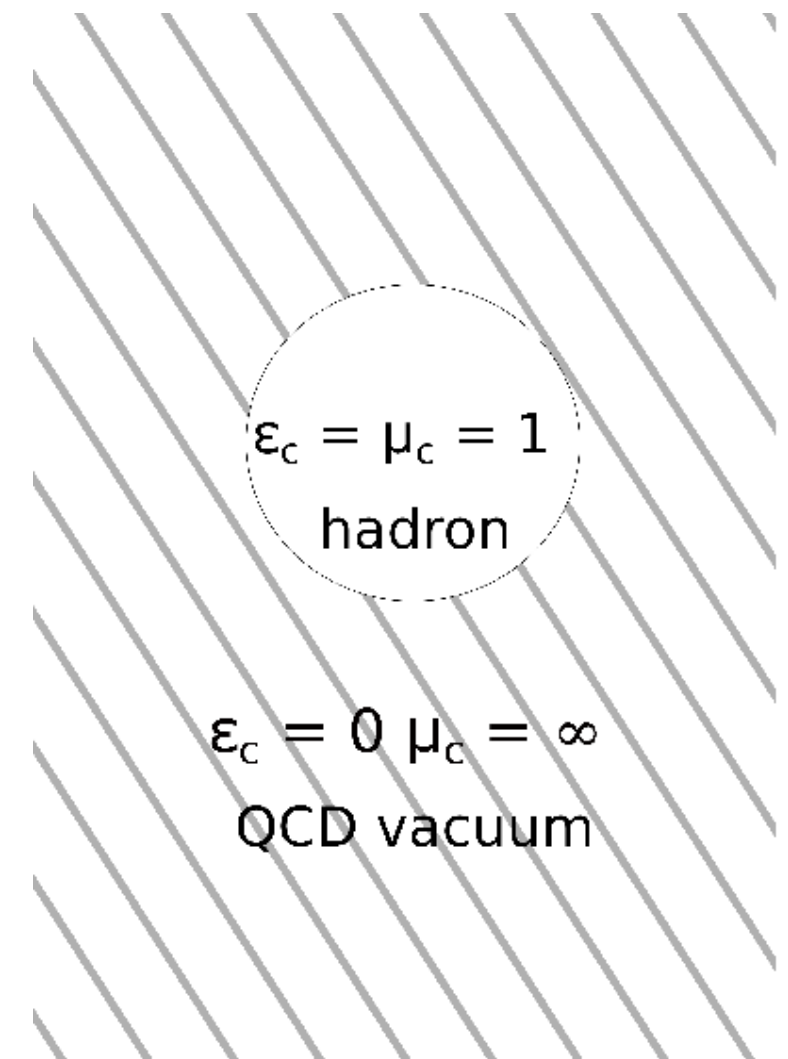
=> glueballs, hybrids, and mixed states.

Modelling: gluons

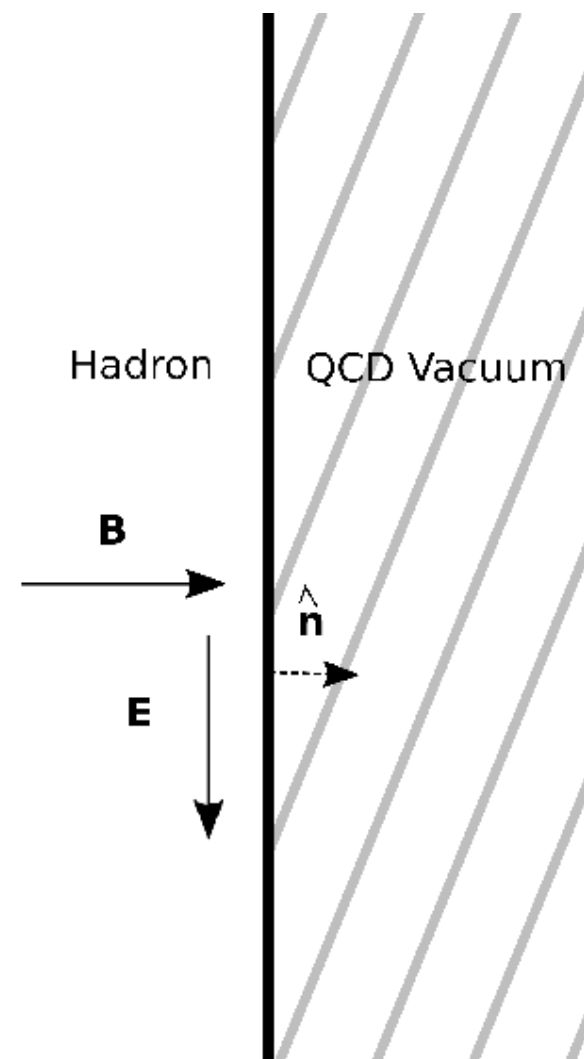
Bag Models

place quarks and gluons in a "bag" and allow them to interact perturbatively.

T. Barnes and F. E. Close, Phys. Lett. B 116, 365 (1982)
T. Barnes, F. E. Close and F. de Viron, Nucl. Phys. B 224, 241 (1983)
M. Chanowitz and S. Sharpe, Nucl. Phys. B 222, 211 (1983)



(a) The color permeability and permittivity of the bag-model.



(b) The color fields at the surface of the bag.

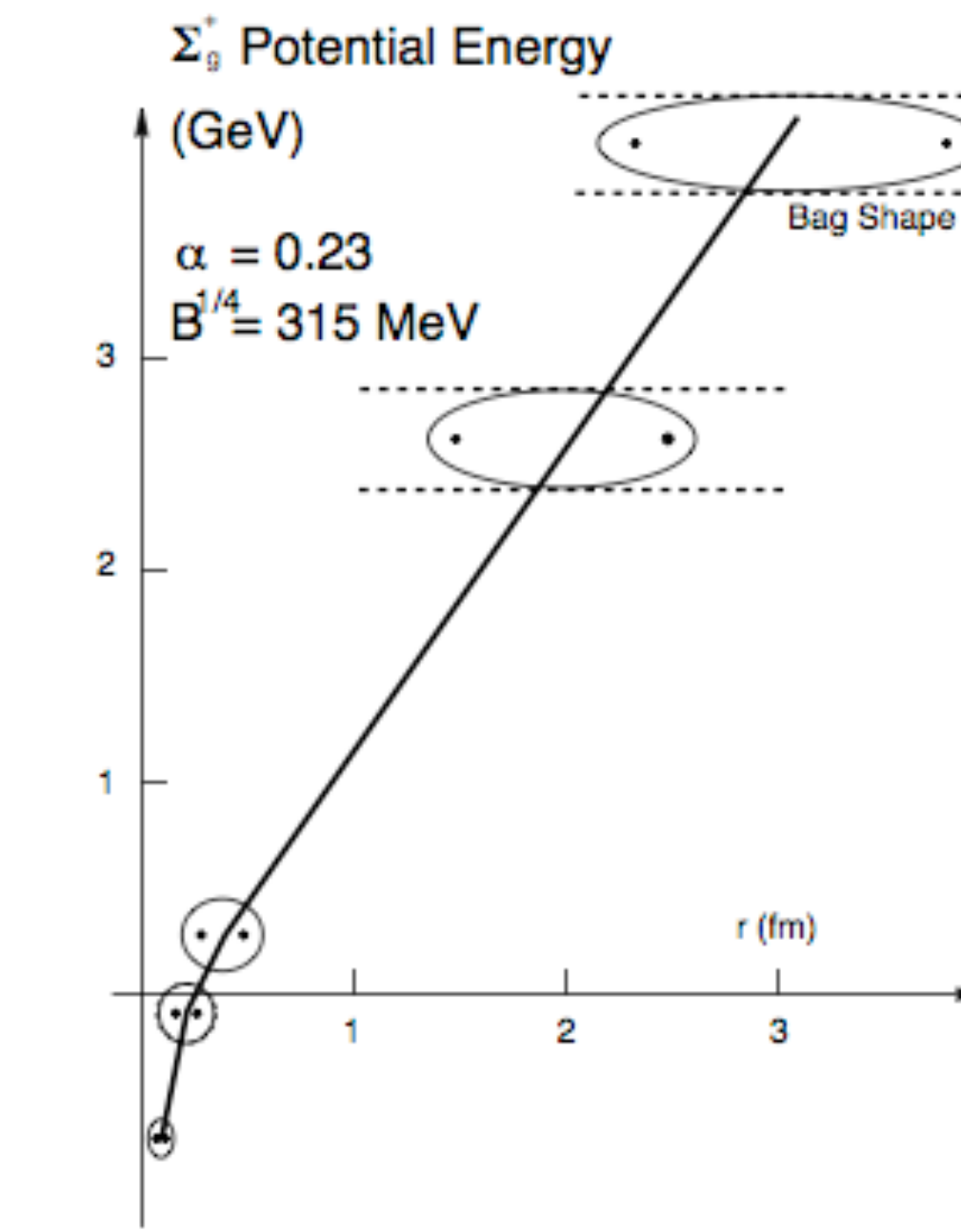
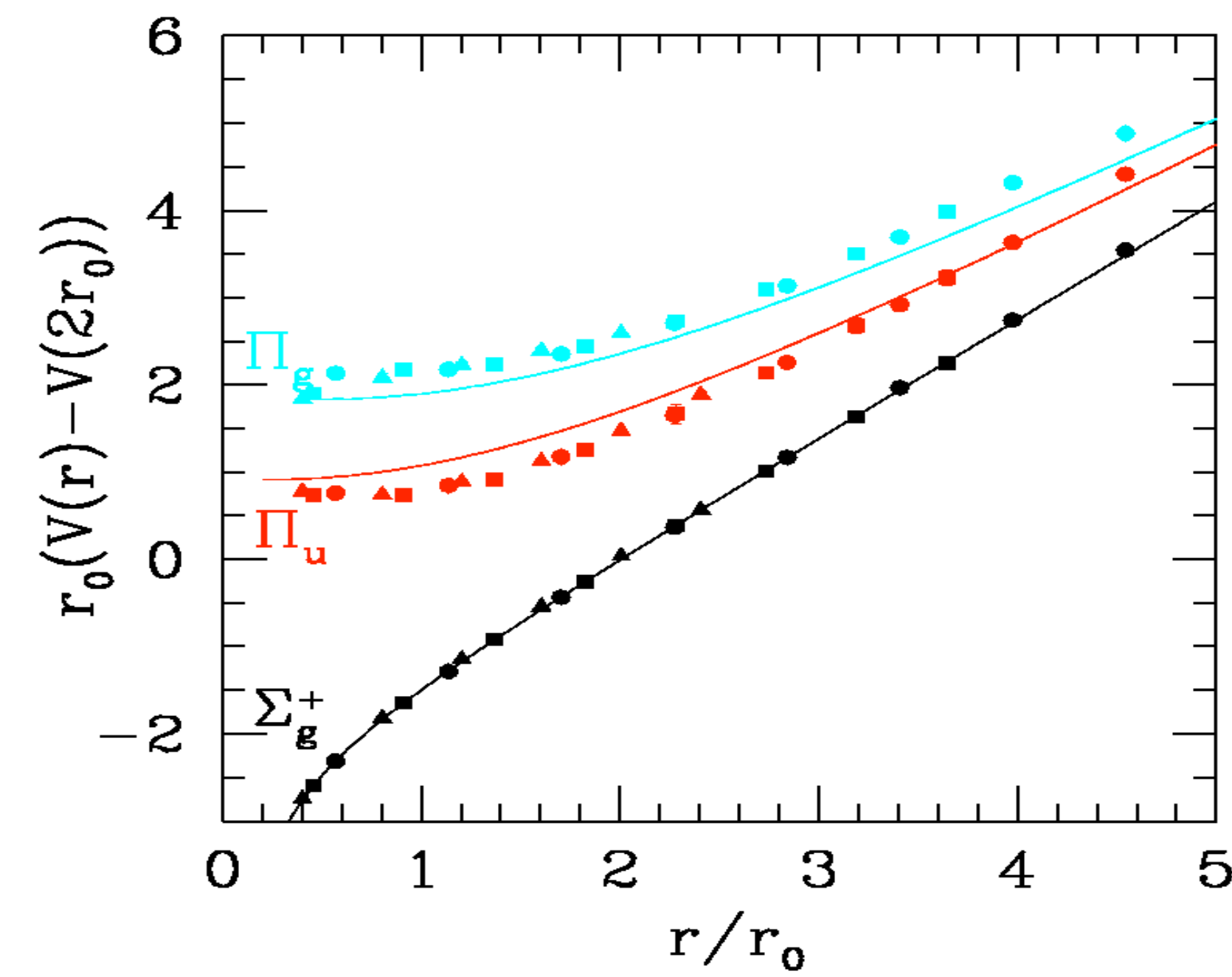
lowest mode is a 1+ TE gluon

Modelling: gluons

Bag Models

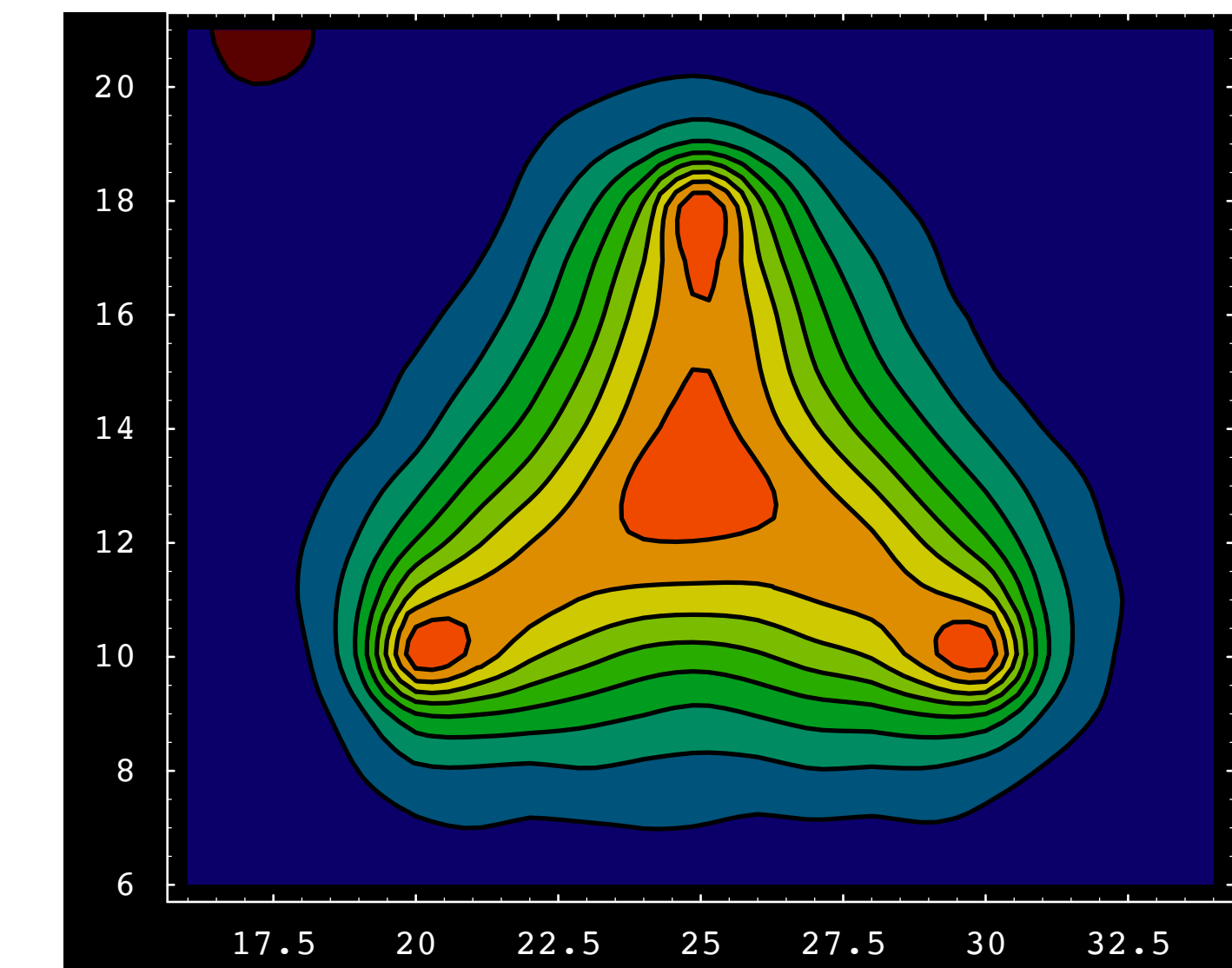
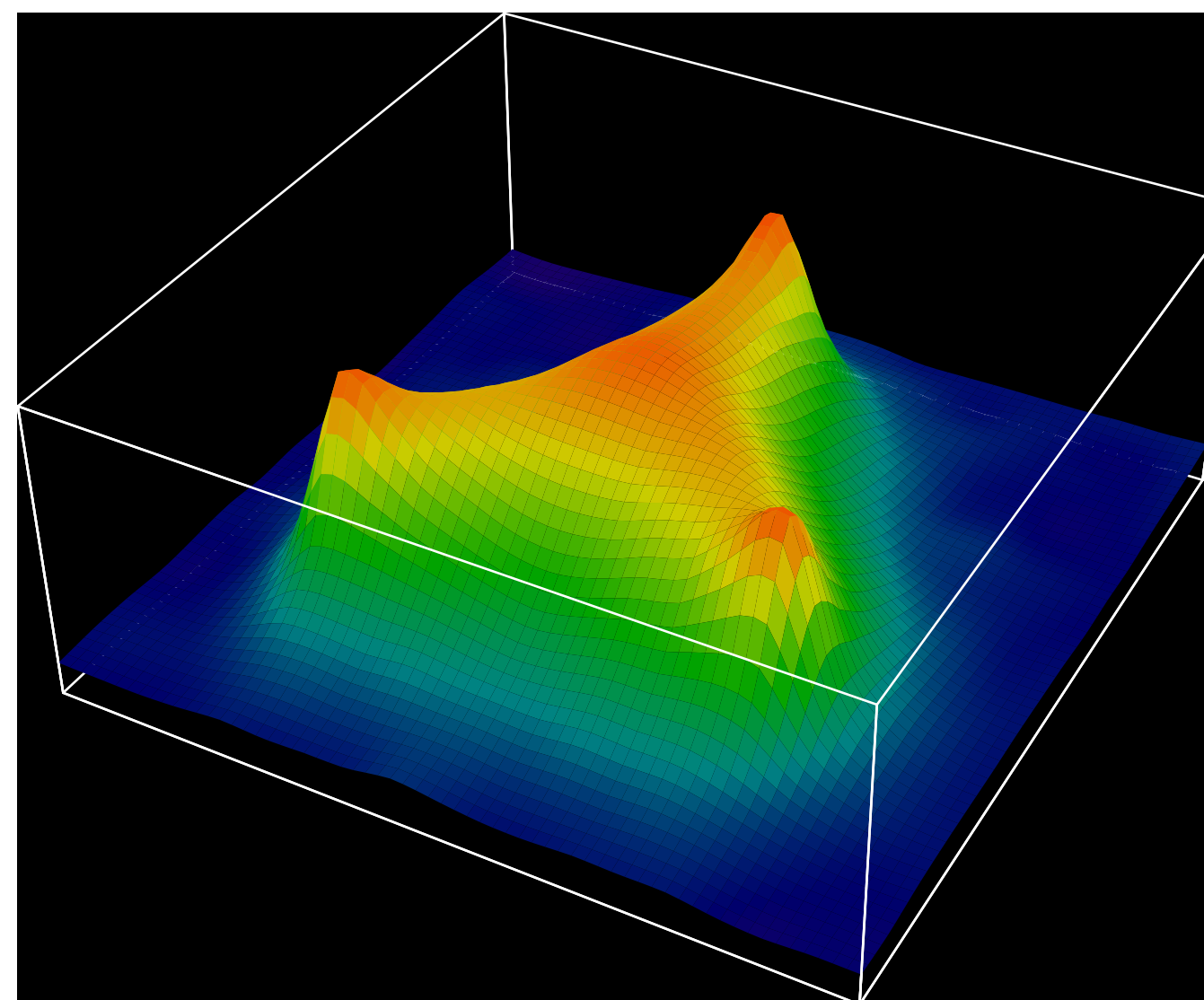
Juge, Kuti, and Morningstar, (98)

HHKR bag model computation



Modelling: gluons

Flux Tube Models



Modelling: gluons

Flux Tube Models

Coupled quarks to a relativistic 2d sheet... the “Quark Confining String Model”.

“The presence of vibrational levels gives ... extra states in quantum mechanics. ... that are absent in the charmonium model.”

$$V_N = \sigma r \left(1 + \frac{2N\pi}{\sigma r^2}\right)^{1/2}$$

GT

$$V_{NG} = \sigma r \left(1 - \frac{D-2}{12\sigma r^2} + \frac{2N\pi}{\sigma r^2}\right)^{1/2}$$

J.F. Arvis, PLB127, 106 (83);
Luescher

Giles and Tye, PRL37, 1175 (76).

T. Allen and M.G. Olsson, PLB434,
110 (98)

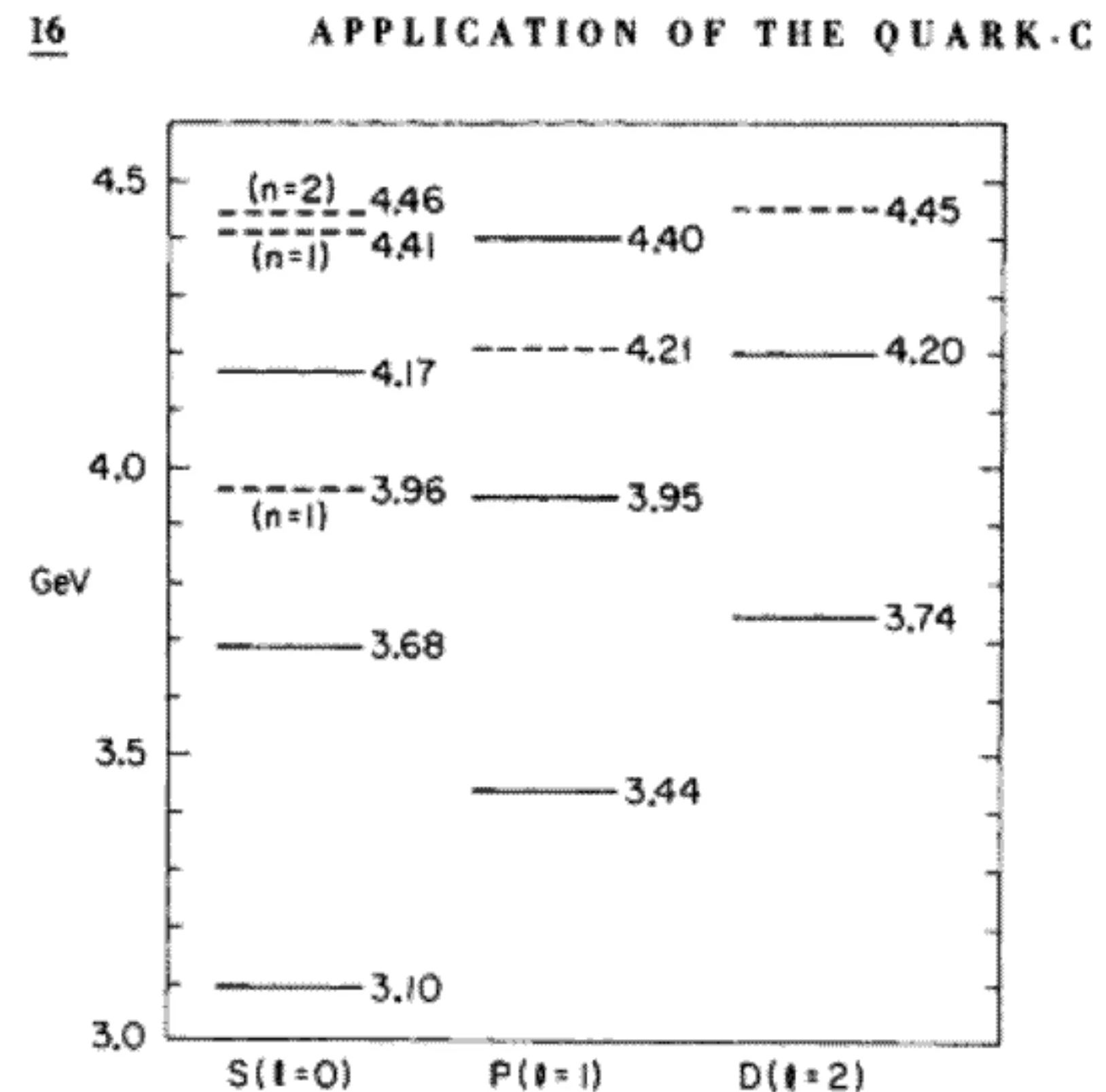


FIG. 4. The nonrelativistic spectroscopy of the charm string. $\psi(3.10)$ and $\psi(3.68)$ are fitted to obtain $M = 1.154$ GeV and $k = 0.21$ GeV 2 . The dashed lines are the vibrational levels absent in the charmonium model. Levels

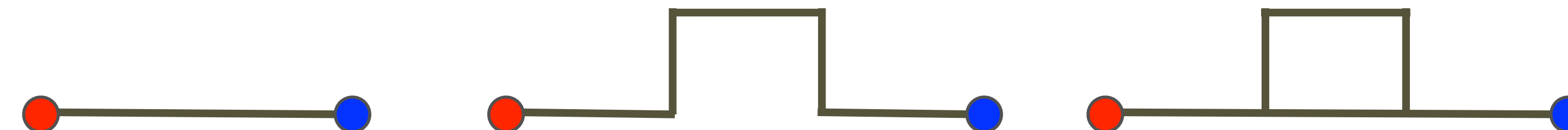
Modelling: gluons

Flux Tube Models

Isgur and Paton, PRD31, 2910 (85) .

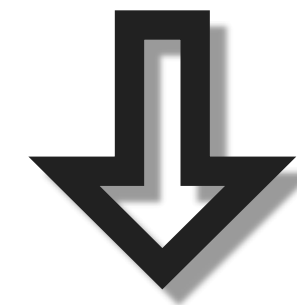
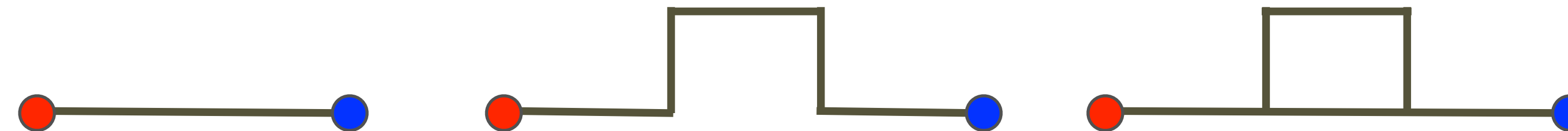
strong coupling Hamiltonian lattice gauge theory

$$H = \frac{g^2}{2a} \sum_{\ell} E_{\ell}^a E_{a\ell} + \sum_n m \bar{\psi}_n \psi_n + \frac{1}{a} \sum_{n,\mu} \psi_n^\dagger \alpha_\mu U_\mu(n) \psi_{n+\mu} + \frac{1}{ag^2} \sum_P \text{tr}(N - U_P - U_P^\dagger)$$

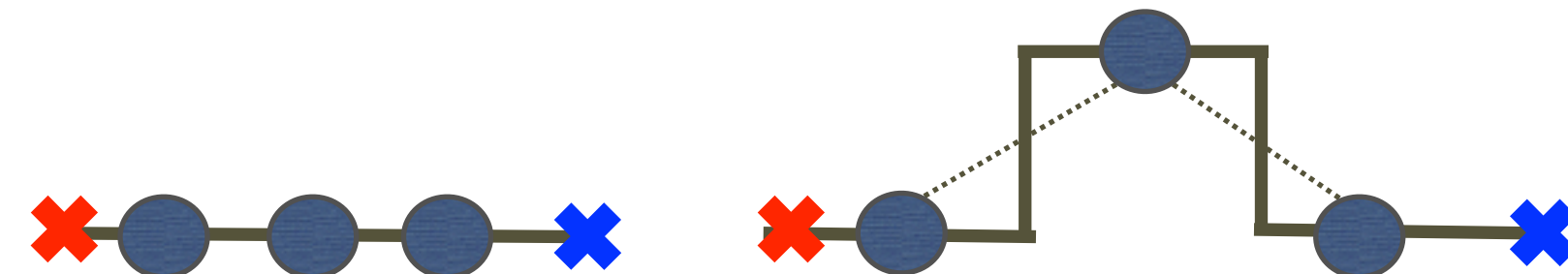


Modelling: gluons

Flux Tube Models



adiabatic



small oscillation

nonrelativistic beads

$$m_b = b a$$

Modelling: gluons

Flux Tube Models

string Hamiltonian

$$H = b_0 R + \sum_n \left[\frac{p_n^2}{2ba} + \frac{b}{2a} (y_n - y_{n+1})^2 \right]$$

$$s_{m\lambda} = \sum_n y_n(\lambda) \sqrt{\frac{2}{N+1}} \sin \frac{nm\pi}{N+1}$$

$$y_n(\lambda) = \sum_m s_{m\lambda} \sqrt{\frac{2}{N+1}} \sin \frac{nm\pi}{N+1}$$

$$H = b_0 R + \sum_{n\lambda} \left[\frac{p_n^2}{2ba} + \frac{ba}{2} \omega_n^2 s_{n\lambda}^2 \right]$$

$$\omega_n = \frac{2}{a} \sin \frac{\pi n}{2(N+1)}$$

$$\alpha_{n\lambda} = \sqrt{\frac{b_0 \omega_n}{2}} s_{n\lambda} + i \frac{p_{n\lambda}}{\sqrt{b_0 a \omega_n}}$$

$$\omega_1 \rightarrow \frac{\pi}{R}$$

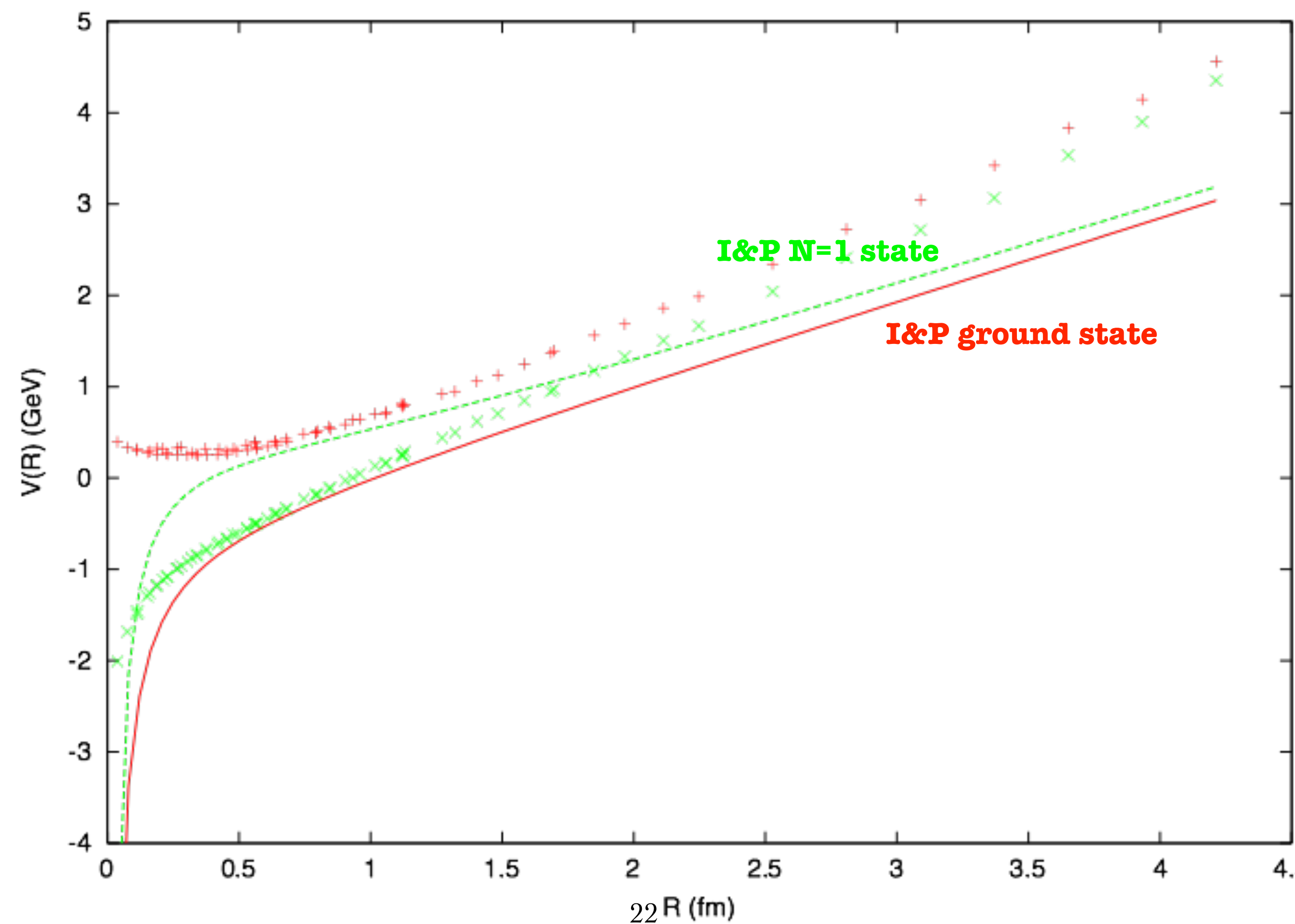
$$H = b_0 R + \sum_{n\lambda} \omega_n \left(\alpha_{n\lambda}^\dagger \alpha_{n\lambda} + \frac{1}{2} \right)$$

$$H = b_0 R + \left(\frac{4}{\pi a^2} R - \frac{1}{a} - \frac{\pi}{12R} \right) + \sum_{n\lambda} \omega_n \alpha_{n\lambda}^\dagger \alpha_{n\lambda}$$

Modelling: gluons

Flux Tube Models

compare to lattice



Modelling: gluons

Coulomb gauge QCD formalism

$$H_{QCD} = \int d^3x \left[\psi^\dagger (-i\alpha \cdot \nabla + \beta m) \psi + \frac{1}{2} (\mathcal{J}^{-1/2} \Pi \mathcal{J} \cdot \Pi \mathcal{J}^{-1/2} + B \cdot B) - g \psi^\dagger \alpha \cdot A \psi \right] + H_C$$

$$H_C = \frac{1}{2} \int d^3x d^3y \mathcal{J}^{-1/2} \rho^A(\mathbf{x}) \mathcal{J}^{1/2} \hat{K}_{AB}(\mathbf{x}, \mathbf{y}; \mathbf{A}) \mathcal{J}^{1/2} \rho^B(\mathbf{y}) \mathcal{J}^{-1/2}$$

$$\mathcal{J} \equiv \det(\nabla \cdot D)$$

$$\rho^A(\mathbf{x}) = f^{ABC} \mathbf{A}^B(\mathbf{x}) \cdot \boldsymbol{\Pi}^C(\mathbf{x}) + \psi^\dagger(\mathbf{x}) T^A \psi(\mathbf{x})$$

$$\hat{K}^{AB}(\mathbf{x}, \mathbf{y}; \mathbf{A}) \equiv \langle \mathbf{x}, A | \frac{g}{\nabla \cdot \mathbf{D}} (-\nabla^2) \frac{g}{\nabla \cdot \mathbf{D}} | \mathbf{y}, B \rangle.$$

$$D^{AB} \equiv \delta^{AB} \nabla - g f^{ABC} A^C$$

Modelling: gluons

Coulomb gauge QCD formalism

Evaluate K with the aid of a nontrivial vacuum Ansatz

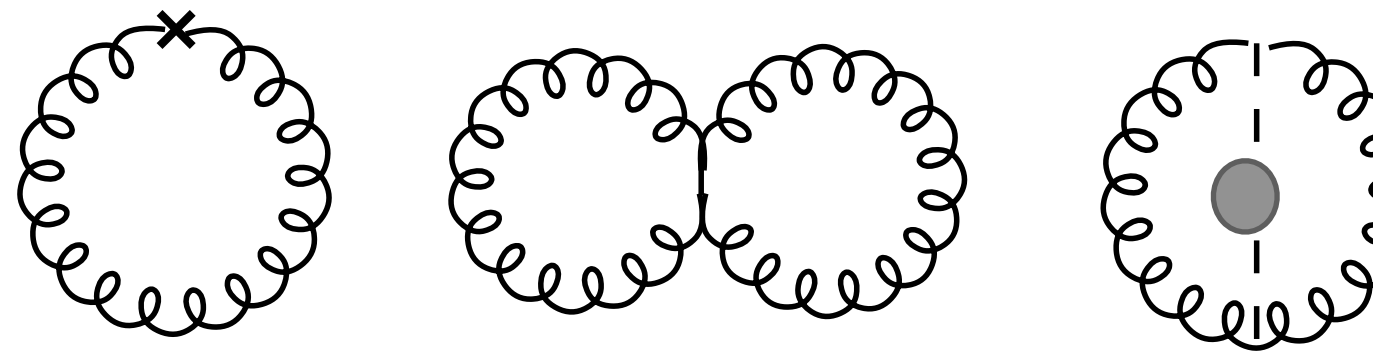
$$\langle A | \omega \rangle = \Psi_0[A] = \exp \left[-\frac{1}{2} \int \frac{d^3 k}{(2\pi)^3} A^a(k) \omega(k) A^a(-k) \right]$$

Obtain ω by solving the gap equation

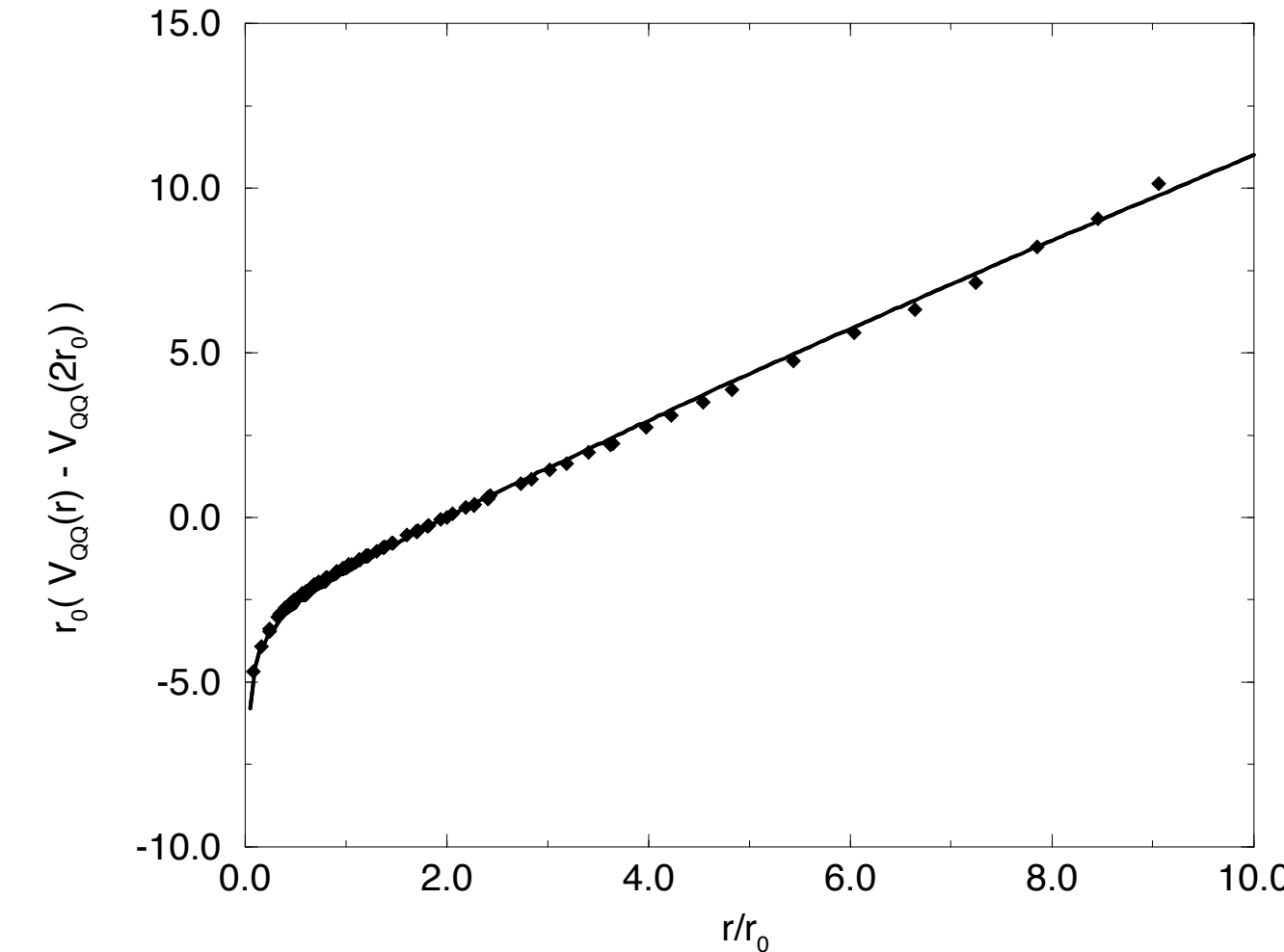
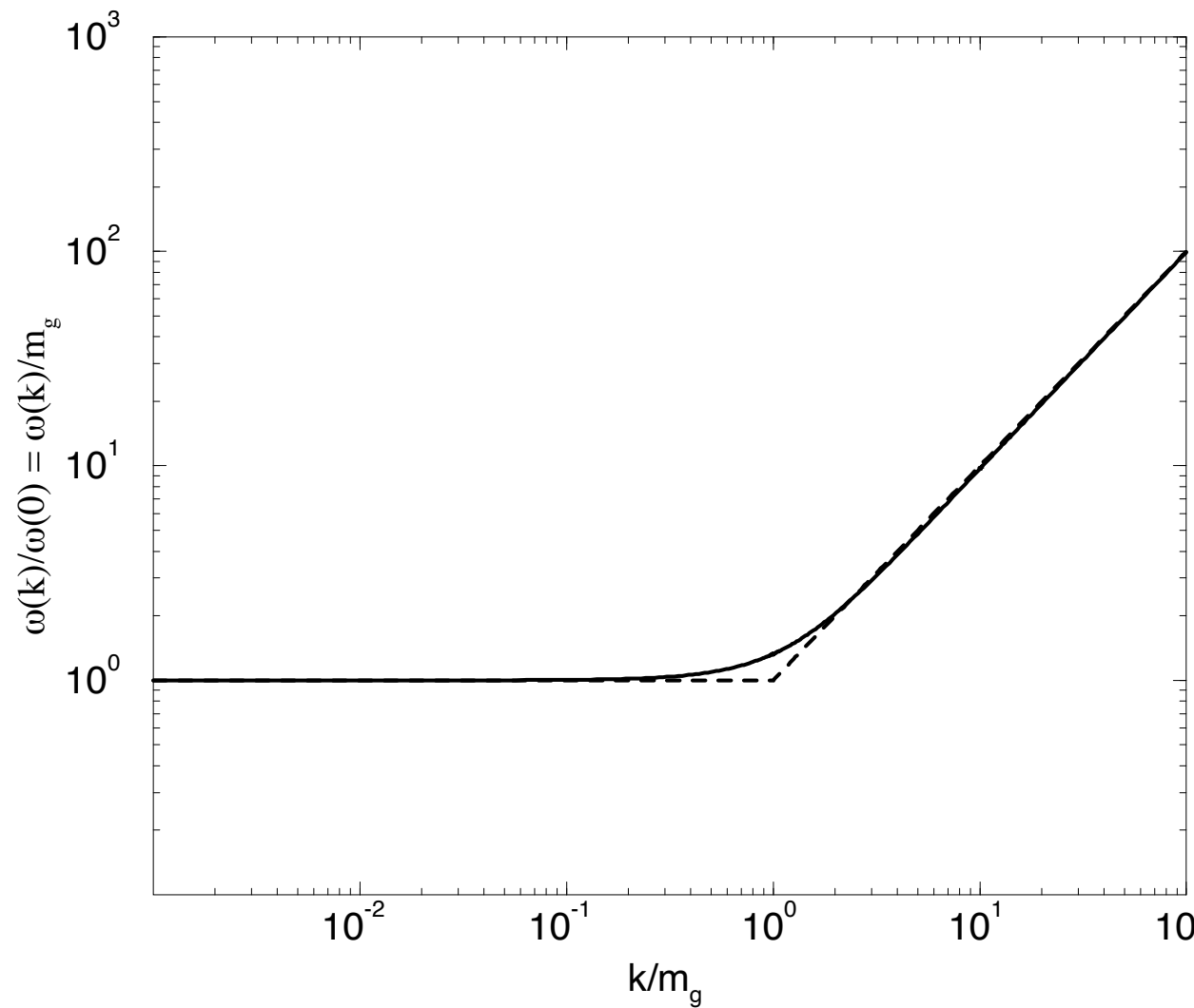
$$\frac{\delta}{\delta \omega} \langle \omega | H | \omega \rangle = 0$$

Modelling: gluons

Coulomb gauge QCD formalism



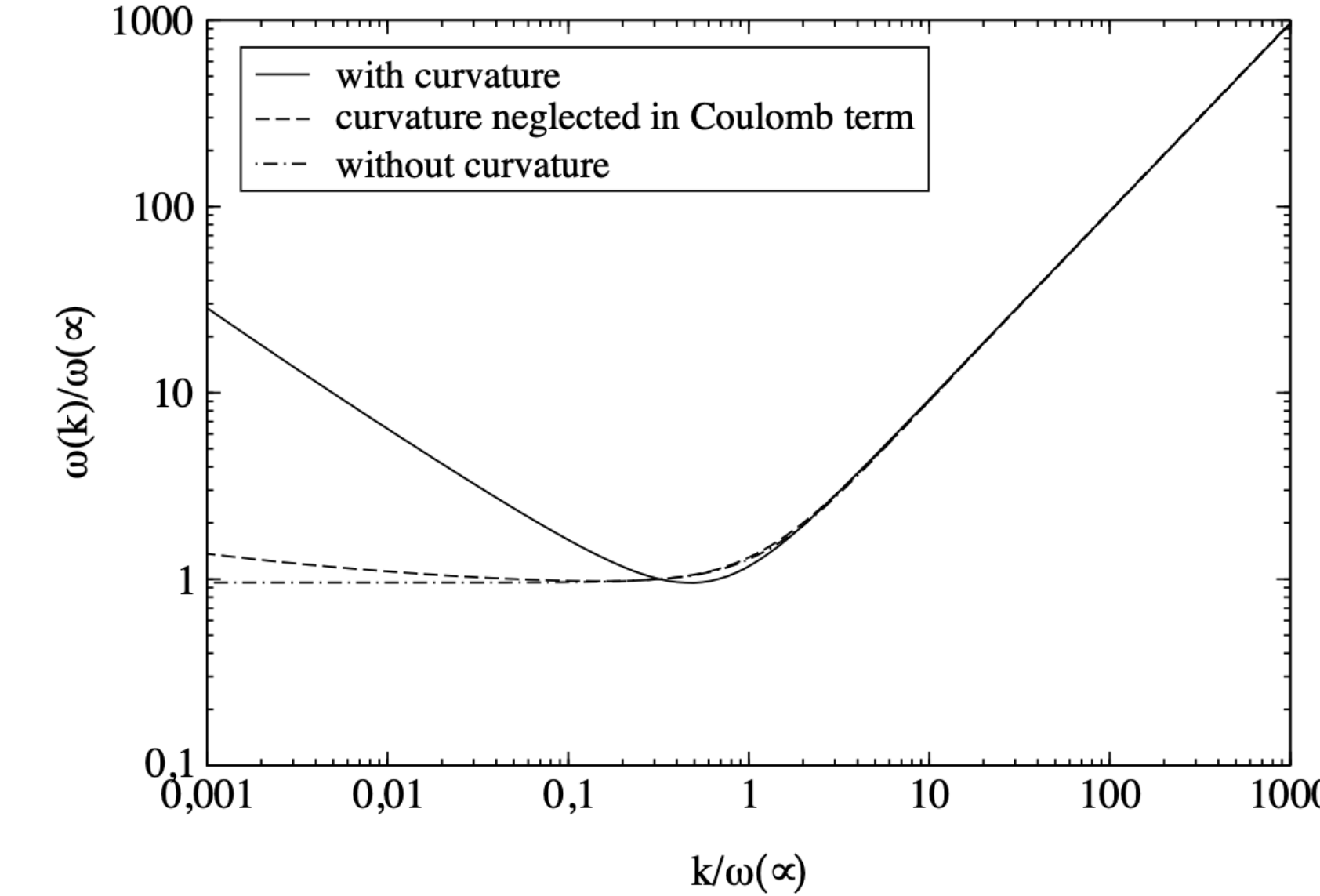
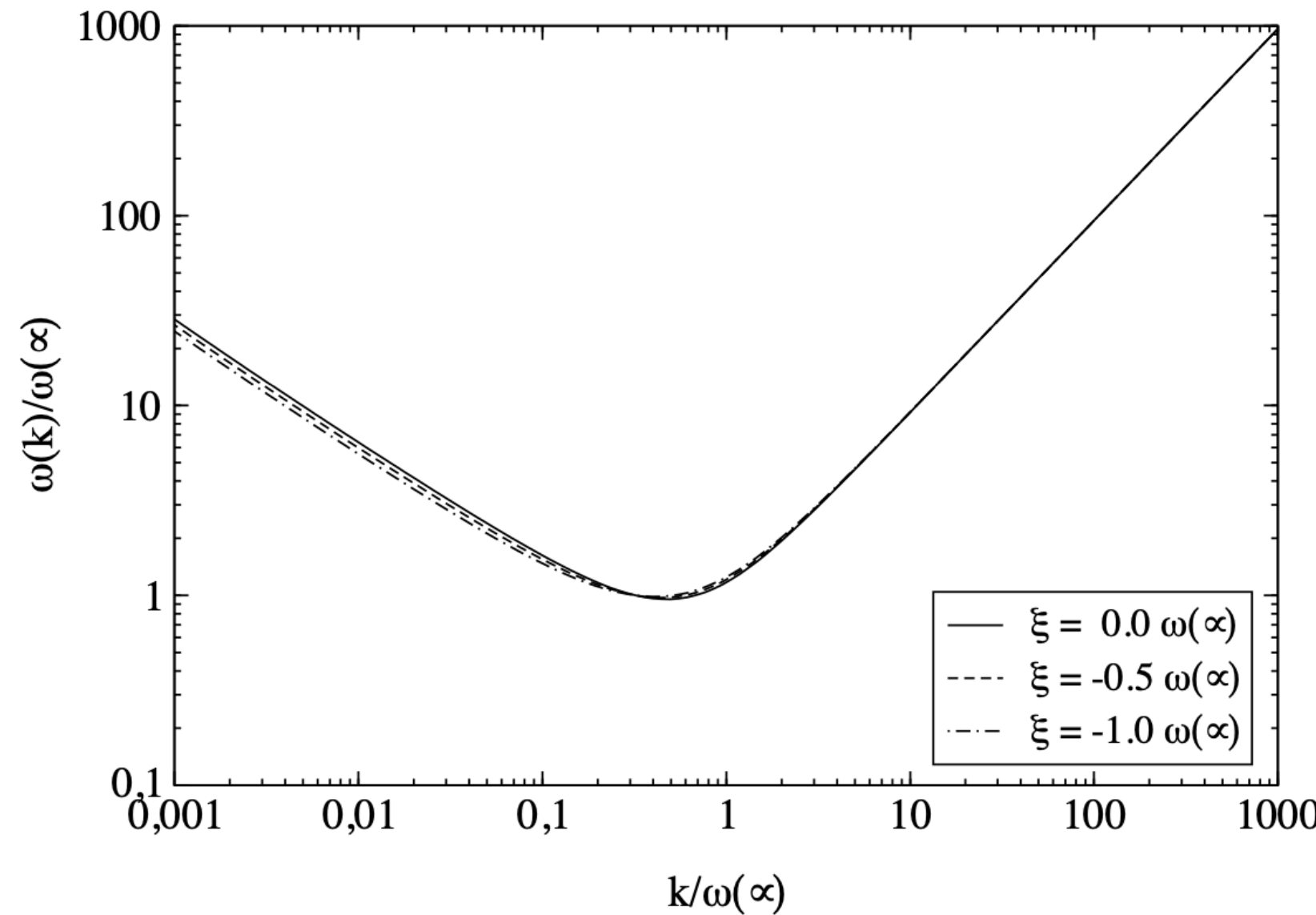
$$\begin{aligned}
 Z_\Pi^2(\Lambda)\omega^2(q; \Lambda) &= Z_A^2(\Lambda)q^2 + Z_m(\Lambda)\Lambda^2 + g^2(\Lambda)\frac{N_c}{4} \int^\Lambda \frac{d\mathbf{k}}{(2\pi)^3} \frac{(3 - (\hat{\mathbf{k}} \cdot \hat{\mathbf{q}})^2)}{\omega(k; \Lambda)} + \\
 &+ \frac{N_c}{4} \int^\Lambda \frac{d\mathbf{k}}{(2\pi)^3} K^{(0)}(\mathbf{k} + \mathbf{q}; \mathbf{A}) (1 + (\hat{\mathbf{k}} \cdot \hat{\mathbf{q}})^2) \frac{\omega^2(k; \Lambda) - \omega^2(q; \Lambda)}{\omega(k; \Lambda)}
 \end{aligned}$$



Modelling: gluons

Coulomb gauge QCD formalism

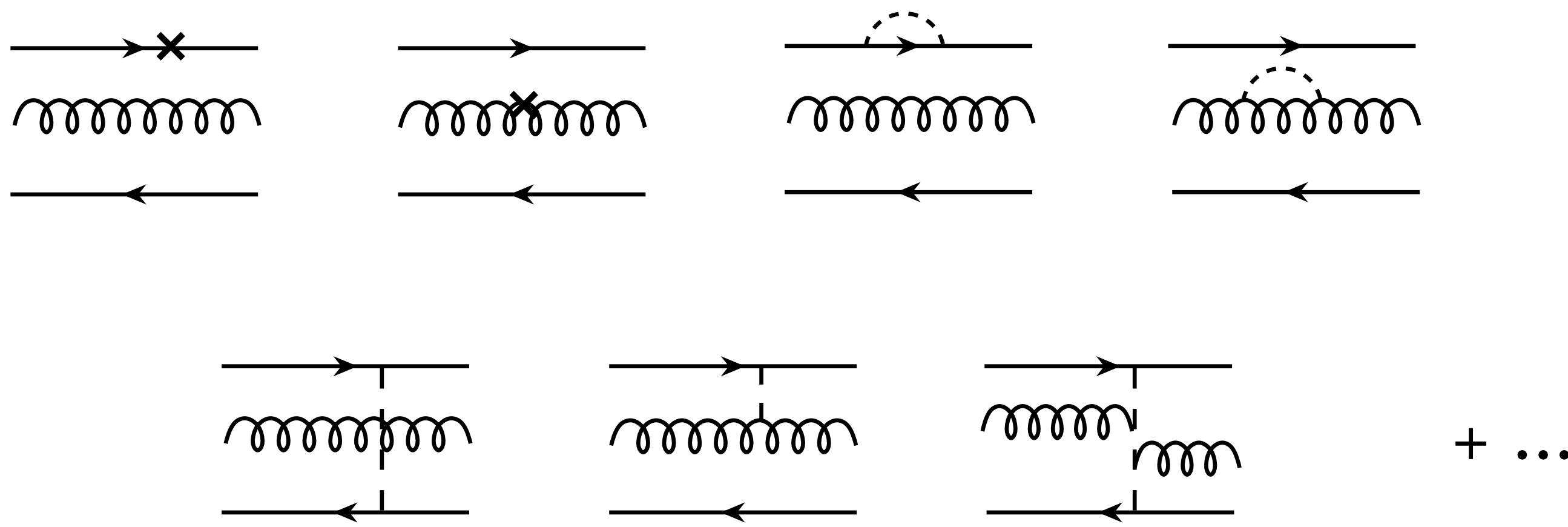
$$\tilde{\Psi}[A] = \langle A | \omega \rangle = \mathcal{N} \exp \left[-\frac{1}{2} \int d^3x \int d^3x' A_i^{\perp a}(\mathbf{x}) \omega(\mathbf{x}, \mathbf{x}') A_i^{\perp a}(\mathbf{x}') \right]$$
$$\Psi[A] = \mathcal{J}^{-\frac{1}{2}}[A] \tilde{\Psi}[A]$$



Variational solution of the Yang-Mills Schrödinger equation in Coulomb gauge,
C. Feuchter & H. Reinhardt, hep-th/0408236.

Modelling: gluons

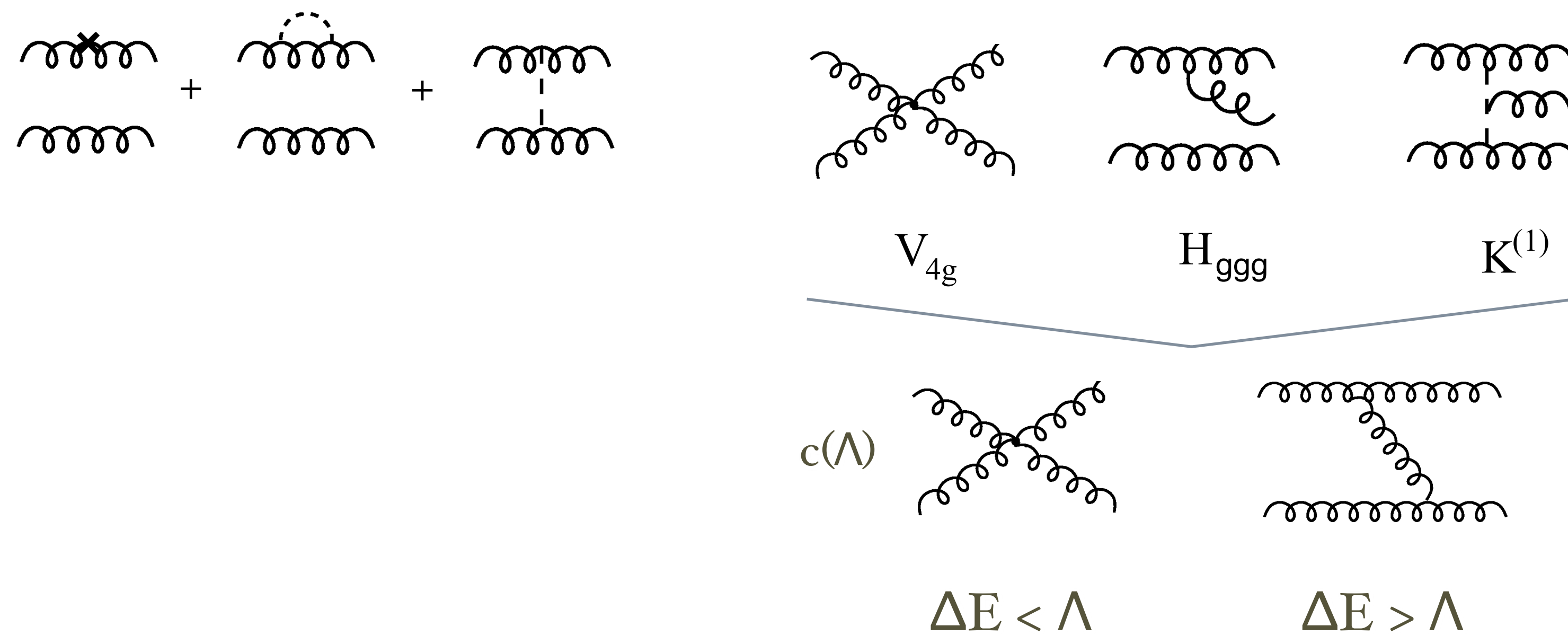
Coulomb gauge QCD formalism | Hybrids



$$\begin{aligned}
 |JM[LS\ell j_g\xi]\rangle &= \frac{1}{2}T_{ij}^A \int \frac{d^3q}{(2\pi)^3} \frac{d^3k}{(2\pi)^3} \Psi_{j_g;\ell m_\ell}(\mathbf{k}, \mathbf{q}) \sqrt{\frac{2j_g + 1}{4\pi}} D_{m_g \mu}^{j_g *}(\hat{k}) \chi_{\mu, \lambda}^{(\xi)} \\
 &\times \left\langle \frac{1}{2}m \frac{1}{2}\bar{m} |SM_S \right\rangle \langle \ell m_\ell, j_g m_g |LM_L \rangle \langle SM_S, LM_L |JM \rangle b_{\mathbf{q} - \frac{\mathbf{k}}{2}, i, m}^\dagger d_{-\mathbf{q} - \frac{\mathbf{k}}{2}, j, \bar{m}}^\dagger a_{\mathbf{k}, A, \lambda}^\dagger |0\rangle.
 \end{aligned}$$

Modelling: gluons

Coulomb gauge QCD formalism | Glueballs



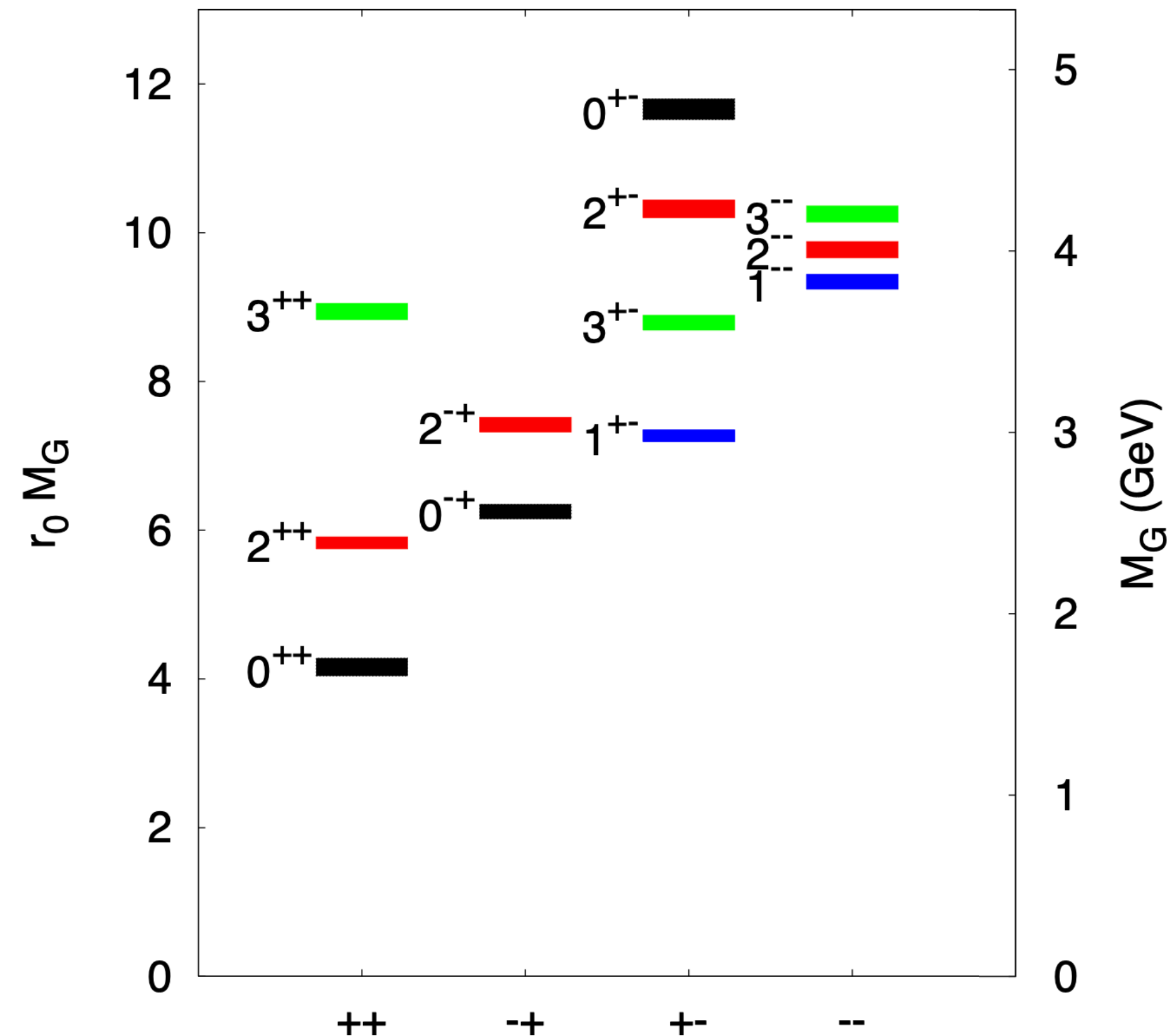
$$|JM; \lambda, \lambda'\rangle = \frac{1}{\sqrt{2(N_c^2 - 1)}} \sqrt{\frac{2J+1}{4\pi}} \int \frac{d^3k}{(2\pi)^3} \psi(k) D_{M,\lambda-\lambda'}^{J*}(\phi, \theta, -\phi) \Pi a^\dagger(k, \lambda, A) a^\dagger(-k, \lambda, A) |0\rangle$$

$$|JM; \eta\rangle = \frac{1}{\sqrt{2}} (|JM; \lambda, \lambda'\rangle + \eta |JM; -\lambda, -\lambda'\rangle)$$

Modelling: gluons



glueballs à la lattice

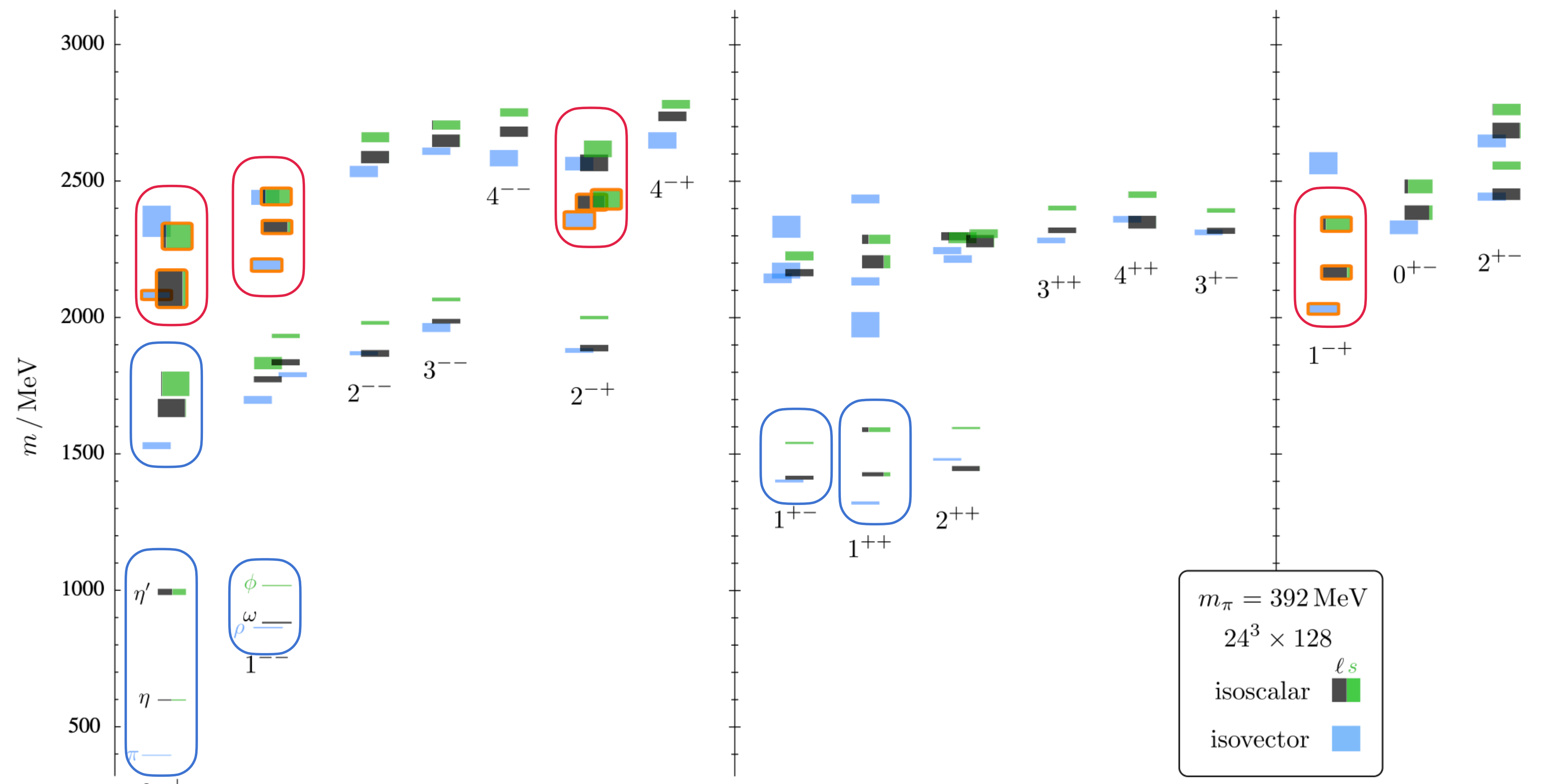


Modelling: gluons



hybrids à la lattice

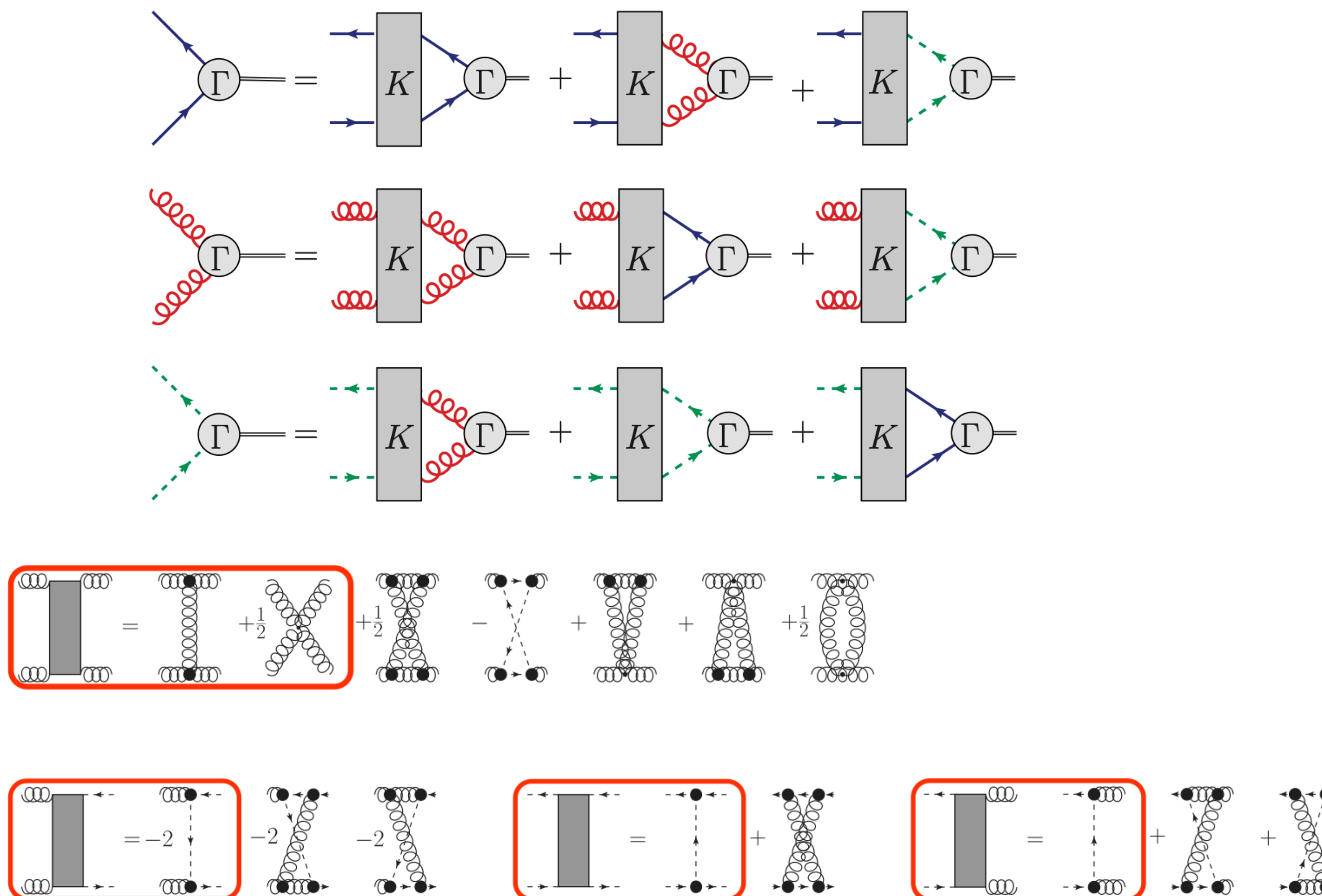
11



Toward the excited isoscalar meson spectrum from lattice QCD,
[HadSpec] J.J. Dudek et al. Phys.Rev.D 88 (2013) 9, 094505.

Modelling: gluons

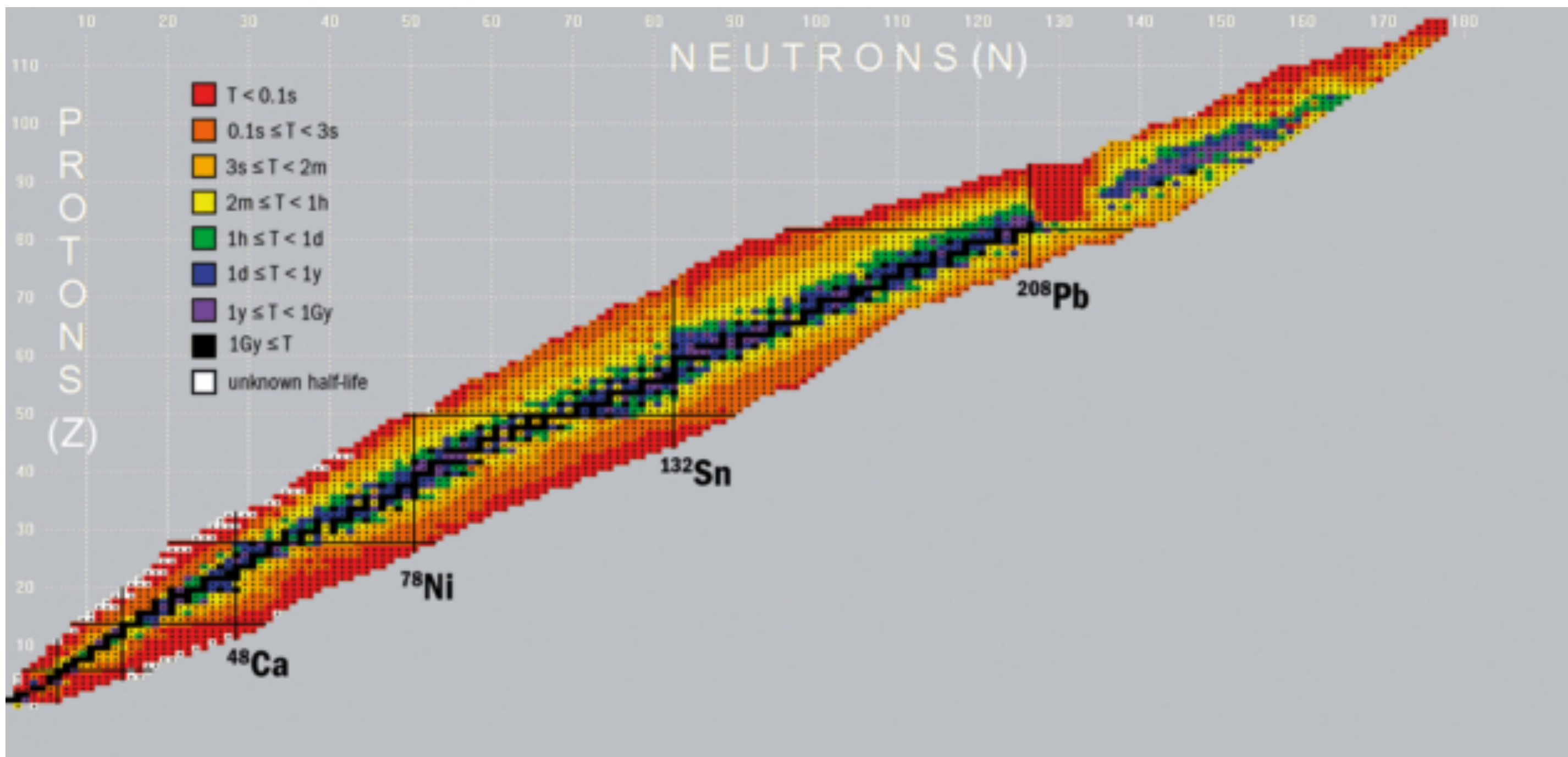
Bethe-Salpeter formalism



multiquarks

$$|M\rangle = |q\bar{q}\rangle + |q\bar{q}g\rangle + \boxed{|q\bar{q}q\bar{q}\rangle} + \dots$$

There are a lot of multiquarks!



Multi-quark States



“Vi har nu en model, der på smukke ste vis forklarer data og for første gang indeholder alle de begrænsninger, data giver,” sagde fysikeren Tim Burns fra Swansea University ved offentliggørelsen.

Multi-electron States

1946: Wheeler suggests that Ps_2 might be bound

[Wheeler, J. A. Polyelectrons. Ann. NY Acad. Sci. 48, 219–238 \(1946\).](#)

1946: Ore proves it is unbound

1947: Hylleraas & Ore prove it is bound

[Hylleraas, E. A. & Ore, A. Binding energy of the positronium molecule. Phys. Rev. 71, 493–496 \(1947\).](#)

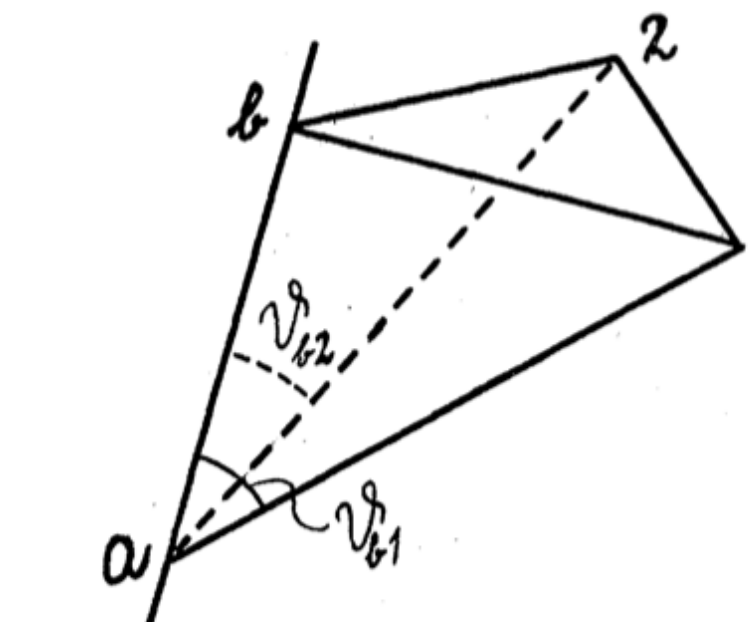


FIG. 1. Coordinate system for the positronium molecule.

2007: Ps_2 is observed

[Cassidy, D.B.; Mills, A.P. \(Jr.\) \(2007\). "The production of molecular positronium". Nature 449 \(7159\): 195–197](#)

Multi-quarks through the ages

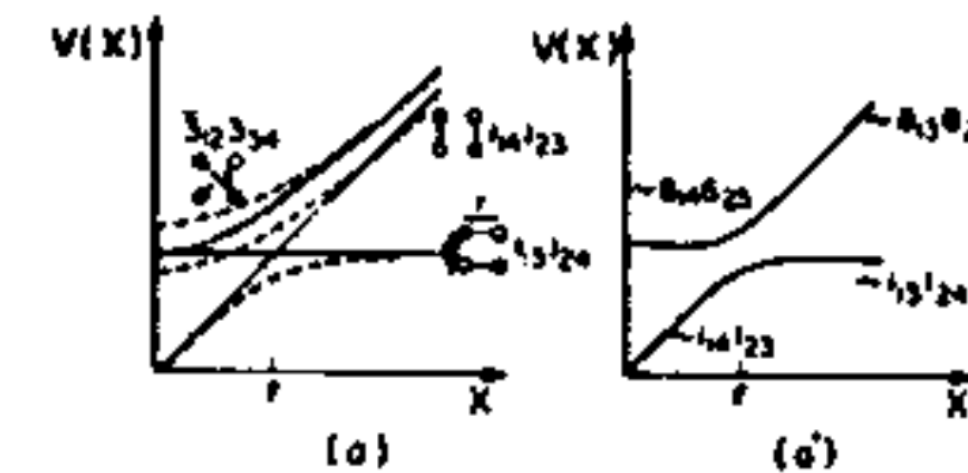
B. The Multiquark Fiasco

Multiquark physics has a somewhat unfortunate history. A confluence of dubious experimental results and dubious theoretical models in the late 1970's and early 1980's created, indeed, a multiquark fiasco. I am not competent to discuss what went wrong experimentally, but let me review the theoretical side of this fiasco in order to place it in perspective and thereby, I hope, point the way toward a better understanding of multiquark systems.

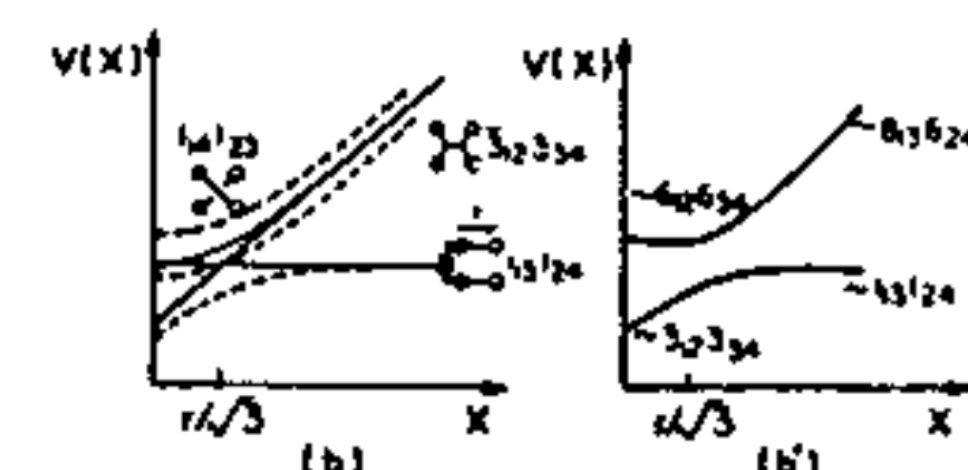
The story is basically one of throwing caution to the winds. Modelers from at least four different camps were, it seems to me, guilty:



UIPT-85-18
March, 1985

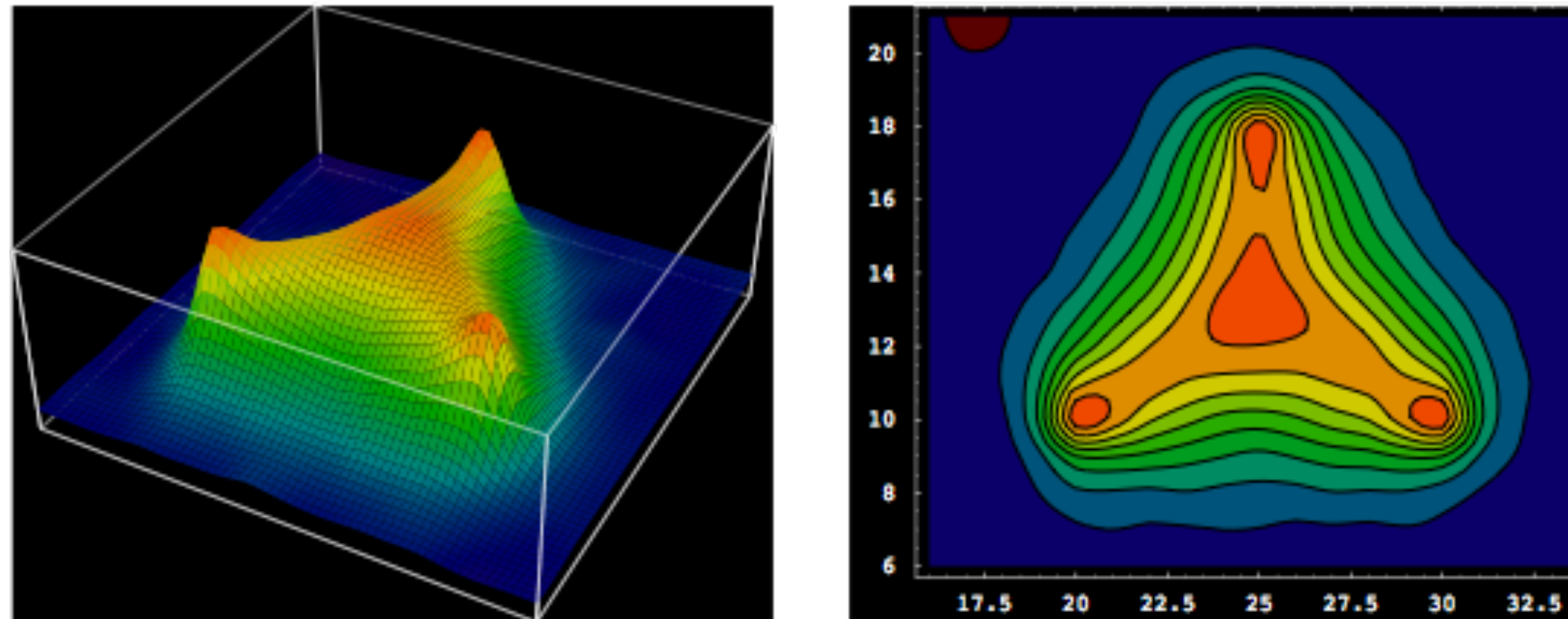
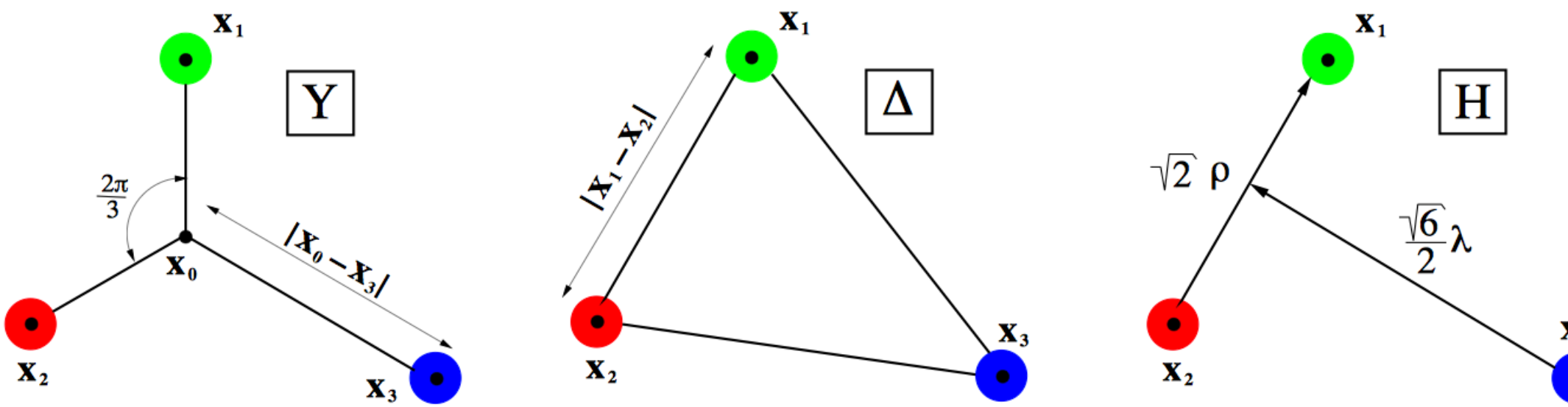


(a)



(b)

What is the interaction?

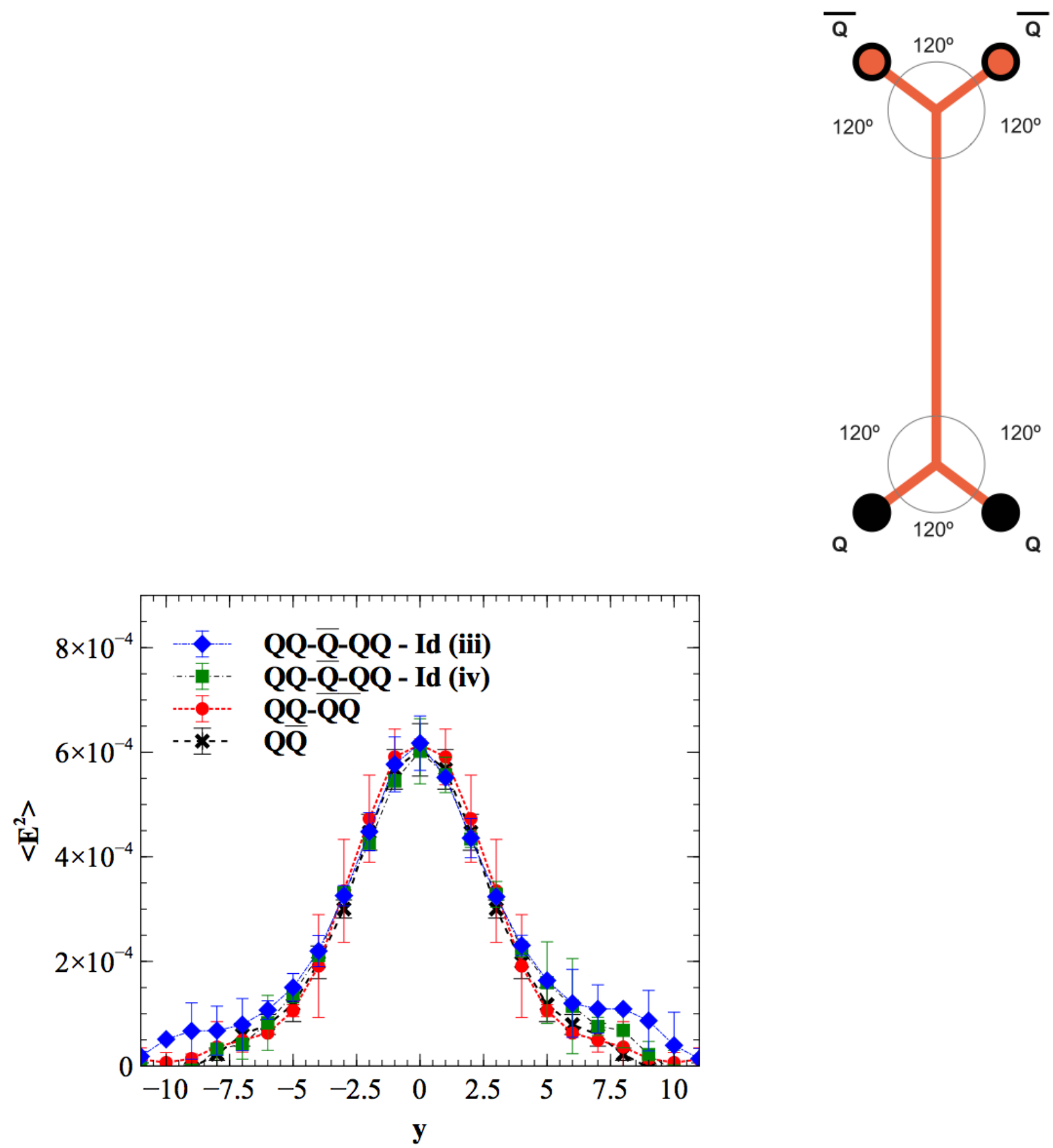


H. Ichie, V. Bornyakov, T. Streuer and G. Schierholz, “The flux distribution of the three quark system in SU(3)”, arXiv:hep-lat/0212024.

C. Alexandrou, P. De Forcrand and A. Tsapalis, Phys. Rev. D 65, 054503 (2002).

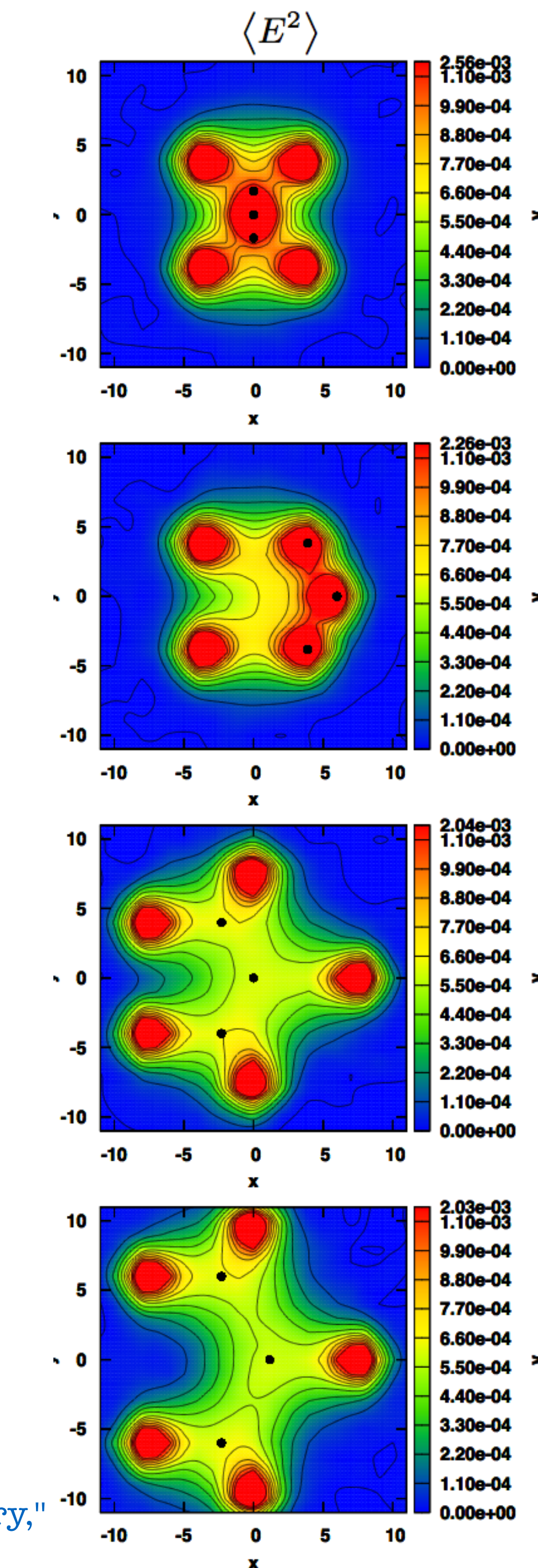
T. T. Takahashi, H. Suganuma, Y. Nemoto and H. Matsufuru, Phys. Rev. D 65, 114509 (2002).

What is the interaction?



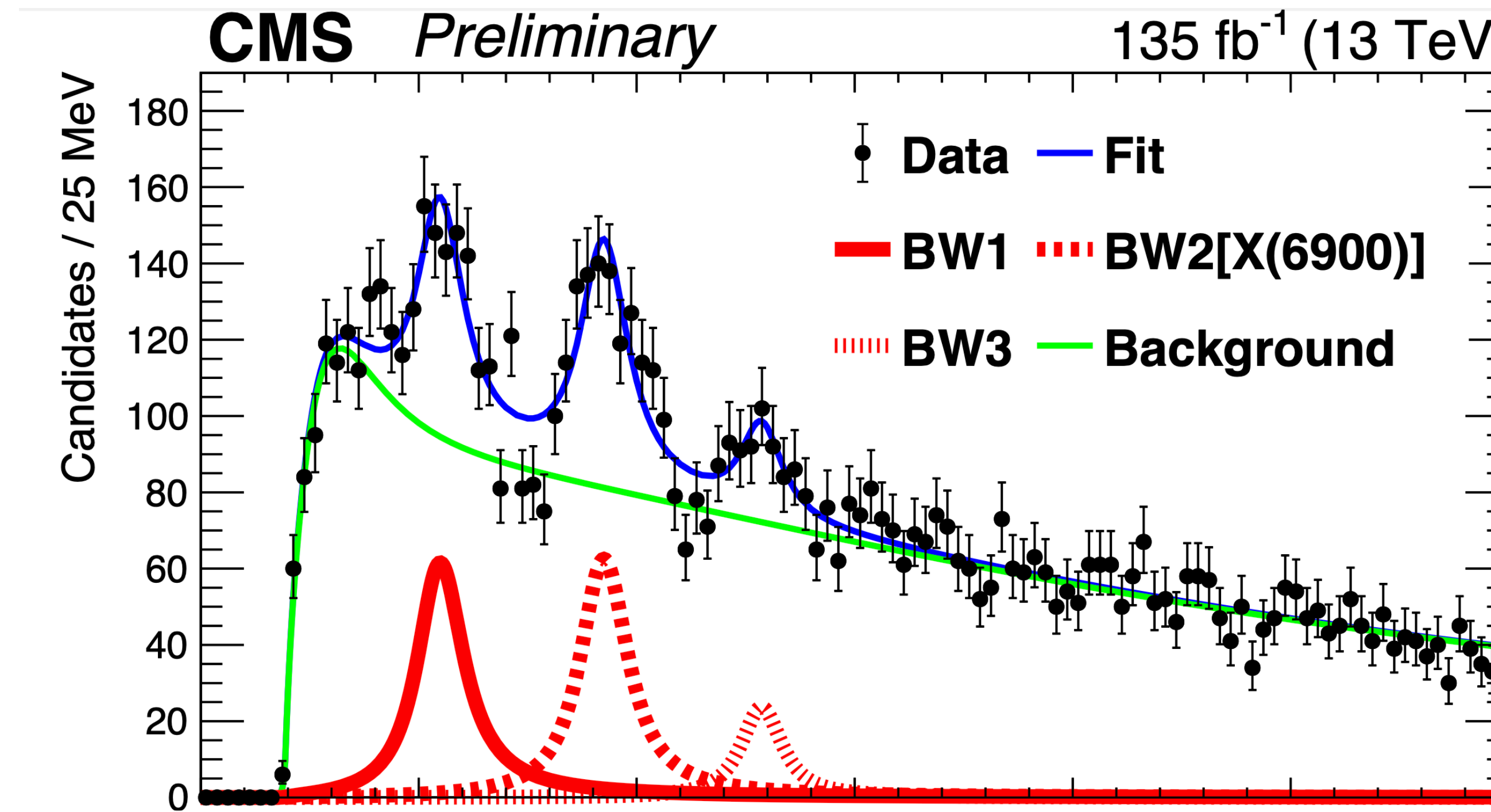
N. Cardoso and P. Bicudo,
 ``Color fields of the static pentaquark system computed in SU(3) lattice QCD,"
 Phys. Rev. D {87}, no. 3, 034504 (2013)

S. Furui, A.M. Green and B. Masud,
 ``An analysis of four quark energies in SU(2) lattice Monte Carlo using the flux tube symmetry,"
 Nucl. Phys. A {582}, 682 (1995)



an example application

Multiquark Exotics $cc\bar{c}\bar{c}$



<https://cds.cern.ch/record/2815336>

An Example Problem

A simple nonrelativistic constituent model

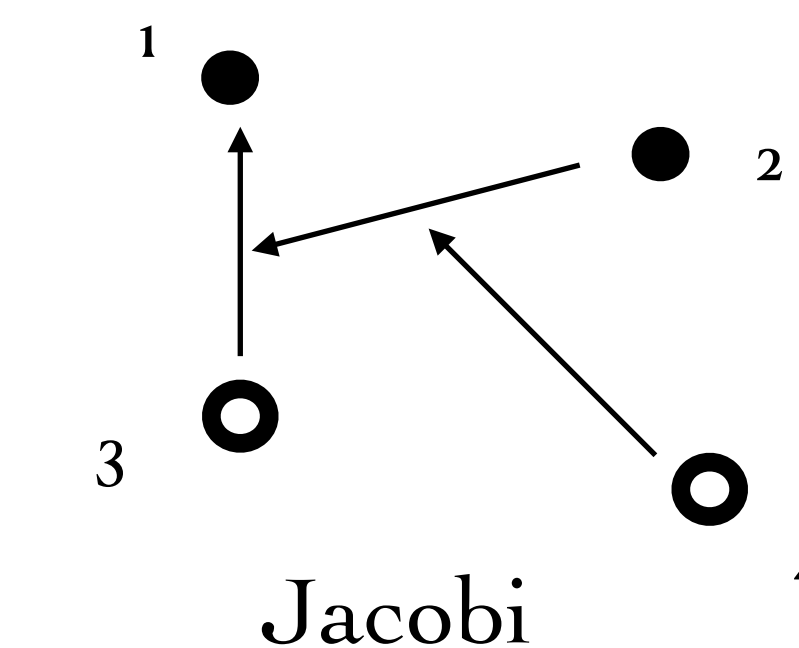
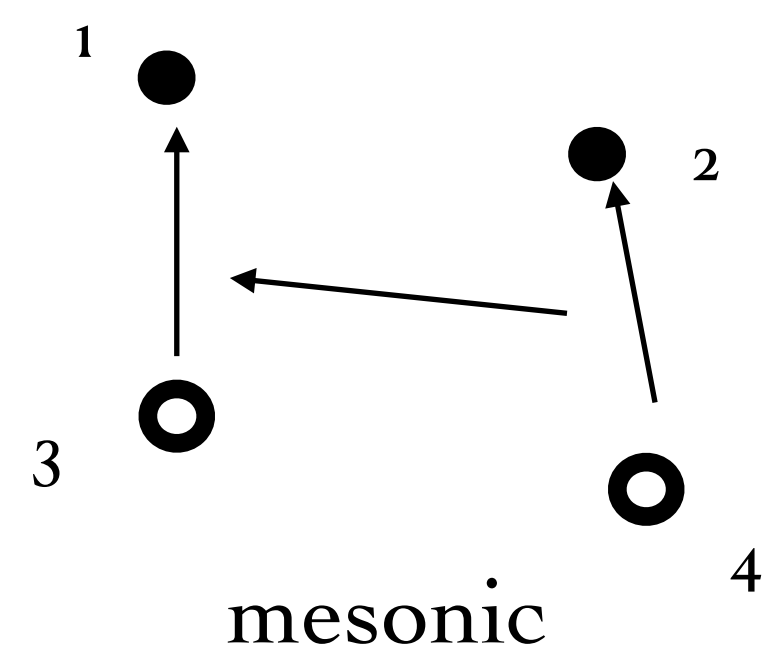
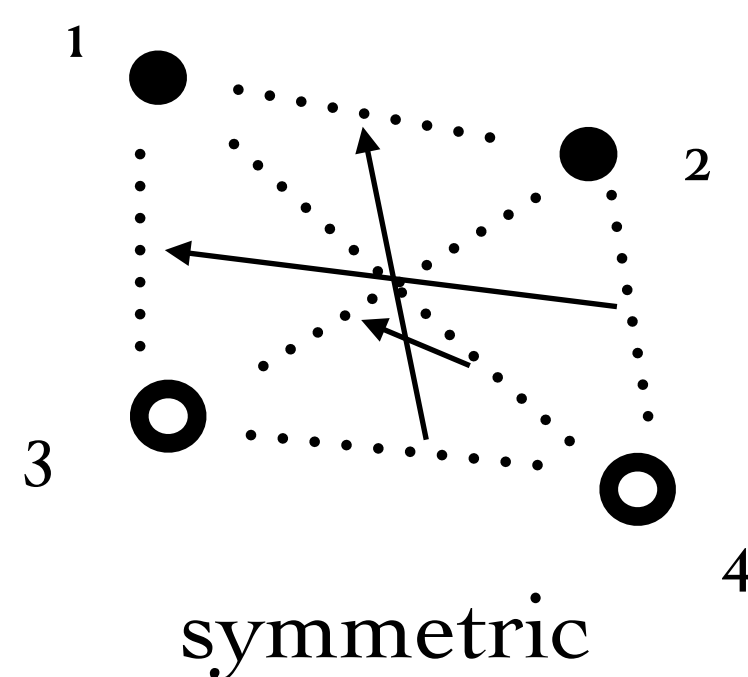
$$H = - \sum_{i=1}^4 \frac{\nabla_i^2}{2m_i} + \frac{1}{2}k \sum_{i < j} r_{ij}^2 \vec{\lambda}_i \cdot \vec{\lambda}_j$$



Possible colour states:

$$|1_{13}1_{24}\rangle, |1_{23}1_{14}\rangle \quad \text{or} \quad |\bar{3}3\rangle, |6\bar{6}\rangle \quad \text{or} \quad |1_{13}1_{24}\rangle, |8_{13}8_{24}\rangle.$$

Possible coordinate systems:



An Example Problem

Symmetric-3/6 form:

$$H = -\frac{1}{2}(\nabla_x^2 + \nabla_y^2 + \nabla_z^2) \cdot \begin{pmatrix} 1 & 0 \\ 0 & 1 \end{pmatrix} + \frac{\kappa}{2} \begin{pmatrix} 2x^2 + 2y^2 + \frac{4}{3}z^2 & -\sqrt{2}(x^2 - y^2) \\ -\sqrt{2}(x^2 - y^2) & x^2 + y^2 + \frac{10}{3}z^2 \end{pmatrix}$$

How does one solve this problem?

[We would like as full a spectrum as possible, including possible resonances.]

Computational Methods

Variational Resonating Group

J.A. Wheeler, PR52, 1107 (1937)

T. Kato, Prog Theor Phys 6, 394 (1951); L. Hulthen, Ark Mat Astr Fys A35, 25, (1948).

$$\psi = \sum_{c,I,S,\alpha,\beta} \mathcal{C}_c \phi_I \chi_S \psi_\alpha(\rho_1, \lambda_1) \psi_\beta(\rho_2, \lambda_2) F_{cIS\alpha\beta}(R)$$

$$\mathcal{L}u_L = \left(\frac{d^2}{dR^2} - \frac{L(L+1)}{R^2} + k^2 \right) u_L + \int W^{(L)}(R, R') u_L(R') dR' = 0$$

$$\delta \left(S_L + \frac{i}{2k} \int u_L \mathcal{L}u_L \right) = 0$$

$$u_L = \sum_i c_i \begin{cases} \gamma_i \chi_i^{(L)}, & R < R_c \\ kR[h_L^{(-)}(kR) + s_i h_L^{(+)}(kR)], & R > R_c \end{cases}$$

Computational Methods

Variational Resonating Group

Vary wrt the c_i to obtain

$$\sum_j \mathcal{M}_{ij} c_j = \mathcal{M}_i$$

$$\mathcal{M}_{ij} = K_{ij} - K_{i0} - K_{0j} + K_{00} \quad \mathcal{M}_j = K_{00} - K_{j0} \quad K_{ij} = \int \phi_i \mathcal{L}_L(\phi_j) dR$$

$$K_{ij} = \gamma_i \gamma_j \left[\int_0^{R_c} \chi_i(R) \left(\frac{d^2}{dR^2} - \frac{L(L+1)}{R^2} + k^2 \right) \chi_j(R) dR + \int_0^\infty \int_0^\infty \chi_i(R) W^{(L)}(R, R') \chi_j(R') dR dR' \right]$$

Choose the $\chi_i^{(L)}$ such that all integrals can be done analytically. Solve the linear equations, evaluate the functional at the stationary point, and obtain S.

Computational Methods

Lanczos Algorithm

1. Let $v_1 \in \mathbb{C}^n$ be an arbitrary vector with Euclidean norm 1.
2. Abbreviated initial iteration step:
 1. Let $w'_1 = Av_1$.
 2. Let $\alpha_1 = w'^*_1 v_1$.
 3. Let $w_1 = w'_1 - \alpha_1 v_1$.
3. For $j = 2, \dots, m$ do:
 1. Let $\beta_j = \|w_{j-1}\|$ (also Euclidean norm).
 2. If $\beta_j \neq 0$, then let $v_j = w_{j-1}/\beta_j$,
else pick as v_j an arbitrary vector with Euclidean norm 1 that is orthogonal to all of v_1, \dots, v_{j-1}
 3. Let $w'_j = Av_j$.
 4. Let $\alpha_j = w'^*_j v_j$.
 5. Let $w_j = w'_j - \alpha_j v_j - \beta_j v_{j-1}$.
4. Let V be the matrix with columns v_1, \dots, v_m . Let $T =$

$$\begin{pmatrix} \alpha_1 & \beta_2 & & & & 0 \\ \beta_2 & \alpha_2 & \beta_3 & & & \\ \beta_3 & \alpha_3 & \ddots & & & \\ \ddots & \ddots & \ddots & \beta_{m-1} & & \\ & & \beta_{m-1} & \alpha_{m-1} & \beta_m & \\ 0 & & \beta_m & \alpha_m & & \end{pmatrix}.$$

[work with a discrete (grid) basis ->
simple to evaluate $H|\varphi\rangle!$]

[overcomes stability problems(!)]

Computational Methods

Lanczos Algorithm

Hydrogen naive 3d approach

```
./BoxHydrogen -N 320 -x 14      [33M x 33M !!]
[slow convergence in Lanczos iterations...]

295: -0.4990305889 -0.1245724433 -0.0326180510
296: -0.4990305889 -0.1245748623 -0.0327418135
297: -0.4990305889 -0.1245771746 -0.0328625434
298: -0.4990305889 -0.1245793873 -0.0329804546
299: -0.4990305889 -0.1245815035 -0.0330955698
```

Helium naive 6d Cartesian discretization

```
./BoxHeliumC -N 26 -x 12      (309M^2)

37: -1.9144083947 -1.4707632674 -1.3666560990
38: -1.9144083947 -1.4707925755 -1.3677339189
39: -1.9144083947 -1.4708129613 -1.3686194909
```

run into trouble as we need a larger grid

Computational Methods

Guided Random Walks

T. Barnes, G.J. Daniell ,and D.Storey, Nucl. Phys. B₂₆₅ [FS15] (1986) 253.

T. Barnes and E.S. Swanson, PRB₃₇, 9405 (1988)

T. Barnes, F.E. Close, E.S Swanson, PRD₅₂, 5242 (1995)

A simple and more direct version of the Greens function quantum Monte Carlo method, leveraging the mapping between random walks and the Euclidean time Schrödinger equation

Computational Methods

Guided Random Walks

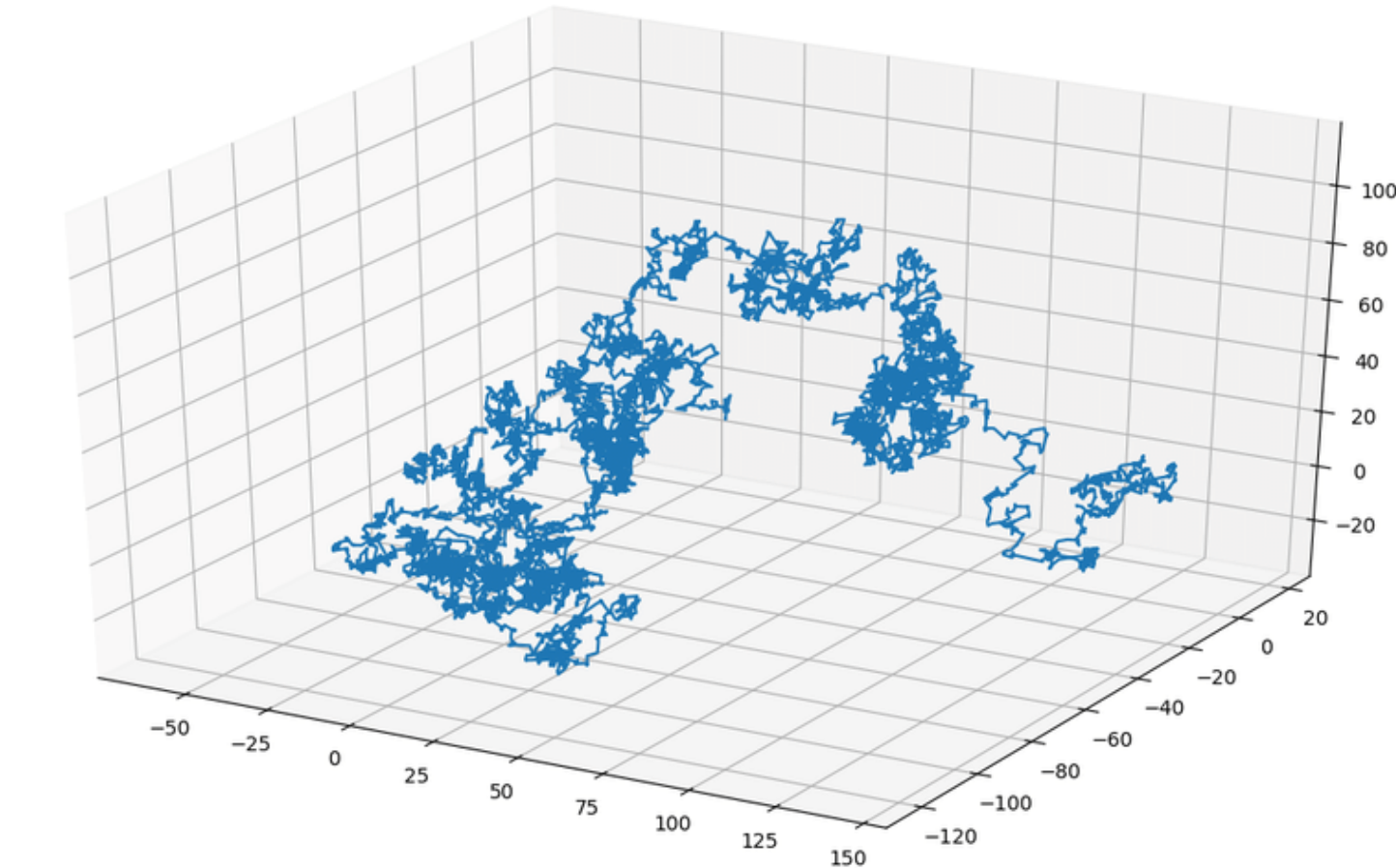
$$-\dot{\psi}(x') = \langle x' | H\psi | x' \rangle = \langle x' | H_0 | x' \rangle \psi(x') + \sum_{x \neq x'} \langle x' | H_I | x \rangle \psi(x)$$

Associate a weight with each walk

$$w(\tau) = \exp[- \int_0^\tau a(\tau) d\tau] .$$

$$-\dot{Q}(x', \tau) = \left[\sum_{x \neq x'} r(x, x') + a(\tau) \right] Q(x', \tau) - \sum_{x \neq x'} r(x, x') Q(x, \tau)$$

Walk to large Euclidian time and extract the energy.



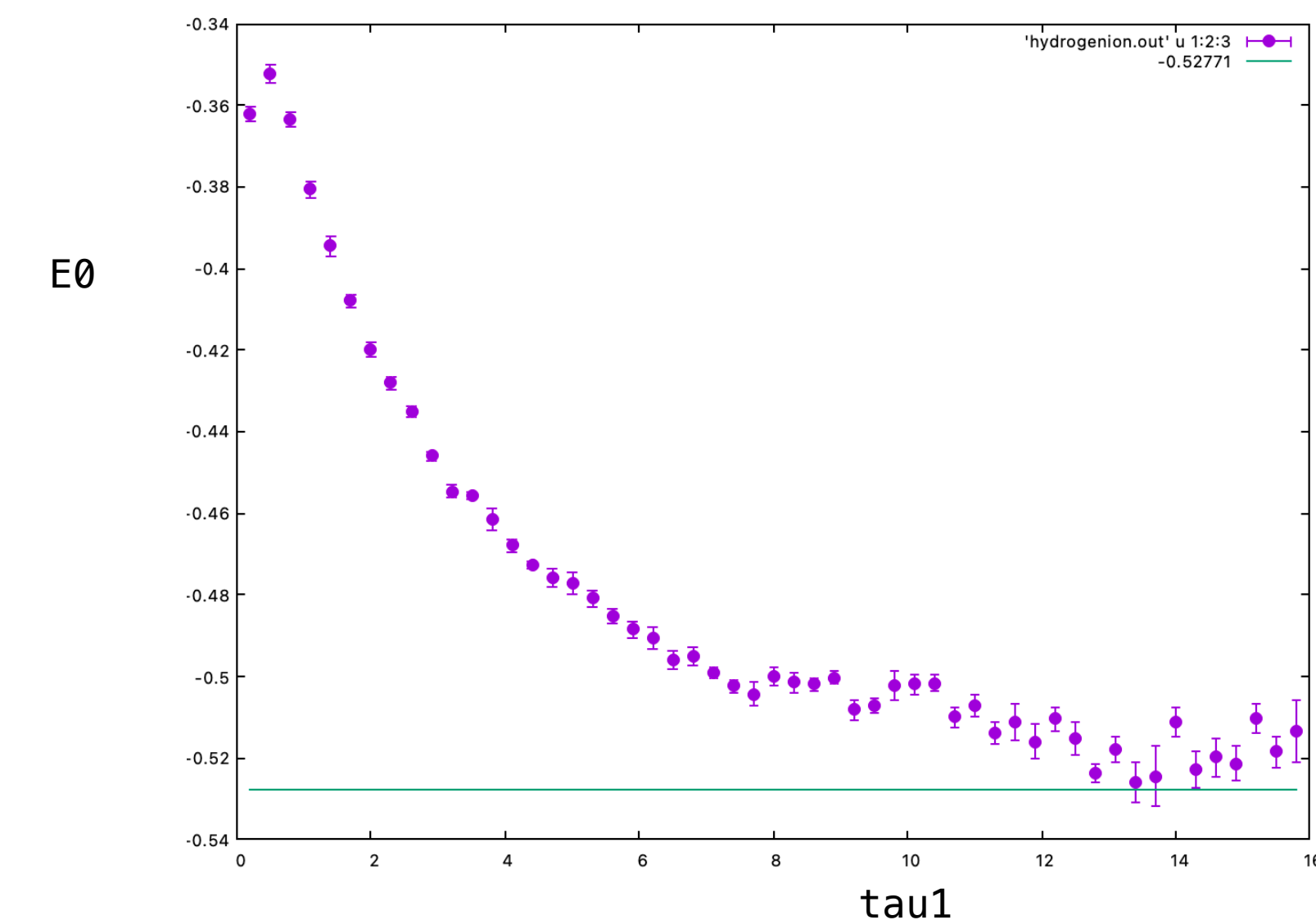
$$r(x \rightarrow x') = - \langle x' | H_I | x \rangle \frac{\varphi(x')}{\varphi(x)}$$

$$w_{trans} = \prod_{x \rightarrow x'} \left[- \frac{\langle x' | H_I | x \rangle}{r(x, x')} \right]$$

Computational Methods

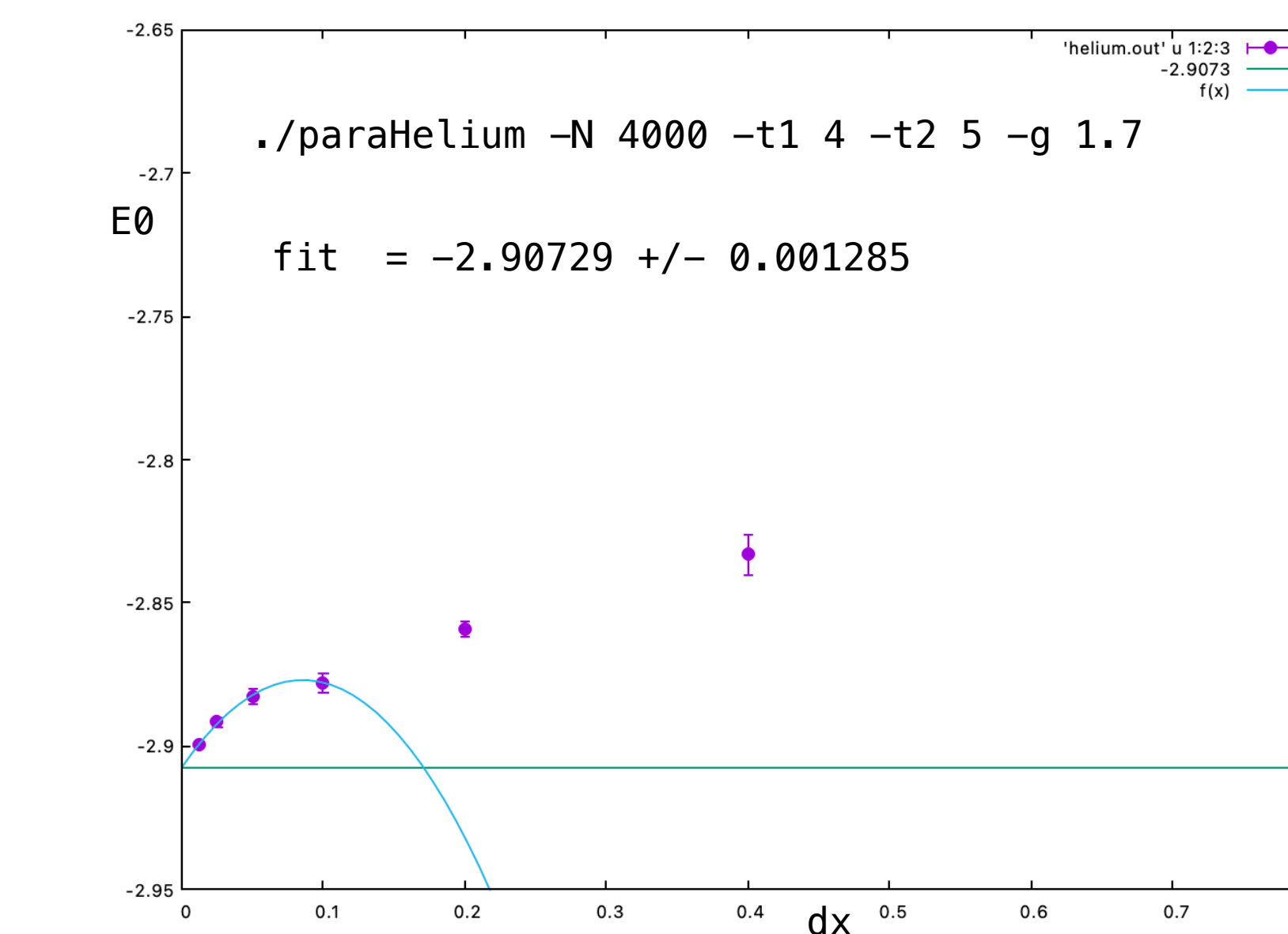
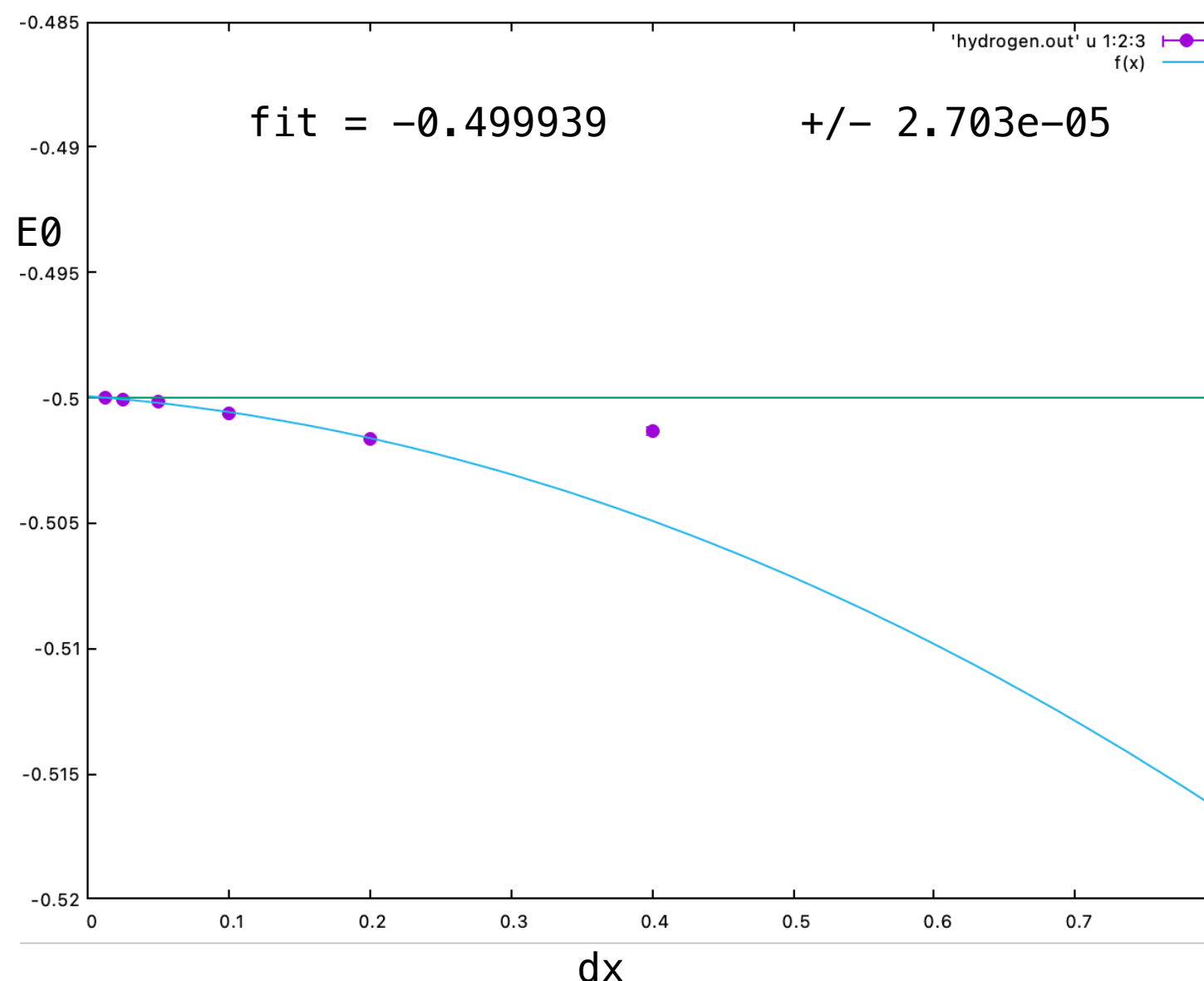
Guided Random Walks

hydrogen ion



hydrogen

para helium, $E_0 = -2.9073$



Computational Methods

Guided Random Walks

Ps2

```
SWANSONE@PHYAST-LWQG1H7VT0 GRW % time ./Ps2 -N 9000 -g .4 -t1 14 -t2 15 -d .1  
-0.51502 +/- 0.00903268  
. ./Ps2 -N 9000 -g .4 -t1 14 -t2 15 -d .1 317.81s user 0.28s system 688% cpu 46.204 total  
  
SWANSONE@PHYAST-LWQG1H7VT0 GRW % time ./Ps2 -N 9000 -g .4 -t1 14 -t2 15 -d .05  
-0.520122 +/- 0.0102292  
. ./Ps2 -N 9000 -g .4 -t1 14 -t2 15 -d .05 1273.68s user 1.35s system 715% cpu 2:58.29 total  
  
SWANSONE@PHYAST-LWQG1H7VT0 GRW % time ./Ps2 -N 9000 -g .4 -t1 14 -t2 15 -d .025  
-0.513579 +/- 0.00678113  
. ./Ps2 -N 9000 -g .4 -t1 14 -t2 15 -d .025 4996.82s user 11.28s system 735% cpu 11:21.18 total
```

Computational Methods

Variational

Once again, the grid is our friend

$$E_0 \sim \sum_{iC} |\psi_{iC}|^2 \cdot \left[\sum_{C'} V_i^{CC'} \frac{\psi_{iC'}}{\psi_{iC}} + \frac{2}{2m\delta^2} - \frac{1}{2m\delta^2} \frac{\psi_{i+1C}}{\psi_{iC}} - \frac{1}{2m\delta^2} \frac{\psi_{i-1C}}{\psi_{iC}} \right]$$

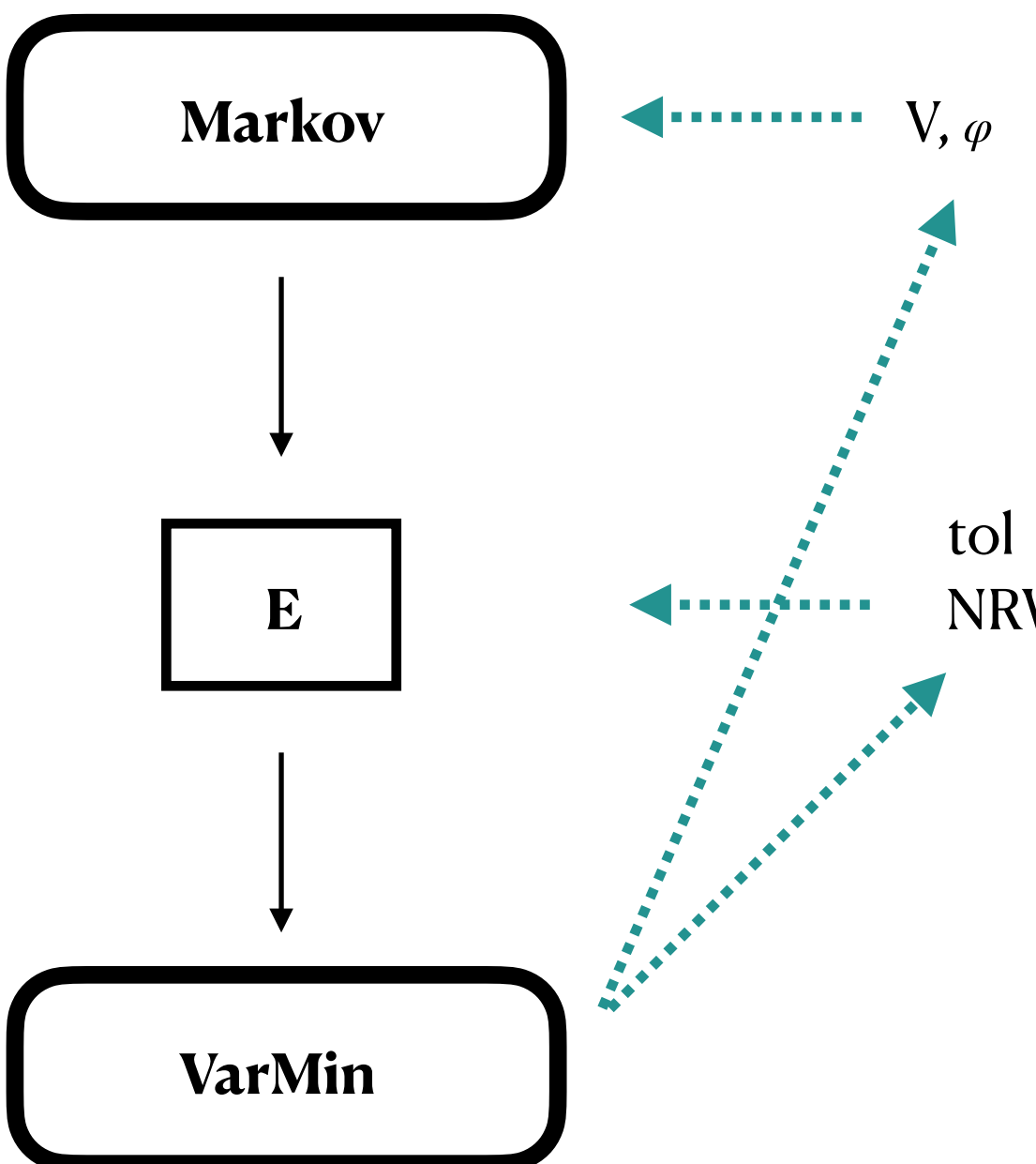
- evaluate with adaptive parallelized MCMC
- minimize the Ansatz with a variety of schemes (simulated annealing -> simplex walk -> differential evolution)
- minimizing a function with errors? -> adjust MCMC statistics as required as the minimum is approached
- user interface requires V and the Ansatz

Computational Methods

Variational

Ps2

Eo[Suzuki]=-0.51600



```
VAR % ./Ps2Var
fcn eval time (ms): 102

test eval -0.494706
*** resetting NRW to 40000 [0.0728424 | 0.00226158]
quick scan: -0.500108 +/- 0.00185215
params: 0.52 0.07
number of function evaluations: 80

*** resetting NRW to 40000 [0.138703 | 0.00438151]
anneal: -0.500108 +/- 0.00185215
params: 0.52 0.07
number of function evaluations: 401

*** resetting NRW to 40000 [0.14088 | 0.00377591]
diff evo: -0.499023 +/- 0.00129373
params: 0.517881 0.0758662
number of function evaluations: 79

*** resetting NRW to 40000 [0.247881 | 0.00477687]
simplex: -0.499023 +/- 0.00129373
params: 0.517881 0.0758662
number of function evaluations: 6

final min: -0.499023 +/- 0.00129373

high stats estimate -0.500641 +/- 0.000200992 << 3%
```

Computational Methods

Complex Scaling

The idea:

"complexify" coordinates:

$$U(\theta)rU^\dagger(\theta) = r \exp(i\theta)$$

$$U(\theta)pU^\dagger(\theta) = p \exp(-i\theta)$$

to reveal poles of the Schrödinger equation

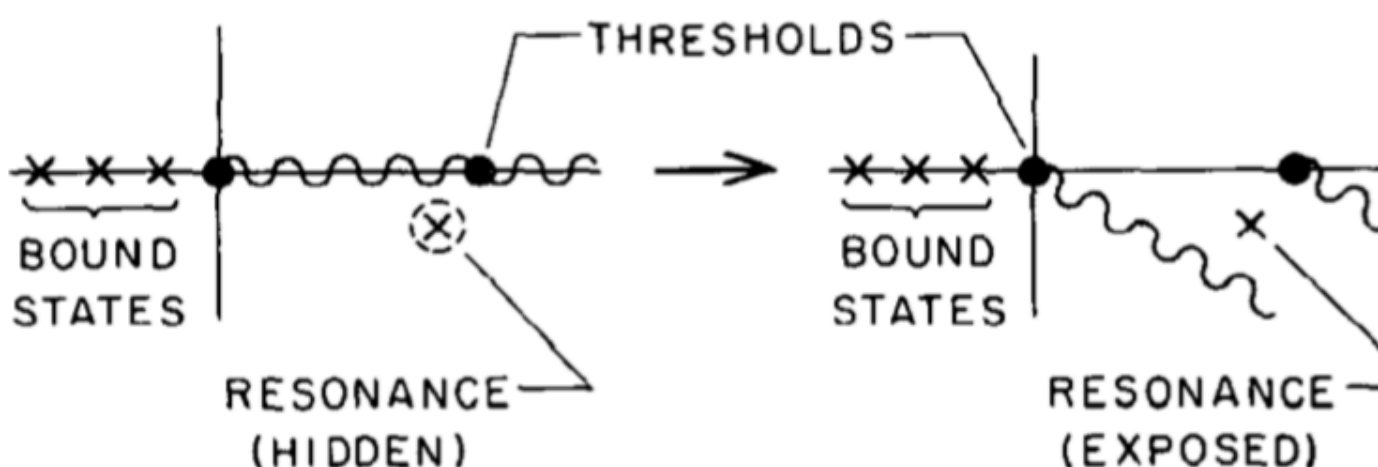
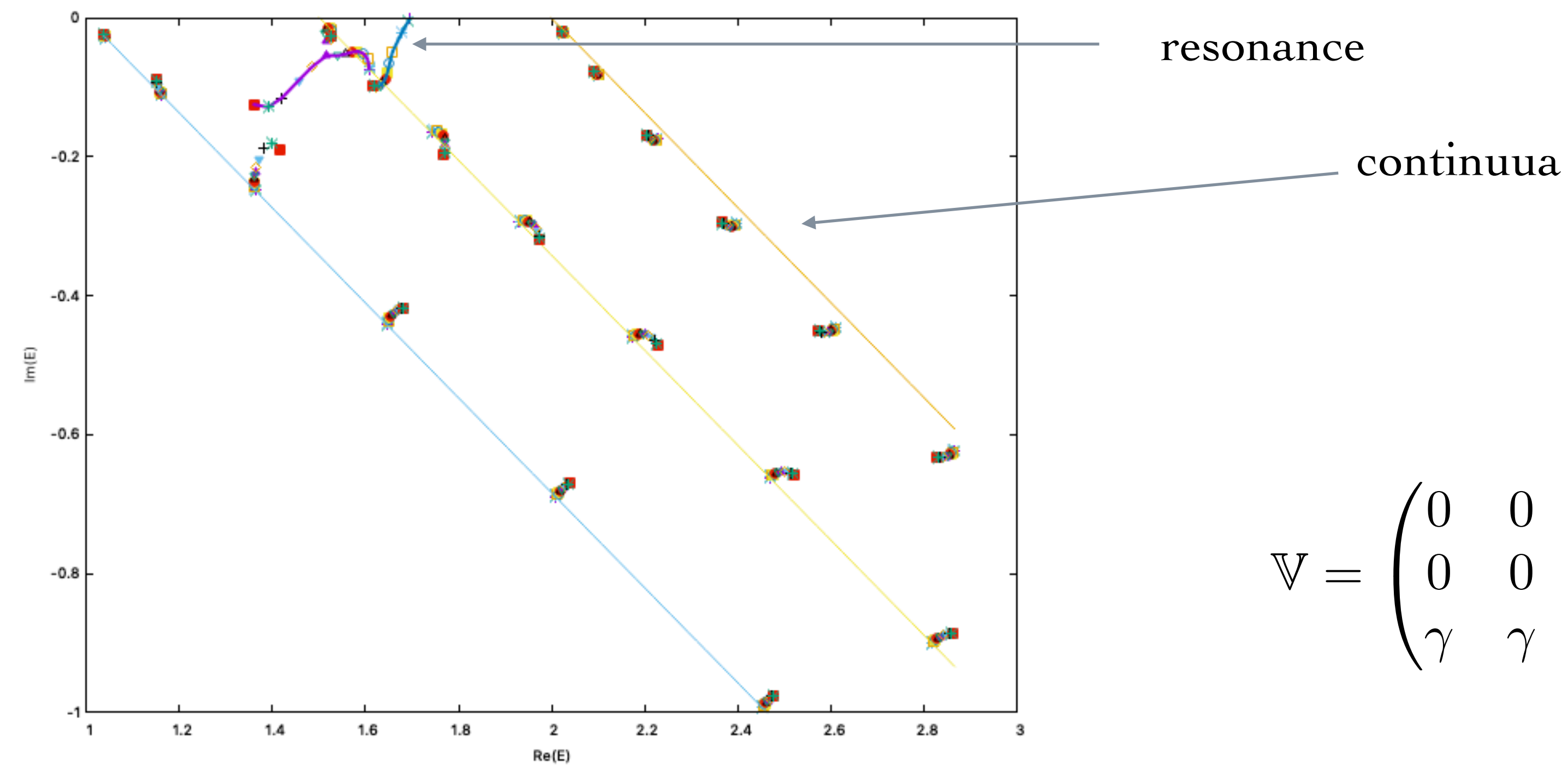


Figure 3 Effect of dilatation transformation on a many-body Hamiltonian. Again bound states and thresholds are invariant. However, as the continua rotate, complex resonance eigenvalues may be exposed. Such eigenvalues correspond to poles of the rcsolvent $R_\phi(z)$, but are "hidden" on a higher sheet if $\theta=0$, and will be exposed if the cuts are appropriately moved.

Computational Methods

Complex Scaling

Ex. Poles in a three-channel model

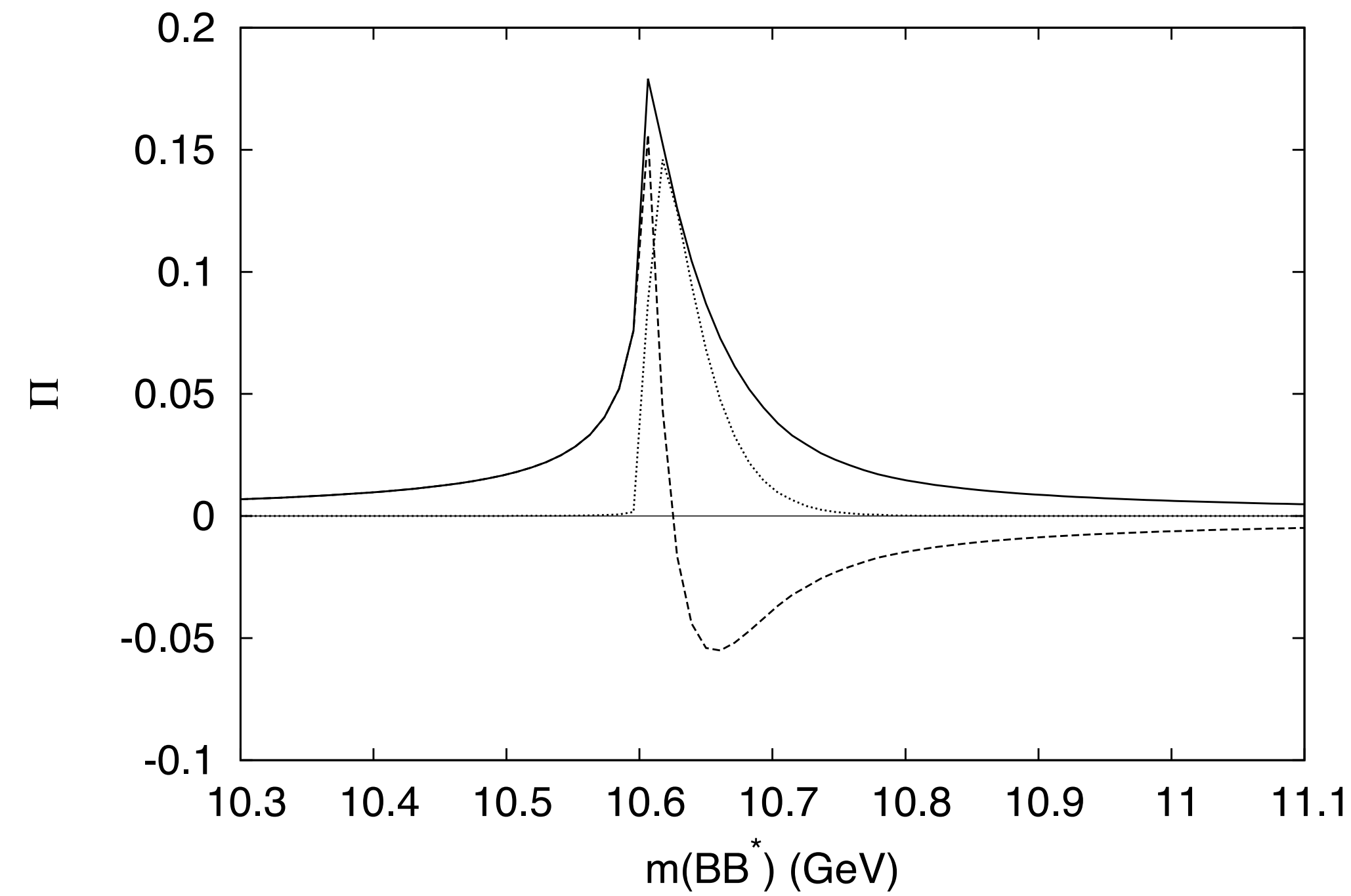
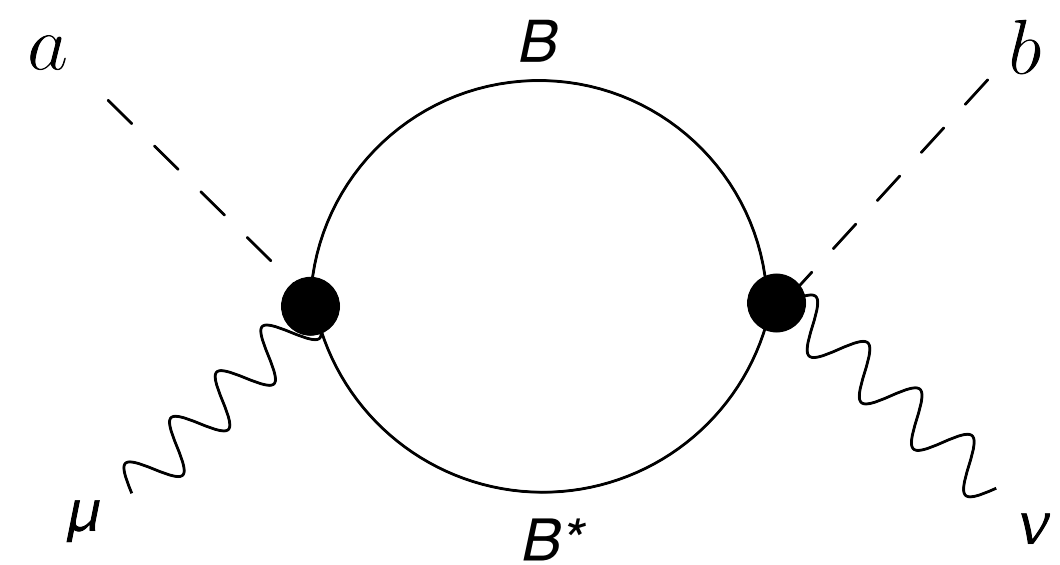


$$\mathbb{V} = \begin{pmatrix} 0 & 0 & \gamma \\ 0 & 0 & \gamma \\ \gamma & \gamma & -1.8 \end{pmatrix}$$

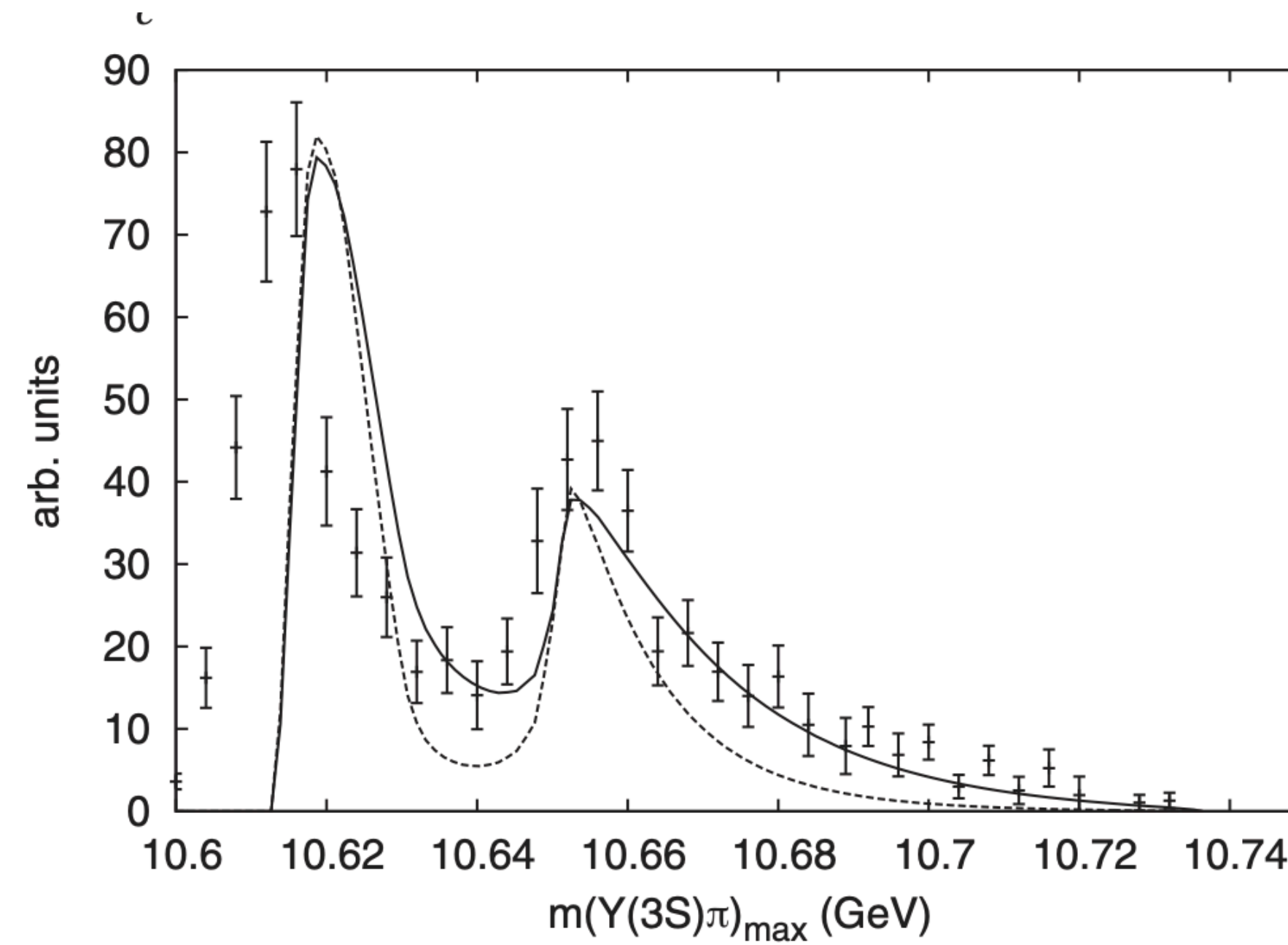
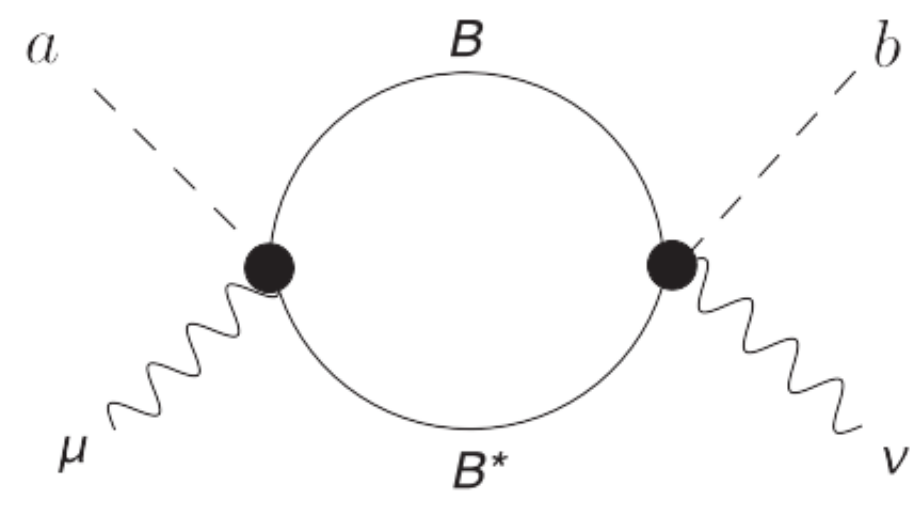
Real Scaling, System-in-a-box, Luescher,...

other things that can happen

Loop diagrams can have sharp features



$\Upsilon(5s) \rightarrow \Upsilon(3S)\pi\pi$



Swanson, PRD91 034009 (2015)

$$Y \rightarrow \pi\pi J/\psi(h_c)$$

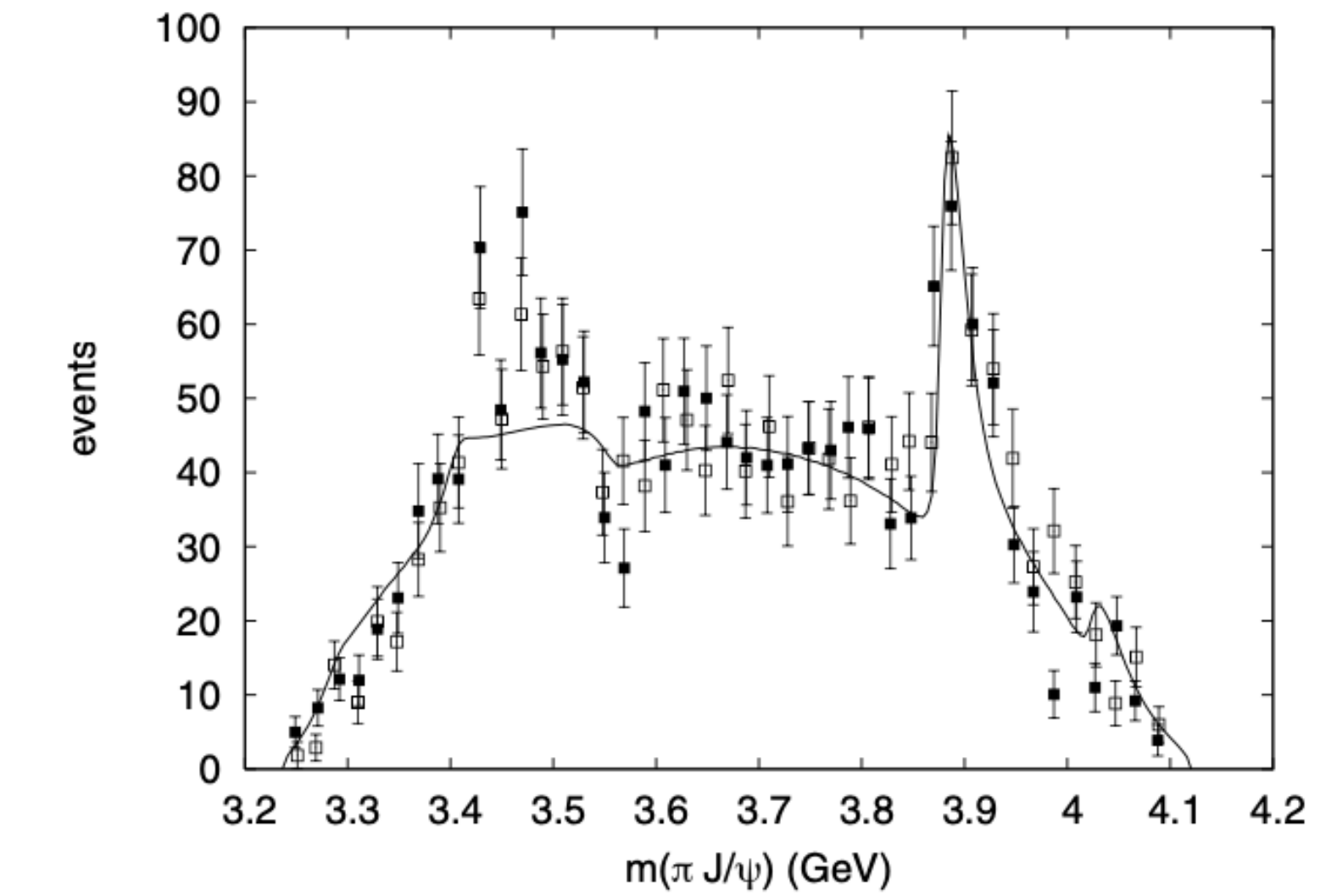
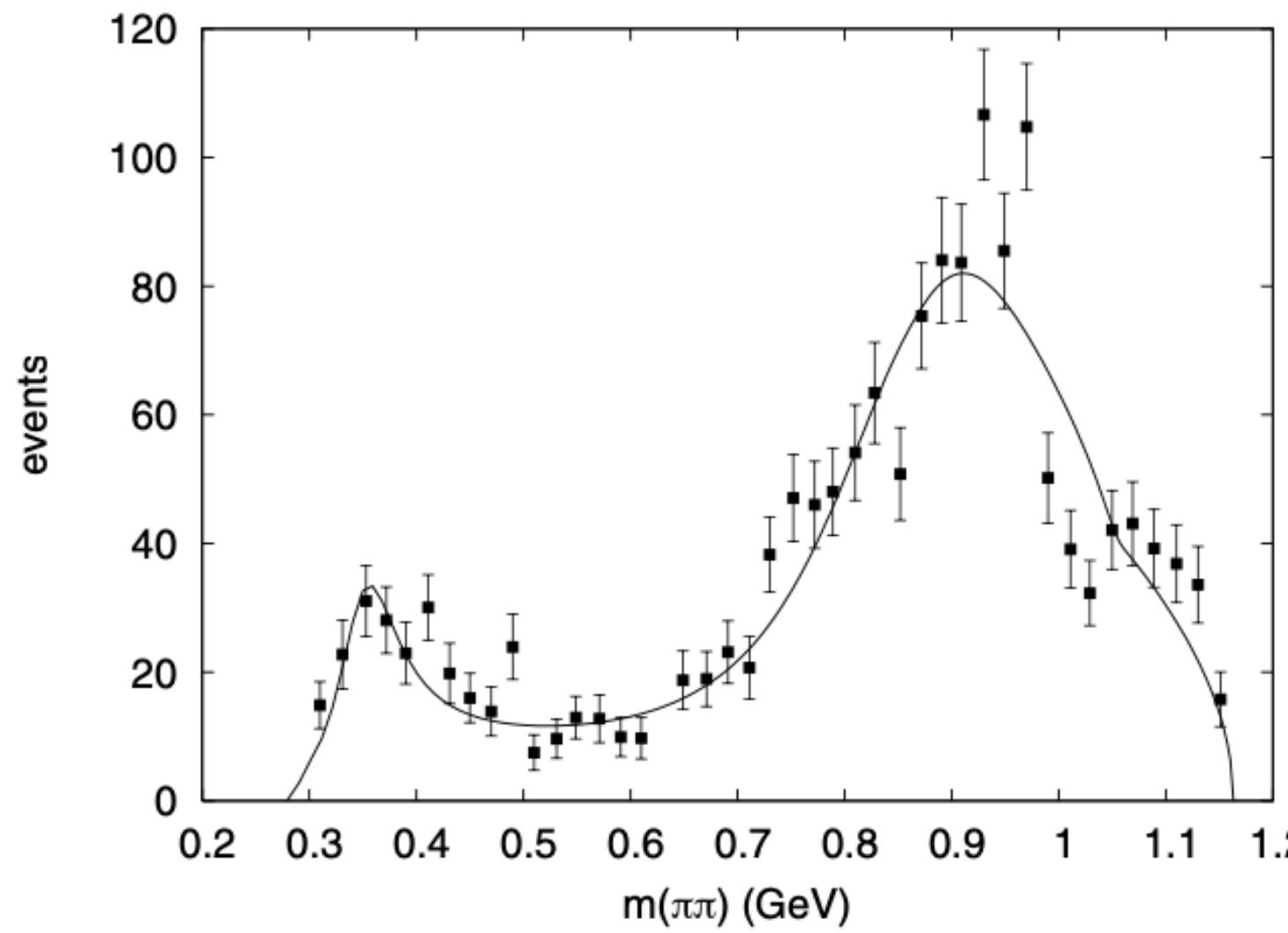
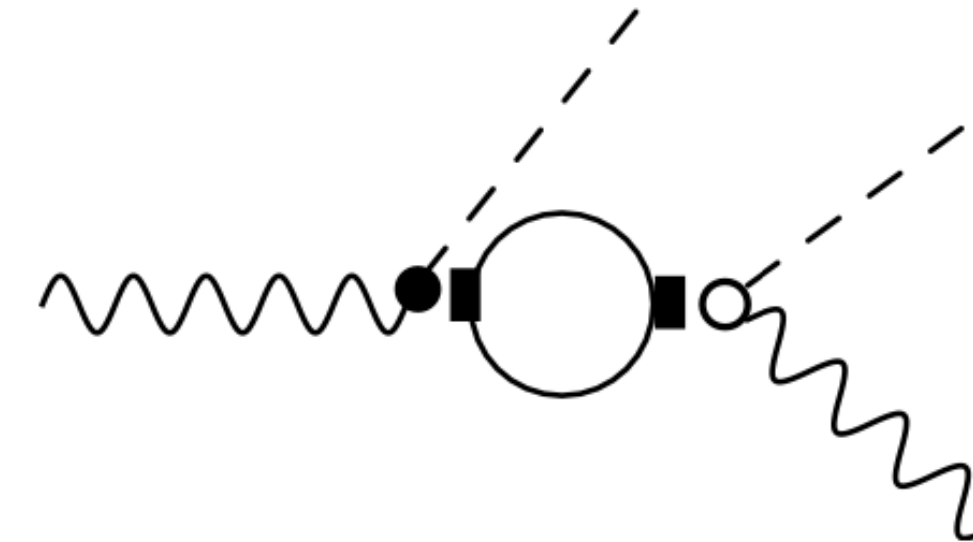


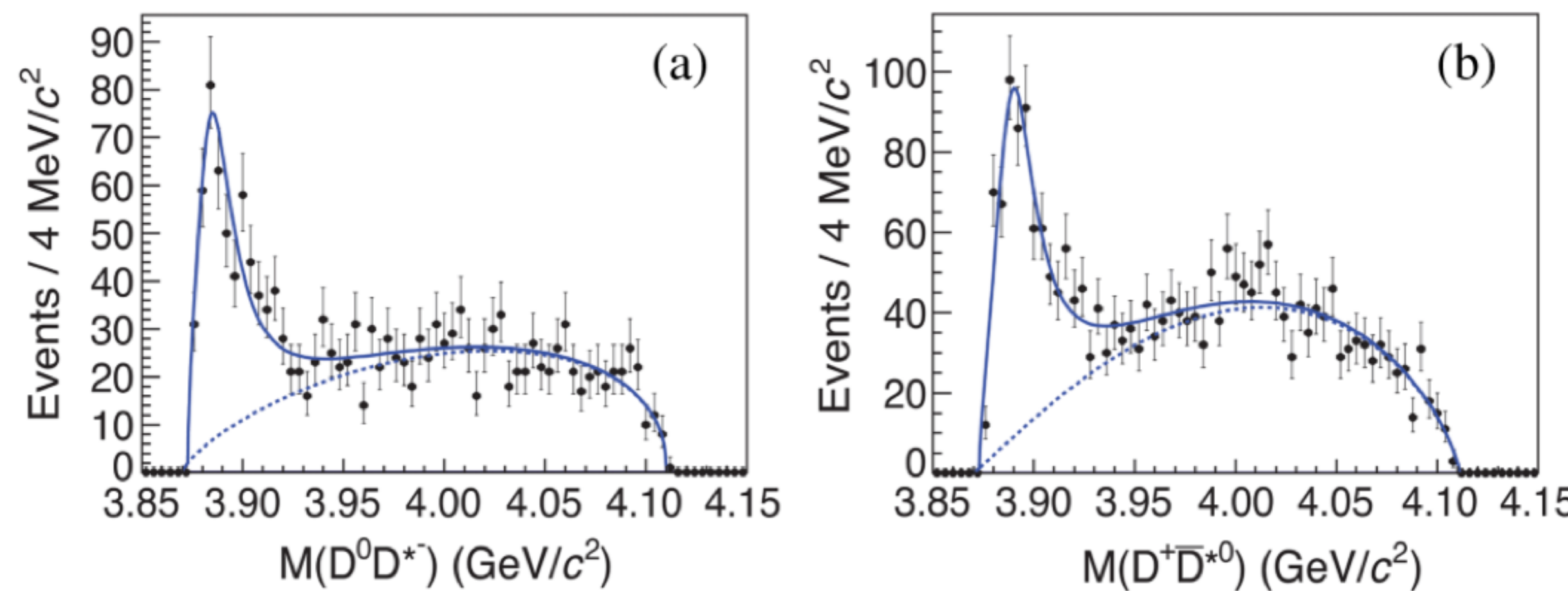
Fig. 4. $e^+e^- (\sqrt{s} = 4.26 \text{ GeV}) \rightarrow \pi\pi J/\psi$. Left panel: invariant $\pi\pi$ mass distribution. Right panel: invariant $\pi J/\psi$ mass distribution. Filled squares: $\pi^- J/\psi$; open squares: $\pi^+ J/\psi$. Data from Ref. 7.

Zc(3900)

$$e^+ e^- \rightarrow \pi D \bar{D}^* \quad \sqrt{s} = 4.26$$

$$M = 3883.9 \pm 1.5 \pm 4.2$$

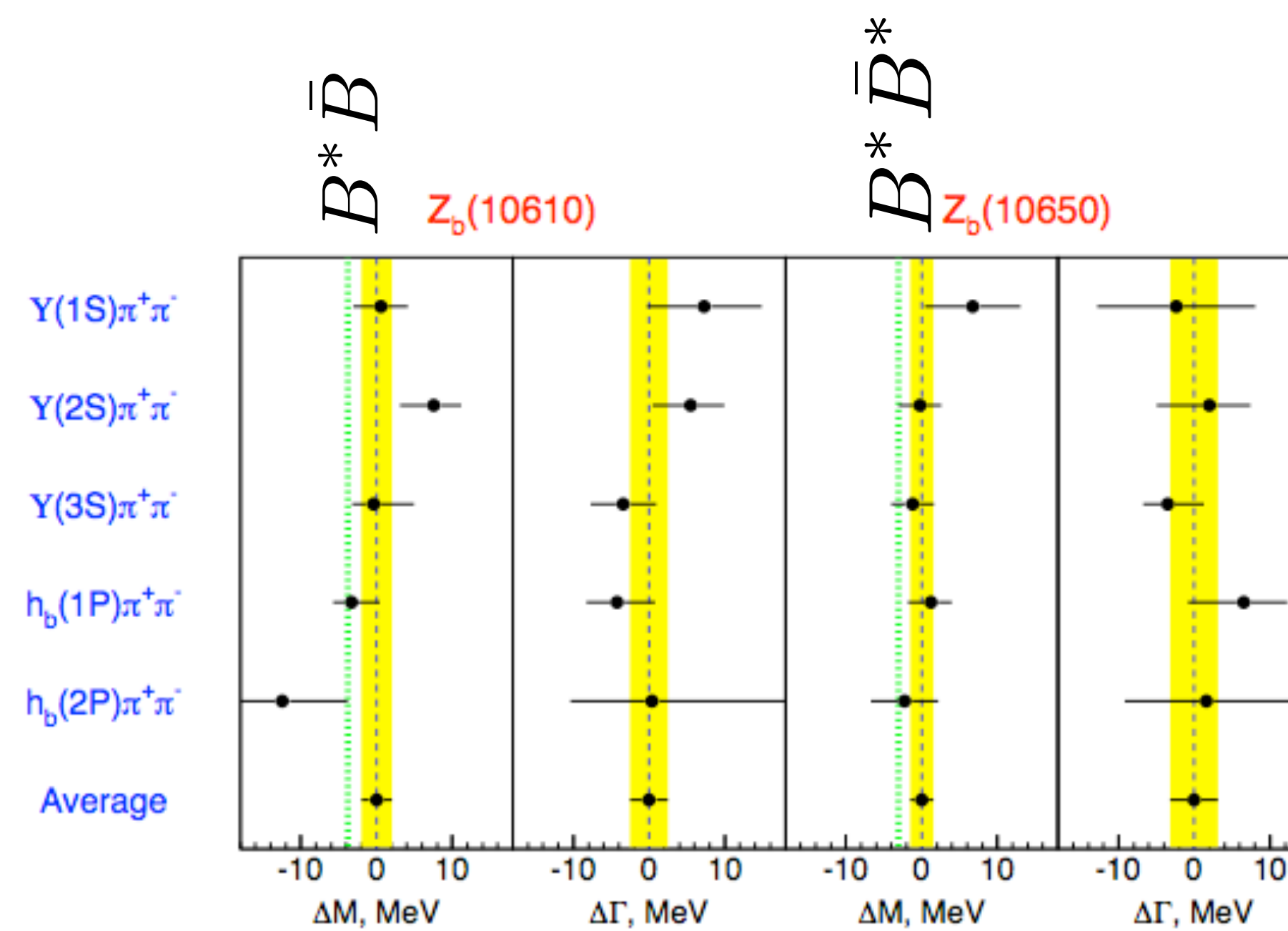
$$\Gamma = 24.8 \pm 3.3 \pm 11.0$$



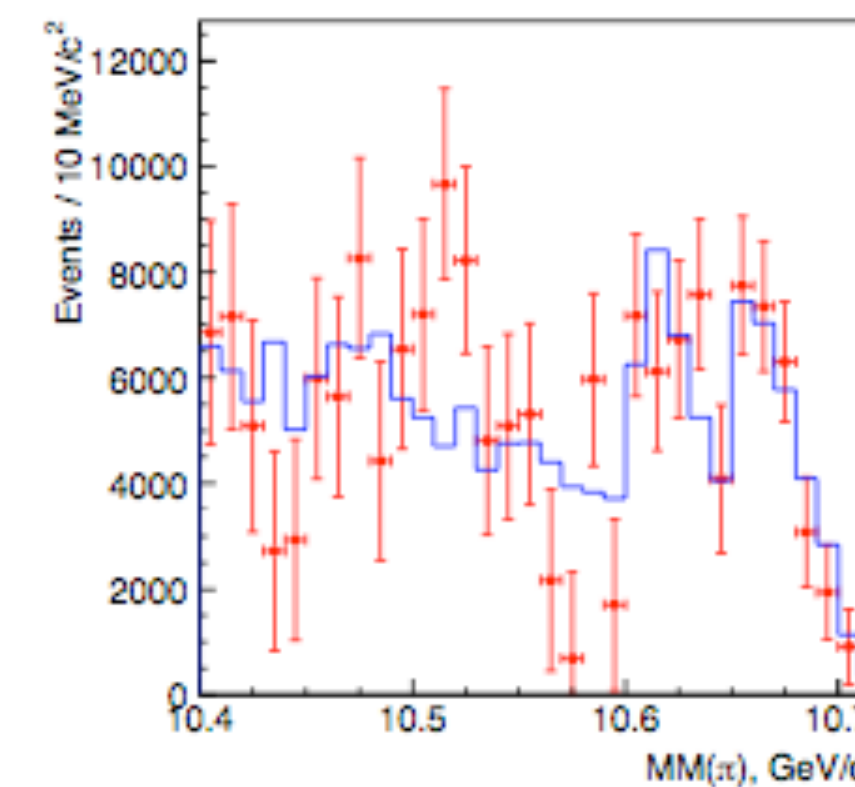
$Z_b^+(10610)$ $Z_b^+(10650)$

Adachi et al. [Belle] 1105.4583

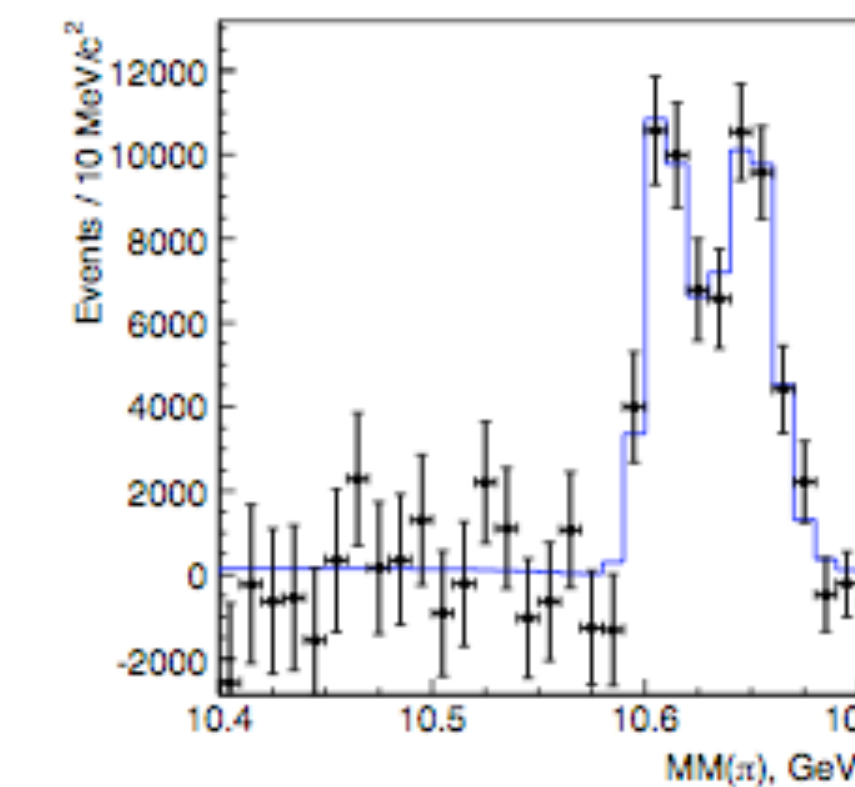
$$I^G J^P = 1^+ 1^+$$



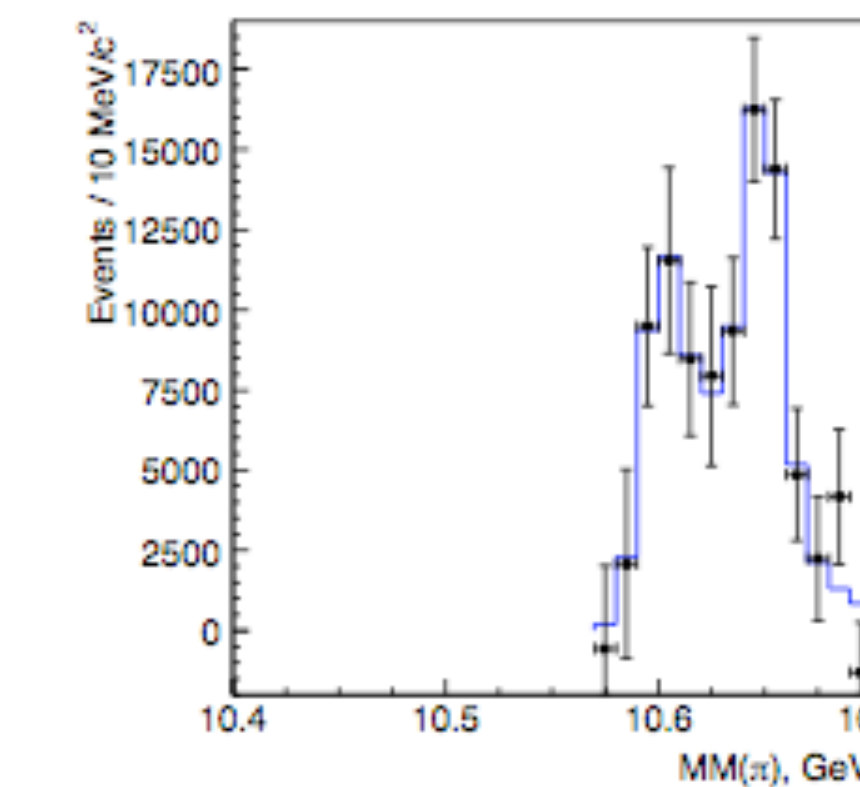
$\Upsilon(2S)$



$h_b(1P)$

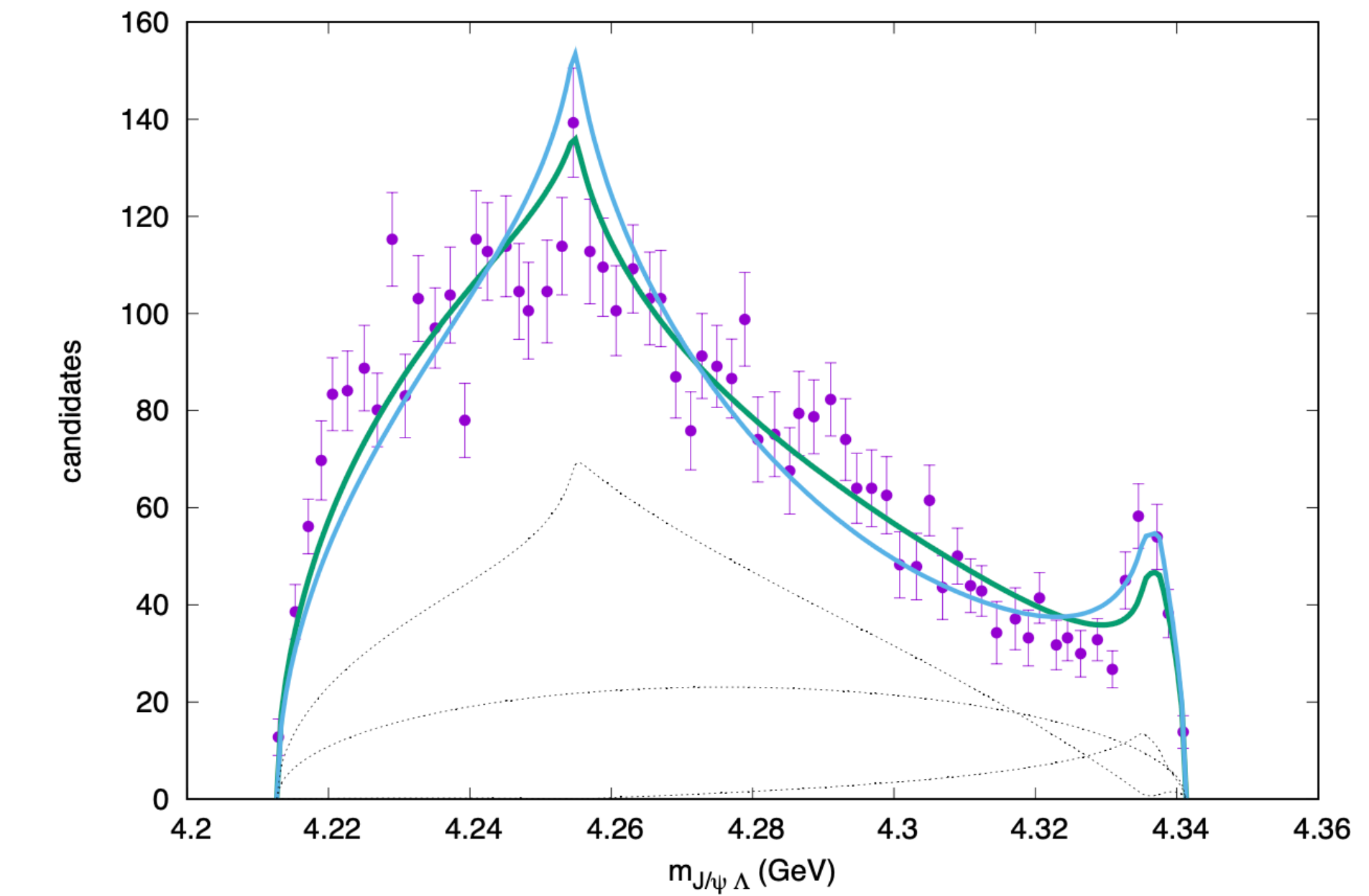
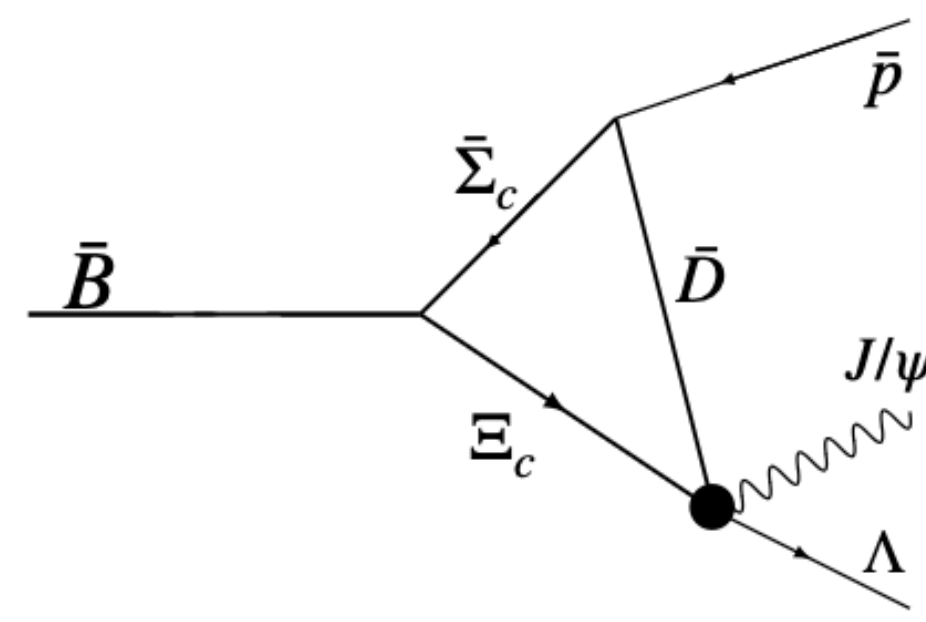


$h_b(2P)$

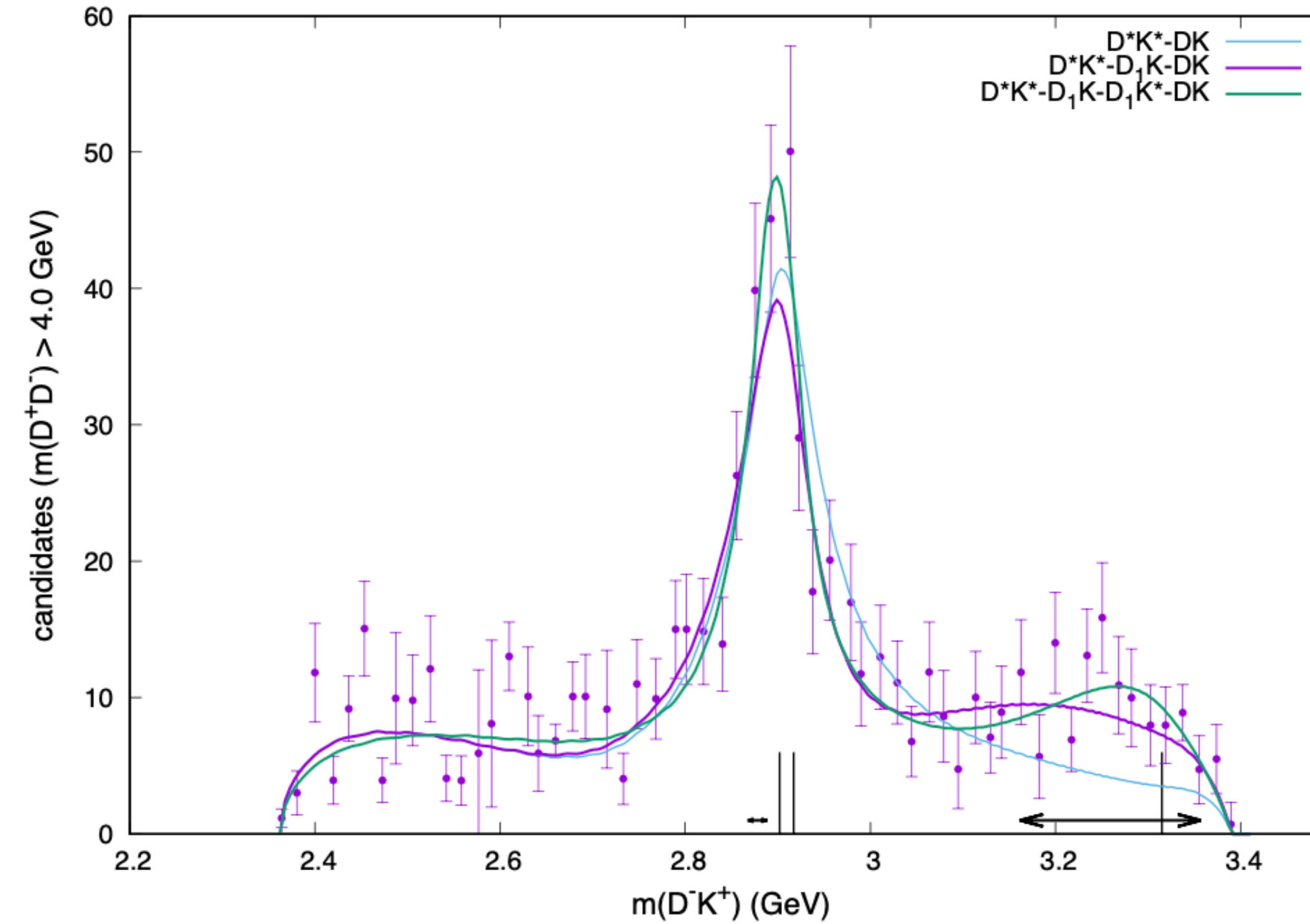
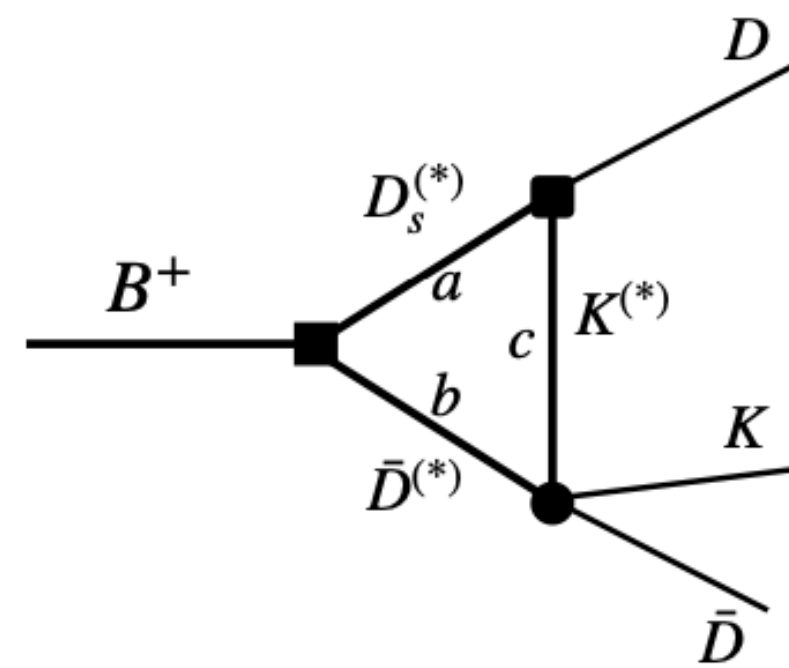


The 'triangle' diagram has a log singularity in certain kinematical regions.

LHCb state $P_{\psi s}^{\Lambda}(4338)$

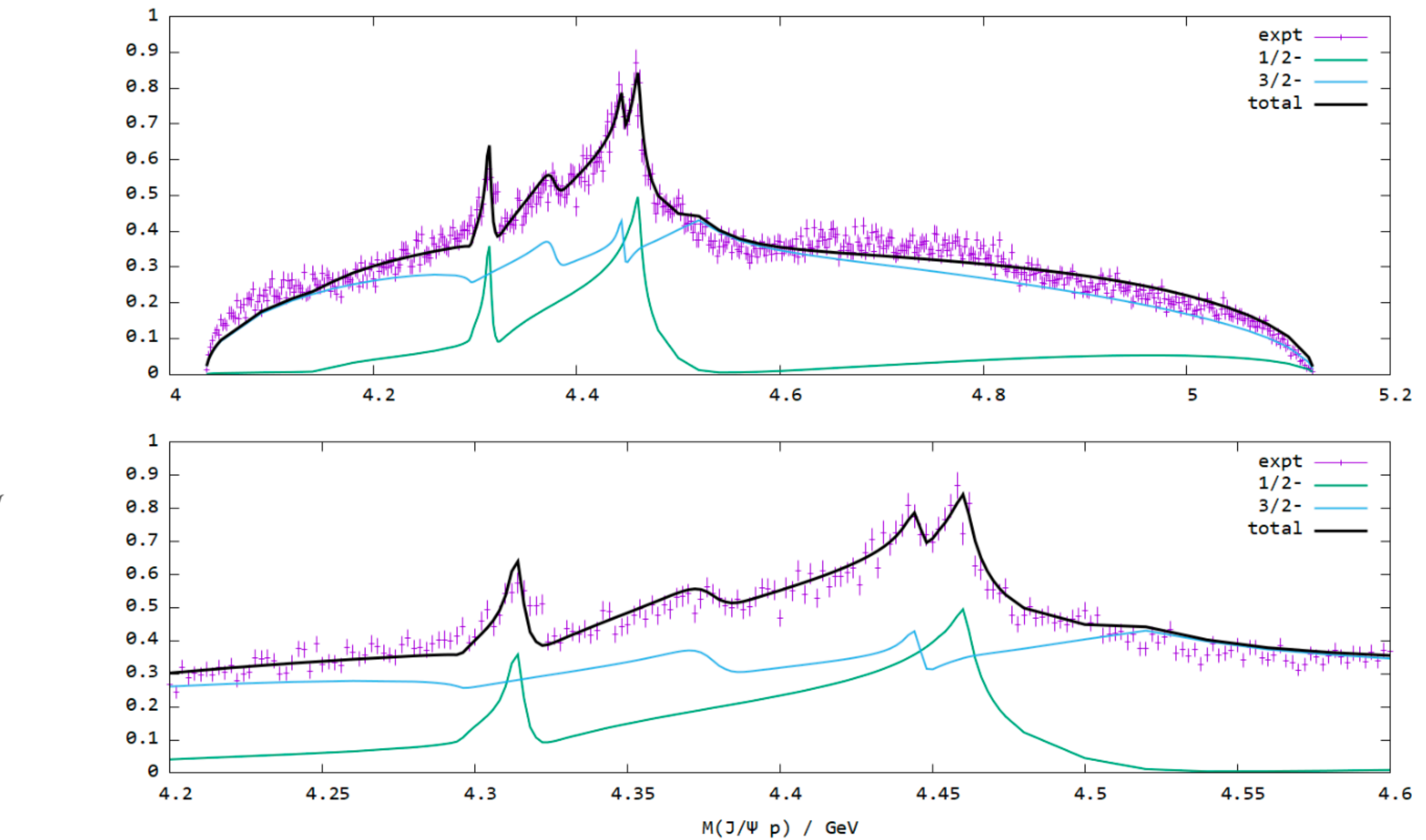
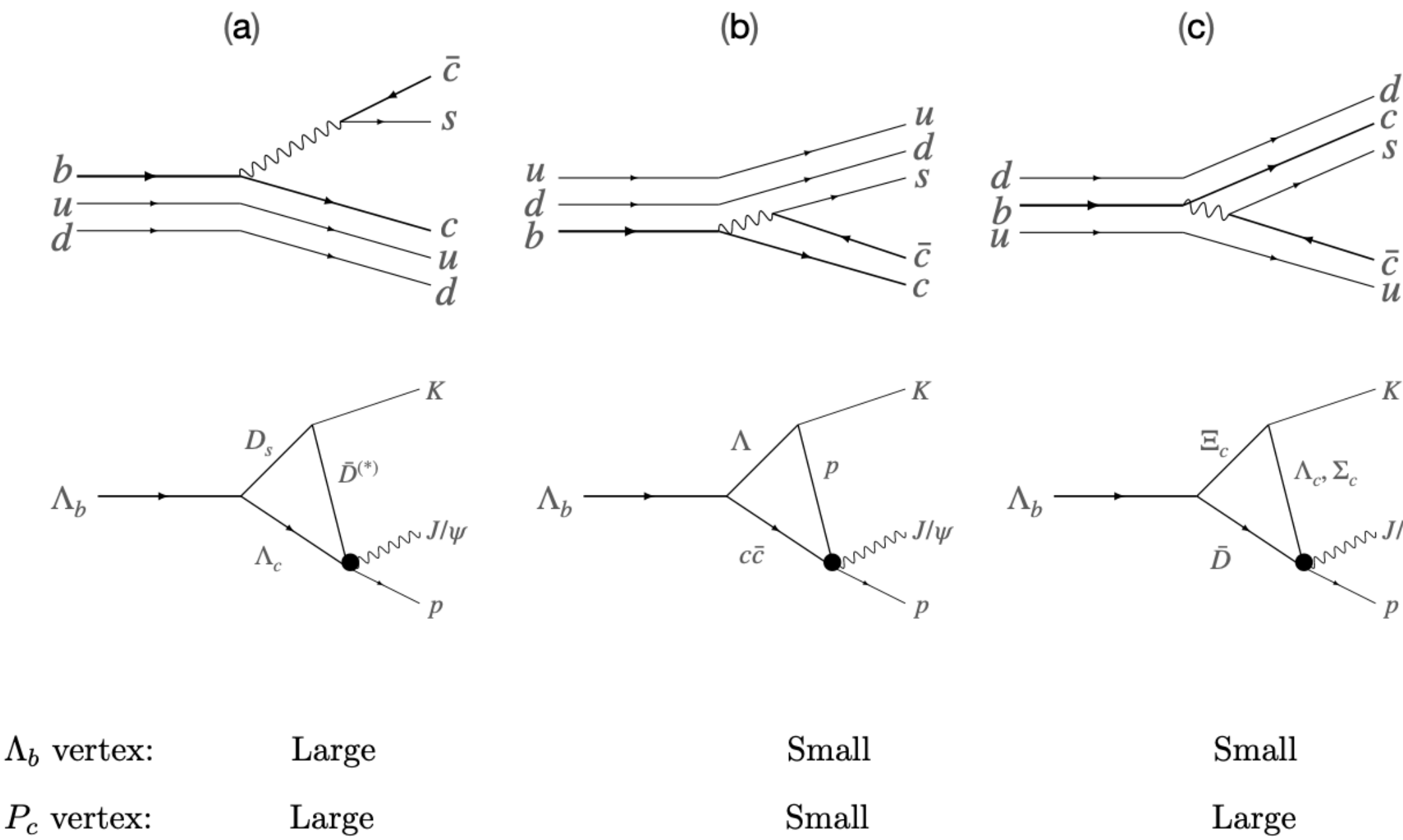


LHCb X(2900) $ud\bar{c}\bar{s}$



Burns & Swanson, PLB 813, 136057 (2021)

LHCb Pentaquark states $P_c(4312)$, $P_c(4380)$, $P_c(4440)$



Burns & Swanson, PRD106, 054029 (2022)

What are the common features here?

- "state" lies just above thresholds
- S-wave quantum numbers
- tree level production is suppressed (eg, colour suppressed electroweak transitions)
- widths will depend on channel

Conclusions

We are fortunate to have QCD to guide the search for effective degrees of freedom and their interactions.

But this is not enough. Lattice field theory helps determine the *emergent* degrees of freedom and properties.

Old ideas (bag, flux tube) are giving way to approaches that are closer to QCD (Bethe-Salpeter, many-body, EFT, dispersion relations, Born-Oppenheimer).

The role of non-resonant interactions in generating amplitude "structure" is a recent (~2010) development.

The role of coupled channels has long been appreciated and still awaits a definitive treatment.

+ ÆRIC MEC HEHT GEWYRCAN

Diquarks and the New Charmonia

[Maiani, Piccinini, Polosa, Riquer; PRD71, 014028 \(2005\)](#)

[Bigi, Maiani, Piccinini, Polosa, Riquer; PRD72, 114016 \(2005\)](#)

$$M([cq]_S) = 1933$$

$$M([cq]_V) = 1933$$

[Maiani, Riquer, Piccinini, Polosa; PRD72, 031502 \(2005\)](#)

[Maiani, Polosa, Riquer; PRL99, 182003 \(2007\)](#)

[Maiani, Polosa, Riquer; arXiv:0708.3997](#)

Assume a spin-spin interaction

$$|0^{++}\rangle = |[cq]_S[\bar{c}\bar{q}]_S; J=0\rangle \quad (1)$$

$$|0^{++}'\rangle = |[cq]_V[\bar{c}\bar{q}]_V; J=0\rangle \quad (2)$$

$$|1^{++}\rangle = \frac{1}{\sqrt{2}} (|[cq]_S[\bar{c}\bar{q}]_V; J=1\rangle + |[cq]_V[\bar{c}\bar{q}]_S; J=1\rangle) \quad (3)$$

$$|1^{+-}\rangle = \frac{1}{\sqrt{2}} (|[cq]_S[\bar{c}\bar{q}]_V; J=1\rangle - |[cq]_V[\bar{c}\bar{q}]_S; J=1\rangle) \quad (4)$$

$$|1^{+-}'\rangle = |[cq]_V[\bar{c}\bar{q}]_V; J=1\rangle \quad (5)$$

$$|2^{++}\rangle = |[cq]_V[\bar{c}\bar{q}]_V; J=2\rangle \quad (6)$$